PHOTOHERMAL INVESTIGATIONS ON CERTAIN ORGANIC MOLECULES AND THEIR PLASMA POLYMERISED THIN FILMS.

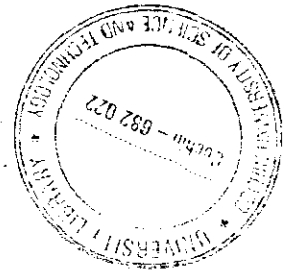

Thesis submitted to

Cochin University of Science and Technology

in partial fulfilment of the requirements for the award of the Degree of

Doctor of Philosophy

By

T.Nandini

LASER AND SPECTROSCOPY LABORATORY

Department of Physics

Cochin University of Science and Technology

Kochi-682 022

INDIA

JANUARY 2005

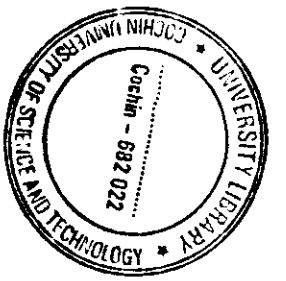

PHOTOTHERMAL INVESTIGATIONS ON CERTAIN ORGANIC MOLECULES AND THEIR PLASMA POLYMERISED THIN FILMS.

Ph.D Thesis submitted to

Cochin University of Science and Technology

in partial fulfilment of the requirements for the award of the Degree of

Doctor of Philosophy

Autor

T.Nandini

ResearchFellow,Department of Physics.

Cochin University of Science and Technology

Kochi-682 022, INDIA

Research Supervisers

Dr K.P.Rajappan Nair

Cochin University of Science and Technology

Kochi-682 022, INDIA

LASER AND SPECTROSCOPY LABORATORY

Department of Physics

Cochin University of Science and Technology

Kochi-682 022, INDIA

JANUARY 2005

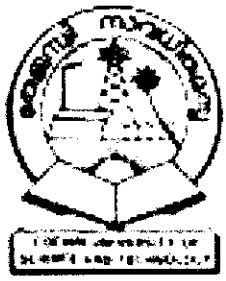

Department of Physics
Cochin University of Science and Technology
Cochin 682 022

CERTIFICATE

Certified that the work presented in this thesis entitled **"Photothermal Investigations on certain Organic Molecules and their Plasma polymerized thin Films"** is based on the bonafide research work done by Ms. T.Nandini under my guidance in the Department of Physics, Cochin University of Science and Technology, Cochin 682 022 and has not been included in any other thesis submitted previously for the award of any degree.

K.P. Rajappa Nair

Cochin- 22
18-01-2005

Prof. K.P Rajappan Nair
Supervising Guide
Dean, Faculty of Science,
CUSAT, Cochin-22

Declaration

I hereby declare that the present work entitled "**PHOTOTHERMAL INVESTIGATIONS ON CERTAIN ORGANIC MOLECULES AND THEIR PLASMA POLYMERISED THIN FILMS**"which will be submitted is based on the original work done by me under the guidance of Dr.K.P. Rajappan Nair,Department of Physics, Cochin University of Science and Technology,has not been included in anyother thesissubmitted previously for theawardof any degree.

Kochi-682 022 **T.Nandini**

27-01-2005

WORDS OF GRATITUDE

I am grateful to my guide Dr.K.P.Rajappan Nair for his valuable guidance and also for the encouragement throughout my work.His constructive commentsand suggestions have played a key role in formulating my aptitude for research

.I am extremely thankful to Dr.S.Jayalakshmi for the invaluable support, inspiration and efforts taken in making samples. She was always encouraging me with a pleasant smile and helped me with timely and fruitful discussions.

I here express my sincere gratitude to Dr.K.P.VijayaKumar , Head of Department of Physics for the help renderd for my research work.

Throughout my research work my senior research collegueDr.JyotsnaRavi helped me a lot in understanding the various aspects ofinstruments and guided me by giving correct advices at proper times.I amgrateful to my collegues B Syamalakumari ,,K.KVijayan, SunnyKuriakose,Mathew George, ,UshaJohn

,Thomas.P.Zacharia,P,Raveendran,for the supportGiven during my research career. The help rendered by Dr.S.Shaji andDr.ShibuEapen Dr.K.Bindu, Alex Mathew and Sajeev.U.S are also equally important.

T.Nandini

CONTENTS

Papers presented in seminars / conferences:

1. Thermal Characterization of Diethylene triamine and its Plasma Polymerized Film using Probe Beam Deflection Method. **T.Nandini**, Jyotsna Ravi, TMA Rasheed, K.P.R.Nair Austin Symbosium March 2004 Austin.U.S.A.

2 .Optical and thermal characterization of plasma polymerised m-toludine,

Jyotsna Ravi,B.Syamalakumari, **T.Nandini**, K.P.R.Nair TMA Rasheed Nineteenth Austin Symbosium March2002 March2-March5 Austin,.U.S.A.

3. Comparative study of the optical and thermal properties of plasma polymerized benzylamine andN-metylaniline B.Syamalakumari Jyotsna Ravi, , **T.Nandini**, TMA Rasheed K.P.R.Nair Nineteenth Austin Symbosium March2002 March2-March5 Austin,.U.S.A.

4 .Optical and thermal characterization of plasma polymerized N-methyl aniline by probe beam deflection technique. B.Syamalakumari Jyotsna Ravi, , **T.Nandini**, TMA Rasheed K.P.R.NairNational Symposium on Atomic,Molecular structure, interactions and Laser Spectroscopy February 22-24 ,2002.

5. Thermal characterization of Plasma polymerized thim film using mirage technique.Jyotsna Ravi,B.Syamalakumari, **T.Nandini**, K.P.R.Nair TMA Rasheed .National Laser symposium 2001.December19-21CATIndore.

6. Determination.of thermal diffusivity of plasma polymerized poly-m-toluidne by probe beam deflectionJyotsna Ravi,B.Syamalakumari, **T.Nandini**, K.P.R.Nair TMA Rasheed Second international Conference and XX 11 Annual Convention of the optical society August27-29,Trivandrum,Kerala,India(2001)

List of Publications

Mirage detection applied to low thermal diffusivity measurementsof weakly absorbing thermally thin plasma polymerized film. Jyotsna Ravi,B.Syamalakumari, **T.Nandini**, K.P.R.Nair TMA Rasheed .Nodestructive testing and evaluation.

Preface

In recent years Photothermal methods emerged as a valuable tool for optical and thermal characterization of wide range of samples offering significant improvements above traditional methods. Essentially it implies an interaction of the modulated radiation with the absorbing sample which leads to non-radiative de-excitation processes and hence to the temperature rise within the sample.

The detection of thermal waves generated by modulated light source can be performed by several direct and indirect ways, photoaccoustic radiometry, optical beam deflection, photo deformation, thermolumniscence and photopyroelectrics. The thermal waves carry information on the thermal and optical properties of the medium in which they propagate and on its structure .One of the most interesting applications of photothermal wave physics is the measurement of the thermal diffusivity of solids, liquids and gases.

One of the advantages of the photothermal wave method is the existence of simple linear relations between two measurable parameters; whose slope can be used to retrieve the diffusivity directly. These linear relations are obtained from theoretical models following a numerical integration of the measurarable magnitude from analytical expressions. However a careful management of them is necessary since some of these linear restrictions are strictly valid only under ideal conditions which are in practice very difficult to achieve.

Thermal diffusivity is a physical quantity which characterizes heat diffusion process through conduction .Usually direct measurement of this quantity is performed using unsteady methods only .All methods allow one to estimate the thermal diffusivity by studying the temperature induced when the sample is heated in an unsteady way.The use of laser as heater improved these methods ,giving rise to a contactless point like heating .Concerning the evaluation of the induced temperaturem the main improvement has been the use of remote detection systems instead of the standard thermal sensors. Infact they can detect very precisely small temperature rises<10^-6K through some physical effects connected to the heating such as the infrared radiation emitted by the sample ,the induced acoustic waves or the mirage effect.

The production of polymer thin film samples has obtained considerable attention for the past few years. Different techniques like plasma polymerisation, electron bombardment, ultra violet radiation and thermal evaporation method can be used for the preparation of polymer thin films from their respective monomers. Among these plasma polymerisation or glow discharge polymerisation has been widely used for polymer thin film preparation.. These films are pinhole free, highly branched and crosslinked, heat resistant, exceptionally dielectric etc. The optical properties like the direct and indirect bandgaps, refractive index etc of certain plasma polymerized thin films prepared are determined from the UV-Vis-NIR absorption and transmission spectra. The possible linkage for the formation of the polymers is obtained by comparing the

FTIR spectra of the monomer and the polymer. Being thermally thin and optically transparent, the thermal diffusivity of these films are determined using the Photothermal beam deflection technique. This technique measure the refractive index gradient established in the sample surface and in the adjacent coupling medium by passing another optical beam (probe beam) through this region and hence the name probe beam deflection. The deflection is detected using a position sensitive detector and its output is fed to a lock-in-amplifier from which the amplitude and phase of the deflection can be directly obtained. The amplitude and phase of the deflection is suitably analysed for determining the thermal diffusivity.

Photothermal beam refraction is a part of a family of thermooptical techniques for absorbance measurements. The accurate measurement of thermal diffusivity and thermal conductivity of liquids is vital not only for practical engineering but for theoretical studies and analysis.In photothermal deflection technique the measurement is based on the deflection of a probe laser beam which passes through the test liquid and a modulated pump laser beam intersects at right angles which illuminates the sample. In these techniques, an optical element is formed within the sample from a temperature rise generated by absorption of pump laser beam. The amplitude and phase of the signal are measured using Lock-in-amplifier

Photoacoustic technique has also been employed for the material characterization which is another important but a much simpler technique. This technique measures the pressure change, one of the photothermal effects by using an electret

microphone. The output of the microphone is also fed to a lock-in-amplifier to obtain the amplitude and phase from which the thermal properties can be obtained The whole work described in the thesis is discussed below.

CHAPTER I Photothermal techniques and its application.1-dimensional and 3-dimensional theory of periodic distribution which forms the basis of Photoacoustic and Photothermal technique beam deflection technique respectively is also included.

CHAPTER II For the analysis of the photothermal signal different methods like the zero crossing detection method, Phase method, Amplitude method etc Thermal wave coupling method, Mutliparameter fitting method are also discussed. these methods are briefed when applied to materials of different category, - thermally thick, thermally thin, optically opaque and optical transparent While dealing with low thermal diffusivity i.e. when the thermal diffusivity of the sample is less than the thermal diffusivity of the coupling medium, the height of the probe beam above the sample surface need be taken into account is discussed..

CHAPTER III Plasma polymerization techniques to emphasis on r.f. plasma polymerization is given in this chapter. This chapter also includes the preparation and optical characterization of different plasma polymerized thin films namely poly Diethylene Triamime, poly PhenylHydrazine poly Furfurylamine and polyPropyl amine. Optical characterization consists of determination of direct and indirect bandgap from the UV-Vis-NIR absorption spectrum, refractive index from transmission spectrum and possible linkage in the polymerization process by comparing the FTIR spectra of the monomer and the corresponding polymer.

CHAPTER IV To determine of thermal diffusivity using transverse PBD technique setup is designed. The measurement of the thermal diffusivity of the three r.f. plasma polymerized thin film samples using two different methods of analysis viz the Phase method and the Amplitude method.in carbontetrachloride is given. There is no contribution from the thermal properties of coupling media to the photothermal signal from the sample. Since the substrate is non-absorbing at the pump wavelength, there is no photothermal signal from the substrate too.

The Probe beam deflection method is used to determine the thermal diffusivity of liquids having low absorptivity.Thermal diffusivity of DiethyleneTriamine, PhenylHydrazine FurfurylAmine were determined by this method.

CHAPTER V Photoacoustic cell is designed and fabricated and the experimental setup has been standardized using silicon wafer and aluminium sheet. Certain $LiNiO_2$ samples are prepared by changing composition and thermal diffusivity is also studied.

CHAPTER VI gives the conclusions and brief summary of the thesis.

CHAPTER I

INTRODUCTION TO PHOTOTHERMAL EFFECTS

1.1 INTRODUCTION TO PHOTOTHERMAL SCIENCE

The ever growing interest in optical communication and the continuing progress in the development of high power lasers motivate the development of sensitive techniques to measure low absorption losses in highly transparent solids, thin films and optical coatings. Photothermal technique encompass a wide range of techniques and phenomena based upon the conversion of absorbed optical energy into heat.Optical energy is absorbed and eventually converted into thermal energy by solids ,liqids and gases. Although the initial absorption processes in many materials is very selective,it is common for excited electronic states in atoms or molecules to loose their excitation energy by a series of non-radiative transitions that result in a general heating of the material.

Absorption of electromagnetic radiation by matter causes absorption, emission and inelastic scattering of light. Except for emission, absorbed energy results in production of several forms of energy like luminescence, photochemical energy, photoelectrical energy or heat. Heat can be produced promptly or at various time delays. This heating induces changes in the sample as well as in the surrounding medium. These changes are referred to as photothermal effects [1,2]. Although it may seem counterintuitive to pursue phenomena based on the transformation of energy to the most chaotic form,heat, these techniques have many advantages for applications in low

absorption environments and in the domain of materials characterization and nondestructive testing. PT material probing is the most important in making significant contribution to the field of science and technology. Photothermal material characterization relies on high sensitivity detection techniques to monitor the effects caused by PT material heating of a sample.

In recent years thermal wave physics emerged as effective research and analytical tool for the characterization of materials.[3,4]The nondestructive and nonintrusive photothermal methods are based on the detection by one means or the other ,of a transient temperature change that characterises the thermal wave generated in the sample after illumination with a pulsed or chopped optical radiation.[5-19]Thedetected photothermal signal depends on the optical absorption coefficient as well as how heat diffuses through the sample [20-24].Dependence of photothermal signal on how heat diffuses through the specimen allows the investigation of transport and structural properties such as thermal diffusivity, thermal effusivity ,thermal conductivity,voids,etc [25-34]). Photothermal methods can be effectively used for the optical characterization of the sample due to its dependence on optical absorption coefficient [35-39].The unique feature of photothermal methods is that the detected photothermal signal depends only on the absorbed light and it is independent of transmitted or scattered light.The two features that make photothermal methods superior to conventional methods is that it can directly monitor the nonradiative path of deexcitation in addition to being sensitive to very small optical absoption coefficient[38-39]. Apart from this ,photothermal effects can amplify the measured optical signal which is referred to as enhancement factor and it is the ratio of the signal obtained using photothermal spectroscopy to that obtained using conventionaltransmission spectroscopy.Enhancement factors depend on thermal and optical properties of the sample ,the power of energy of light source and the optical geometry used

to excite the sample[40].As these parameters can vary externally,photothermal methods can be used even for specimens having relatively poor thermal and optical properties.The merit of these methods also lies in the extremely sensitive detection technique used here in comparison to conventional transmission methods. The various phototermal methods are depicted in Fig.1.The magnitude of photothermal signal depends on the specific method used to detect the photothermal effect and on the type of the sample analysed.

Most of the photothermal effects occur simultaneously. The choice of a suitable PT source depends on the purpose of measurement.. In short PT generation is an example of energy conversion and has in general three kinds of applications. a) PT material probing : do not cause any sample modification. b) PT material processing : causes the sample to change to another useful form. c) PT material destruction: makes the sample useless

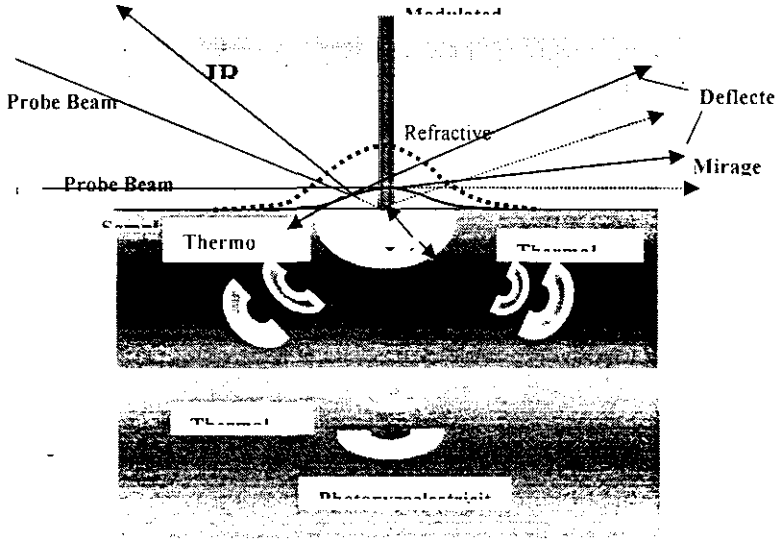

Figure 1: Schematic of the various photothermal effects

The different techniques that are employed in Photothermal methods are shown in Table1.

Detection methods (applicable to sample S or adjacent coupling medium F)	Photothermal Effects
Laser calorimetry (S or F)	Temperature rise
Direct photoacoustic detection (S) Indirect photoacoustic detection (F)	Pressure change
Probe beam refraction (S or F) Probe beam diffraction (S or F) Other optical probes (S or F)	Refractive index change (Thermal or Acoustic)
Probe beam deflection (S) Optical Interference (S)	Surface deformation (Thermal or acoustic)
Photothermal radiometry (S)	Thermal emission change
Transient thermal reflectance (S) Transient piezo reflectance (S) Optical transmission monitoring (S or F)	Reflectivity/Absorptivity change

The detecting parameter changes in all techniques eventhough all techniques are based on the same principle

Temperature rise occurring in the sample can be directly measured using thermocouples, thermistors, or pyroelectric detectors and is called laser calorimetry or photothermal calorimetry [41,42] In the photopyroelectric techniques [43-45] which can be used for the simultaneous measurement of different thermal parameters such as thermal diffusivity,effusivity etc a

thermally thick pyroelectric film(thickness of film greater than thermal diffusion length of the film) is attached to one side of the thermally thick backing medium.The other side of the specimen is illuminated by an intensity modulated opltical radiation.When thermal waves reach the pyroelectric sensor sample interface,the pyroelctric sensor detects an electric current which contain information about the structure and thermal properties of the sample.A variant configuration of the standard photopyroelectric method, well suited for thermal effusivity measurements , is the so called inverse photopyroelectric technique.In this method light is incident directly on the surface of pyroelectric transducer and the substrate is substituted for the sample .Application of IPPE technique for the thermal effusivity of margarines,cultured milk and pastry materials is a typical example of the potential application of this technique for the quality control of the food stuff. [46.47]Direct determination of the thermal conductivity of solids and liquids was recently discussed by Thoen and co-workers.

In photothermal radiometery,[48] the temperature changes are measured indirectly by monitoring the infrared emission and it can be used in situations where a large temperature change has occurred.Although not very sensitive,this method has potential application in non-destructive materials analysis and testing.Using sensitive infrared cameras,it can be used for imaging the thermal properties of large samples.However ,in photothermal radiometry ,a more careful analysis of the spectral detectivity of detector, spectral absorption of the sample and the geometry of the optical equipment are essential.(49] The inherent advantage of this technique is that signal can be obtained remotely [50]. The shapes of the objects can be can be arbitrary. .Nevertless it is better to make sure that the quality for imaging a sample spot

on the detector is constantly good.Signal evaluation may be complicated if the sample is transparent or reflective in the infrared spectral range.

Another temperature dependent parameter exploited is the pressure change. Pressure variations or modulations resulting from the absorption of modulated light by the sample are referred to as optoacoustic or photoacoustic generation [51,52,53]. The pressure wave generated after light excitation contains contributions from various sources such as radiation pressure, electrostriction, thermoelastic expansion (by non radiative transition or thermal energy of chemical reaction), photoinduced volume change, gas evolution, boiling, ablation and dielectric breakdown. The acoustic wave can be detected in the sample itself (i.e. direct photoacoustic detection) or it can be detected via coupling fluid medium adjacent to the sample.

The majority of studies addressing the use of photothemal spectroscopy for chemical analysis have been based on the refractive index measurements. The refractive index change produced upon light absorption may be induced by the pressure wave, density change, a temperature change (by radiationless transition or chemical reaction), molecular alignment, vibration excitation, rotational excitation, electronic excitation, concentration change, photoinduced volume change, creation of electric field (charge creation), clustering and so on. In transparent samples, the temperature dependent changes in refractive index of the sample itself are probed. For opaque samples, the temperature dependent changes in refractive index of the fluid that couples heat out of the sample are measured. Two types of refractive index gradient are produced- Thermal RIG and Acoustic RIG. The thermal RIG is produced by the decreased density of the medium caused by the local temperature rise, decays in time following the diffusional decay of the temperature profile and remains near the initially optically excited region. The

acoustic RIG is associated with the density flectuation of the medium caused by the propagation of PA wave, decays in propagation distance following attenuation of the PA wave and travels at acoustic velocity away from initially optically excited region. The thermal RIG generated by the excitation beam affects the propagation of an optical beam in its viscinity, including its own propagation resulting in a well-known effect of thermal blooming self-defocusing or [54] In other words, spatial dependent refractive index profiles can also result in focussing and defocusing of light. The thermally perturbed sample acts as lens. Light transmitted through an aperture placed beyond the photothermal lens will vary with the strength of the lens. Photothermal methods based on the measurement of the strength of the lens are known as Photothermal lensing spectroscopy [55,56] The thermal RIG also affects the propagation of another weak beam in the viscinity of the excitation beam. Thus, as light exits the medium, with a refractive index gradient, at an angle relative to the incident ray. The detection of bending of light path is utilized in Photothermal deflection method.[57-61]In some experimental measurements a signal that is due the combined effects of deflection and lensing is detected.. These can be generally classified as Photothermal refraction methods [62] and take advantage of the effects of the temperature distribution on the probe beam propagation. The optical path length changes that occur due to the Photothermal induced refractive index change can be measured with interferometry. A periodic refractive index modulation results in a volume phase diffraction grating. The grating will diffract light at an angle that meets requirements from Bragg's law. The amount of light diffracted is proportional to the refractive index change. The diffracted light is measured with a photoelectric detector. Methods used to measure spectroscopic signals based

on volume phase grating formed by the photothermal heating are called Photothermal diffraction spectroscopy.[63,64]

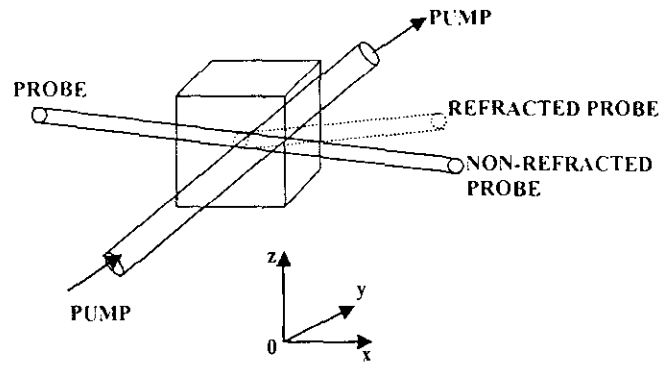

Figure 2: Perpendicular probe beam deflection through the sample

In steady state isobaric conditions, the temperature change due to non-radiative de excitation can result in a variation in the volume expansion coefficient,and a consequent change in the density of the specimen. Though temperature dependent density changes are difficult to measure directly, these changes can affect the samples in several different ways. In solid samples, the density change alters the physical dimensions at sample surface. Sample dimension changes give rise to two optical methods for monitoring temperature changes based on surface deformation. A homogeneous deformation displaces the surface of the sample. Interferometry can be used on reflective samples. Since small displacements of the order of few parts per million of the wavelength of the probe beam light can be measured using interferometry, this method may be used for sensitive measurements. Spatially

heterogeneous expansion (contraction) can also cause the surface angle to change. A probe beam reflected from the surface will change angle when heterogeneous expansion occurs. Measurement of probe beam angle gives rise to the method of PT surface displacement technique [65,66,67]

Temperature changes can also be indirectly measured using methods, which monitor infrared emission since the thermal infrared emission is related to sample temperature. The method of photothermal radiometry [68] can be used to measure the infrared emission changes. Although not very sensitive, this method has great potential application in non-destructive material analysis and testing. Using infrared sensitive cameras, it can be used for imaging the thermal properties of large samples.

Modulated PT heating of many types of metal or semiconductor samples causes modulated reflectivity changes [69] or transmission and scattering changes [70] that can be due to density change or the photoacoustic carrier generation at the surface. Transient thermal reflectance can be used to monitor thermal properties. PT heating can cause changes in absorptivity of the sample. Zapka and Tam have used probe beam absorption measurements to detect the change in the Boltzmann molecular population distribution due to PT heating of a gaseous sample. [71]

Temperature changes resulting from optical absorption are directly related to heat capacity and thermal conductivity. Photothermal signals depend on the thermodynamic and energy transfer properties of the sample. Since the thermal and optical properties are to be known to a high accuracy, absolute sample absorption measurements are difficult. Hence, the dependence on thermodynamic and energy transfer properties allows for the analysis of thermal structure of materials. Photothermal methods have been efficiently used for the measurement of acoustic velocities, thermal diffusion coefficients,

sample temperature, bulk flow rates, phase transition, volume expansion coefficients and heterogeneous thermal conductivities in the solids [72-79].The advent of the coherent , monochromatic and highly unidirectional light source namely laser had led a major renaissance in this field. For an excitation of a sample with a given absorption coefficient, the temperature change will be proportional to the optical power, in the case of continuous excitation or pulsed excitation. The photothermal signal is generally proportional to the temperature change. Thus, the great power and high spectral purity, lasers can deliver high power or pulsed energies over very narrow optical bandwidths thereby enhancing the photothermal signals.. The temperature change is proportional to the optical power or energy, but at the same time is inversely proportional to the volume over which light is absorbed since the heat capacity scales with the amount of substance. The spatial coherence properties of the laser light also allow the light to be focussed to small, diffraction-limited volumes. The small volumes enhance the signal magnitude and allow the photothermal spectroscopy to be used in small volume sample analysis and allow for microscopic analysis of heterogeneous samples.

1.2 **Photoacoustic technique**.[81]

The photoacoustic effect is the generation of acoustic waves in the specimen after illumination with a chopped or pulsed optical radiation.In the case of Photoacoustic technique the excitation beam is not focussed in order to minimize the lateral heat flow. Hence, the heat diffusion can be analysed by one-dimensional calculation of the periodic temperature field.[82]

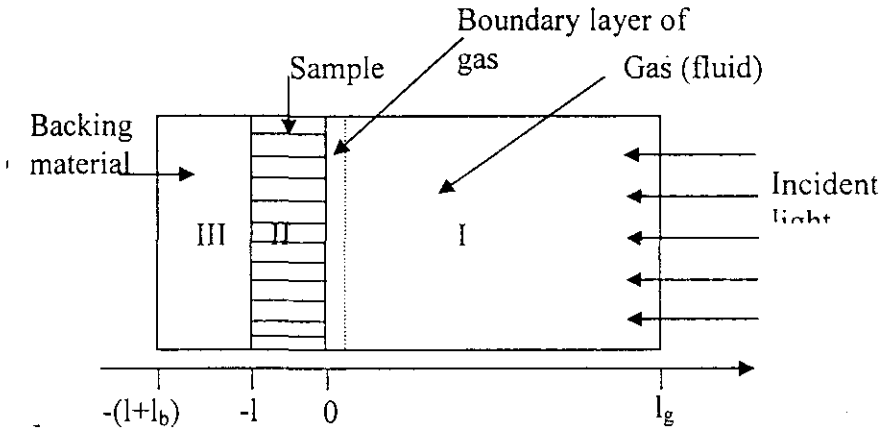

Figure 4: Geometry of 1-D Rosenwaig-Gersho model

Consider a simple cylindrical cell of length L and diameter D as shown in figure 4. Assume that the length L is small compared to the wavelength of the acoustic signal. The sample is considered to be in the form of a disk having diameter D and thickness

The sample is mounted so that its front surface is exposed to the gas (air) within the cell and its back surface is a poor thermal conductor of thickness l_b. The length l_g of the gas column in the cell is then given by $l_g = L-l-l_b$. Further assumption is that the gas and backing materials are not light absorbing.

Let k_i, ρ_i, C_i, α_i represent the thermal conductivity, density, specific heat and thermal diffusivity respectively of the material i. Then $a_i = (\omega/2\alpha_i)^{1/2}$ is the thermal diffusion co-efficient and $\mu_i = 1/a_i$ is the thermal diffusion length of the material. i can take subscripts s, g and b for solid, gas and backing material respectively. ω denotes the chopping frequency of the incident light beam in radians per second.

When. the sinusoidally chopped monochromatic light source with wavelength λ is incident on the solid with intensity $I = (1/2)\, I_0 (1 + \cos \omega t)$

The thermal diffusion equation in the three regions can be written as

$$\frac{\partial^2 \varphi}{\partial t^2} = \frac{1}{\alpha_b} \frac{\partial \varphi}{\partial t} \quad , -l-l_b \le x \le -l \qquad \text{Region III} \qquad (1)$$

$$\frac{\partial^2 \varphi}{\partial t^2} = \frac{1}{\alpha_g} \frac{\partial \varphi}{\partial t}, \; 0 \le x \le -l_g \qquad \text{Region I} \qquad (2)$$

$$\frac{\partial^2 \varphi}{\partial t^2} = \frac{1}{\alpha_s} \frac{\partial \varphi}{\partial t} - A \exp(\beta x)\left[1 + \exp(j\omega t\right], \; -l \le x \le 0 \qquad \text{Region II} \qquad (3)$$

$$\text{with } A = \frac{\beta I_0 \eta}{2k_s}$$

where φ is the temperature and η is the light conversion efficiency. The real part of the complex-valued solution φ(x, t) of the above equations is the solution of physical interest and represents the temperature in the cell relative to the ambient temperature as a function of position and time. Thus, the actual temperature field in the cell is given by

T (x,t) = Re[φ(x, t)]+ ϕ where Re stands for "the real part of " and ϕ is the ambient (room) temperature.

The complex amplitude of the periodic temperature distribution, θ at the solid-gas boundary (x=0) is given by

$$\theta = \frac{\beta I_0}{2k_s\left(\beta^2 - \sigma_s^{\,2}\right)}\left(\frac{(r-1)(b+1)\exp(\sigma_s l) - (r+1)(b-1)\exp(-\sigma_s l) + 2(b-r)\exp(-\beta l)}{(g+1)(b+1)\exp(\sigma_s l) - (g-1)(b-1)\exp(-\sigma_s l)}\right)$$

..... (4)

where $b = \frac{k_b a_b}{k_s a_s}$, $g = \frac{k_g a_g}{k_s a_s}$, $r = (1-j)\frac{\beta}{2a_s}$ and $\sigma_s = (1+j)a_s$.

Due to the periodic heat flow from the solid to the surrounding gas acoustic signal arises. The periodic heating causes the boundary layer of gas to expand and contract periodically. This can be thought of as the action of an acoustic piston on the rest of the gas column, producing an acoustic pressure signal that travels through the entire gas column. The displacement of the gas piston due to the periodic heating can be estimated using the ideal gas law,

$$\delta x(t) = 2\pi\mu_g \frac{\bar{\phi}(t)}{T_o} = \frac{\theta\mu_g}{\sqrt{2}T_o}\exp\left[j\left(\omega t - \frac{\pi}{4}\right)\right] \quad \text{.....} \quad (5)$$

where the average dc temperature of the gas boundary layer is set as dc temperature at the solid surface, $T_0 = \phi + \theta_0$, ϕ being the ambient temperature at the cell walls. Assuming that the rest of the gas responds to the action of the piston adiabatically, the acoustic pressure in the cell due to the displacement of the gas piston can be obtained from the adiabatic gas law PV^γ = constant, where P is the pressure, V is the gas volume in the cell, and γ ratio of the specific heats. Thus the incremental pressure is

$$\delta P(t) = \frac{\gamma P_0}{V_0}\delta V = \frac{\gamma P_0}{l_g}\delta x(t) \quad \text{.....} \quad (6)$$

where P_0 and V_0 are the ambient pressure and volume respectively and $-\delta V$ is the incremental volume. Then from equations (5) & (6)

$$\delta P(t) = Q\exp\left[j\left(\omega t - \frac{\pi}{4}\right)\right] \quad \text{.....} \quad (7)$$

where $$Q = \frac{\gamma P_0 \theta}{\sqrt{2} l_g a_g T_0}$$

The actual physical pressure variation is given by the real part of $\delta P(t)$ and Q specifies the complex envelop of the sinusoidal pressure variation.

Substituting for θ

$$Q = \frac{\beta I_0 \gamma P_0}{2\sqrt{2} k_s l_g a_g T_0 \left(\beta^2 - \sigma_s^2\right)} X$$

$$\left(\frac{(r-1)(b+1)\exp(\sigma_s l) - (r+1)(b-1)\exp(-\sigma_s l) + 2(b-r)\exp(-\beta l)}{(g+1)(b+1)\exp(\sigma_s l) - (g-1)(b-1)\exp(-\sigma_s l)} \right) \quad \ldots\ldots\ldots\ldots (8)$$

Thus, equation (8) can be evaluated for obtaining the amplitude and phase of the acoustic pressure wave produced in the cell by photoacoustic effect. It can be observed that interpretation of the full expression for $\delta P(t)$ is difficult because of the complex expression of Q. Physical insight can be gained easily if certain special cases according to the optical opaqueness of solids are examined. For each category of optical opaqueness, three cases according to the relative magnitude of the thermal diffusion length μ_s, as compared to the physical length l and the optical absorption length μ_β.

Defining $Y = \frac{\gamma P_0 I_0}{2\sqrt{2} l_g T_0}$, $\quad \ldots\ldots\ldots\ldots (9)$

CASE I: Optically Transparent solids ($\mu_\beta > l$)

1. Case Ia : Thermally Thin Solids ($\mu_s >> l$; $\mu_s >> \mu_\beta$)

   We can set $e^{-\beta l} \cong 1-\beta l$, $e^{\pm\sigma l} \cong 1$ and $|r| > 1$ in equation (8) and hence we obtain

$$Q = \frac{(1-i)\beta l}{-2a_g}\left(\frac{\mu_b}{k_b}\right)Y \qquad \ldots\ldots\ldots\ldots (10)$$

Thus the acoustic signal is proportional to βl and varies as f^{-1}. In addition, the thermal properties of the backing material come into play in the expression for Q.

2. Case Ib: Thermally Thin Solids ($\mu s > l$; $\mu s < \mu\beta$)

Here we can set $\exp(-\beta l) \cong 1-\beta l$, $e^{\pm\sigma l} \cong 1 \pm \sigma_s l$ and $|r| < 1$ in equation (8).

Then. $$Q = \frac{(1-j)\beta l}{2a_g}\left(\frac{\mu_b}{k_b}\right)Y \qquad \ldots\ldots\ldots\ldots (11)$$

This equation is identical with equation (10) and hence the acoustic signal behaves in the same fashion.

3. Case Ic: Thermally Thick Solids ($\mu_s > l$; $\mu_s << \mu_\beta$)

In this case we set $\exp(-\beta l) \cong 1-\beta l$, $e^{\pm\sigma l} \cong 0$ and $|r| << 1$ in equation (8)

Now' $$Q = -j\frac{\beta l}{2a_g}\left(\frac{\mu_s}{k_s}\right)Y \qquad \ldots\ldots\ldots\ldots (12)$$

The acoustic signal is now proportional to $\beta\mu_s$ rather than βl. This means that light absorbed within the first thermal diffusion length contributes to the signal, although light is being absorbed throughout the length of the solid. Moreover, μ_s being less than the thickness l, thermal properties of the backing material will not influence the signal. Here the signal varies as $f^{3/2}$.

CASE II: Optically Opaque Solids

1. Case II a: Thermally Thin Solids ($\mu_s >> l$; $\mu_s >> \mu_\beta$)

In equation (8). we set $\exp(-\beta l) \cong 0$, $e^{-\sigma l} \cong 1$ and $|r| >> 1$

Then we obtain $Q = \frac{(1-j)}{2a_g}\left(\frac{\mu_b}{k_b}\right)Y$ . ..... (13)

Here the photoacoustic signal is independent of β. The signal depends on the thermal properties of the backing material and varies as 1/f.

2. Case II b : Thermally Thick Solids ($\mu_s<1$; $\mu_s>\mu_\beta$)

We set $\exp(-\beta l) \cong 0$, $e^{-\sigma l} \cong 0$ and $|r| > 1$ in equation (8)

We obtain $Q = \frac{(1-j)}{2a_g}\left(\frac{\mu_s}{k_s}\right)Y$ . ..... (14)

Though equations (13)& (14) are similar, in the present case there is no contribution from the thermal properties of the backing material.

3. Case II c: Thermally Thick Solids ($\mu_s<<1$; $\mu_s<\mu_\beta$)

We set $\exp(-\beta l) \cong 0$, $e^{-\sigma l} \cong 0$ and $|r| < 1$ in equation (8). Then we obtain

$Q = \frac{-j\beta\mu_s}{2a_g}\left(\frac{\mu_s}{k_s}\right)Y$ ..... (15)

The photoacoustic signal will be proportional to $\beta\mu_s$. The signal is independent of the thermal properties of the backing material and varies as $f^{3/2}$.

The theoretical analysis of the photoacoustic effect applied to different cases discussed above can be suitably applied to the study of any kind of sample.

1.3 PHOTOTHERMAL PROBE BEAM DEFLECTION (PBD) OR MIRAGE EFFECT]

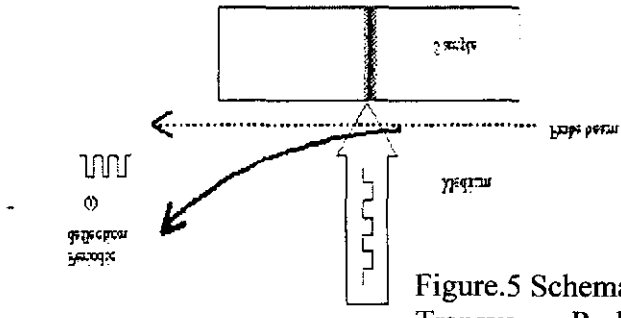

Figure.5 Schematic representation of Transverse Probe beam deflection

In the case of photothermal beam deflection technique, the pump beam or the excitation beam is focussed. Hence, instead of the above 1-D calculation of periodic distribution of temperature, we have to resort to 3D calculations.

The heat diffusion equation in cylindrical geometry[82] is given by

$$\frac{\partial T}{\partial t} = D\left(\frac{\partial^2 T}{\partial r^2} + \frac{1}{r}\frac{\partial T}{\partial r} + \frac{1}{r^2}\frac{\partial^2 T}{\partial \theta^2} + \frac{\partial^2 T}{\partial z^2}\right) \quad \ldots\ldots\ldots\ldots (16)$$

When heat flow takes place in planes through z-axis then the heat diffusion equation becomes

$$\frac{\partial T}{\partial t} = D\left(\frac{\partial^2 T}{\partial r^2} + \frac{1}{r}\frac{\partial T}{\partial r} + \frac{\partial^2 T}{\partial z^2}\right) \quad \ldots\ldots\ldots\ldots (17)$$

The assumption that the homogeneous sample is the absorbing medium and the fluid and the backing are transparent still holds. The heat diffusion equation in three regions can be written as

$$\frac{\partial^2 T_g}{\partial r^2} + \frac{1}{r}\frac{\partial T_g}{\partial r} + \frac{\partial^2 T_g}{\partial z^2} = \frac{1}{D_g}\frac{\partial T_g}{\partial t} \qquad 0 \le z \le l_g \qquad \text{..... (18)}$$

$$\frac{\partial^2 T_s}{\partial r^2} + \frac{1}{r}\frac{\partial T_s}{\partial r} + \frac{\partial^2 T_s}{\partial z^2} = \frac{1}{D_s}\frac{\partial T_s}{\partial t} - A(r,t)\exp(\alpha z)(1+\exp(j\omega t)) \quad -l \le z \le 0 \quad \text{.... (19)}$$

$$\frac{\partial^2 T_b}{\partial r^2} + \frac{1}{r}\frac{\partial T_b}{\partial r} + \frac{\partial^2 T_b}{\partial z^2} = \frac{1}{D_b}\frac{\partial T_b}{\partial t} \qquad -(l+l_b) \le z \le -l \qquad \text{.....(20)}$$

$A(r,t)=\frac{\eta P \alpha}{k_s \pi a^2} e^{\left(\frac{-2r^2}{a^2}\right)}(1+\cos(\omega t))$ is the heat deposited per unit volume where

P is the exciting beam power, α is the optical absorption coefficient, η is the light conversion efficiency, 'a' is the beam radius defined at $1/e^2$ intensity.

The boundary conditions are

$$k_s \frac{\partial T_s}{\partial z}(z=0) = k_g \frac{\partial T_g}{\partial z}(z=0) \qquad \text{.....(21)}$$

$$k_s \frac{\partial T_s}{\partial z}(z=-l) = k_b \frac{\partial T_b}{\partial z}(z=-l) \qquad \text{..... (22)}$$

$$\left.\begin{aligned} &Ts\,(z=-l,\,t)=T_b(z=-l,t) \\ &Ts\,(z=0,t)=T_g(z=0,t) \\ &T_g(z=\infty,t)=T_b(-\infty,t)=0 \qquad \text{with } l_g \sim \infty, l_b \sim \infty \end{aligned}\right\} \qquad \text{..... .(23)}$$

Assume that l_g and l_b are very large compared to the heated area and neglect the backward heat propagation in these two regions.

In order to obtain the periodic steady state temperature, the above differential equations are reduced to simpler partial differential equation by Hankel transformation and Laplace transformation is used to obtain ordinary differential equation from the partial differential equation. Furthermore, the modulated source is replaced by the unit source A® δ (t)

$$-\lambda^2 T_0(\lambda,z,p)+\frac{\partial^2 T_0(\lambda,z,p)}{\partial z^2}=\frac{p}{D_g}T_0(\lambda,z,p) \quad \ldots\ldots\ldots \quad (24)$$

$$-\lambda^2 T_0(\lambda,z,p)+\frac{\partial^2 T_0(\lambda,z,p)}{\partial z^2}=\frac{p}{D_s}T_0(\lambda,z,p)-A_0(\lambda)\exp(\alpha z) \quad \ldots\ldots\ldots(25)$$

$$\frac{\partial^2 T_0(\lambda,z,p)}{\partial z^2}=\frac{p}{D_b}T_0(\lambda,z,p) \quad \ldots\ldots\ldots\ldots\ldots\ldots\ldots\ldots \quad (26)$$

where $= \dfrac{\alpha P \eta}{k_s \pi a^2}\int_0^{\infty} e^{\frac{-2r^2}{a^2}} J_0(\lambda r) r dr$

$$= \frac{\alpha P \eta}{4 k_s \pi} e^{\frac{-\lambda^2 a^2}{8}}$$

1) Assum ing solution of the form to eq (24)

$$T_0(\lambda, z, p) = e^{\sqrt{\lambda^2 + \frac{p}{D}}\, z}$$

The general solution is

$$T_0(\lambda,z,p) = T_s(\lambda,p)e^{-\sqrt{\lambda^2+\frac{p}{D}}z} + B(\lambda,p)e^{\sqrt{\lambda^2+\frac{p}{D}}z}$$

B (λ,p) =0, since the fluid is supposed to be very thick.

Equations (25) and (26) can be solved similarly.

Thus solution to equations (24), (25) and (26) are

$$T_0(\lambda,z,p) = T_s(\lambda,p)e^{-\sqrt{\lambda^2+\frac{p}{D}}z} \qquad \text{.....(27)}$$

$$T_0(\lambda,z,p) = U(\lambda,p)e^{\sqrt{\lambda^2+\frac{p}{D}}z} + V(\lambda,p)e^{-\sqrt{\lambda^2+\frac{p}{D}}z} - \frac{A_0(\lambda)e^{\alpha z}}{\alpha^2-\left(\lambda^2+\frac{p}{D}\right)} \qquad \text{....(28)}$$

$$T_0(\lambda,z,p) = W(\lambda,p)e^{\sqrt{\lambda^2+\frac{p}{D}}z} \qquad \text{.....(29)}$$

After applying the Hankel inversion, to the above three equations the steady periodic state solution obtained is of the form

$$T(r,z,t) = T_0(r,z,p)\Big|_{p=j\omega}\exp(j\omega t) \qquad \text{.....(30)}$$

Thus the expressions for the modulated temperature field in the three regions are

$$T_g(r,z,t) = \int_0^\infty T_s(\lambda)\exp\left(-\beta_g z\right)\exp(j\omega t)J_0(\lambda r)\lambda d\lambda \qquad \text{.....(31)}$$

$$T_b(r,z,t) = \int_0^\infty W(\lambda)\exp\left(\beta_b(z+l)\right)\exp(j\omega t)J_0(\lambda r)\lambda d\lambda \qquad \text{.....(32)}$$

$$T_s(r,z,t) = \int_0^{\infty}\left[U(\lambda)\exp(\beta_s z) + V(\lambda)\exp(-\beta_s z) - E(\lambda)\exp(\alpha z)\right] x \exp(j\omega t) J_0(\lambda r)\lambda d\lambda \quad \ldots (33)$$

where

$$E(\lambda) = \frac{P\eta}{\pi k_s}\frac{\exp\left(\frac{-\lambda^2 a^2}{8}\right)}{\left(-\lambda^2 - j\frac{\omega}{D_s} + \alpha^2\right)} \quad \ldots\ldots\ldots\ldots\ldots\ldots(34)$$

The final temperature distribution is obtained by substituting the following expressions in the above equations.

$$T_s(\lambda) = -E(\lambda) + U(\lambda) + V(\lambda) \quad \ldots\ldots\ldots\ldots\ldots\ldots(35)$$

$$W(\lambda) = -E(\lambda)\exp(-\alpha l) + U(\lambda)\exp(-\beta_s l) + V(\lambda)\exp(\beta_s l) \quad \ldots\ldots\ldots\ldots\ldots\ldots(36)$$

$$U(\lambda) = \left[(1-g)(b-r)\exp(-\alpha l) + (g+r)(1+b)\exp(\beta_s l)\right]\frac{E(\lambda)}{H(\lambda)} \quad \ldots\ldots\ldots\ldots\ldots\ldots(37)$$

$$V(\lambda) = \left[(1+g)(b-r)\exp(-\alpha l) + (g+r)(1-b)\exp(-\beta_s l)\right]\frac{E(\lambda)}{H(\lambda)} \quad \ldots\ldots\ldots\ldots\ldots\ldots(38)$$

and

$$H(\lambda) = (1+g)(1+b)\exp(\beta_s l) - (1-g)(1-b)\exp(-\beta_s l) \quad \ldots$$

$\ldots\ldots\ldots\ldots(39)$

with $g = \frac{k_g \beta_g}{k_s \beta_s}$ $\quad b = \frac{k_b \beta_b}{k_s \beta_s}$ $\quad r = \frac{\alpha}{\beta_s}$

$$\overline{T_s(\lambda)} = \frac{P\eta}{4k_s\pi}\frac{r}{\beta_s}\frac{e^{-\lambda^2\omega^2/8}}{r^2-1}\left[\frac{2(b-r)e^{-\alpha l}+(1+b)(r-1)e^{\beta_s l}+(1-b)(r+1)e^{-\beta_s l}}{(1+g)(1+b)e^{\beta_s l}-(1-g)(1-b)e^{-\beta_s l}}\right] \quad \ldots(40)$$

The surface temperature can be written as

$$T_s(0,t) = \int_0^{\infty} \overline{T_s(\lambda)} J_0(\lambda r)\lambda d\lambda \exp(j\omega t) \quad \ldots\ldots\ldots\ldots (41)$$

The geometry for the mirage deflection is as shown in figure 5. The propagation of the beam through the spatially varying index of refraction is given by

$$\frac{d}{ds}\left(n\ \frac{dr_0}{ds}\right) = \nabla_{\perp} n(r,t) \quad \ldots\ldots\ldots\ldots(42)$$

where r_0 is the perpendicular displacement of the beam from its original direction, n is the uniform index of refraction and $\nabla_{\perp}n(r,t)$ is the gradient of the index of refraction perpendicular to S(the ray path). This relation can be integrated over the ray path S

$$\frac{dr_0}{ds} = \frac{1}{n}\int_{path} \nabla_{\perp} n(r,t)ds \quad \ldots\ldots\ldots\ldots(43)$$

Since the deviation is small, one can get the expression of the deflection

$$= \frac{1}{n}\frac{\partial n}{\partial T}\int_{-\infty}^{+\infty} \nabla T_g \times ds$$

$$\theta(t) \quad \theta = \frac{dr_0}{ds} = \frac{1}{n}\frac{\partial n}{\partial T}\int \nabla_{\perp} T(r,t)ds \quad \ldots\ldots\ldots\ldots(44)$$

In our case, the probe beam is propagating through the fluid along the x-direction. Hence, the probe deflects with components in x-y plane and z-x plane so that after calculating the vector product in the integrand of the above

expression, we get the transverse (θ_t) and the normal (θ_n) components of the deflection, respectively.

$$\theta_n = -\frac{1}{n}\frac{dn}{dT}\int_{-\infty}^{+}\frac{\partial T_g}{\partial z}dx\,\hat{j} \qquad \text{.....(45)}$$

$$\theta\theta_t = \frac{1}{n}\frac{dn}{dT}\int_{-\infty}^{+\infty}\sin\alpha\alpha\frac{\partial T_g}{\partial r}dx\,\hat{k} \qquad \text{.....(46)}$$

θ_n and θ_t are the deflections normal and parallel to the sample surface.

Using the standard result

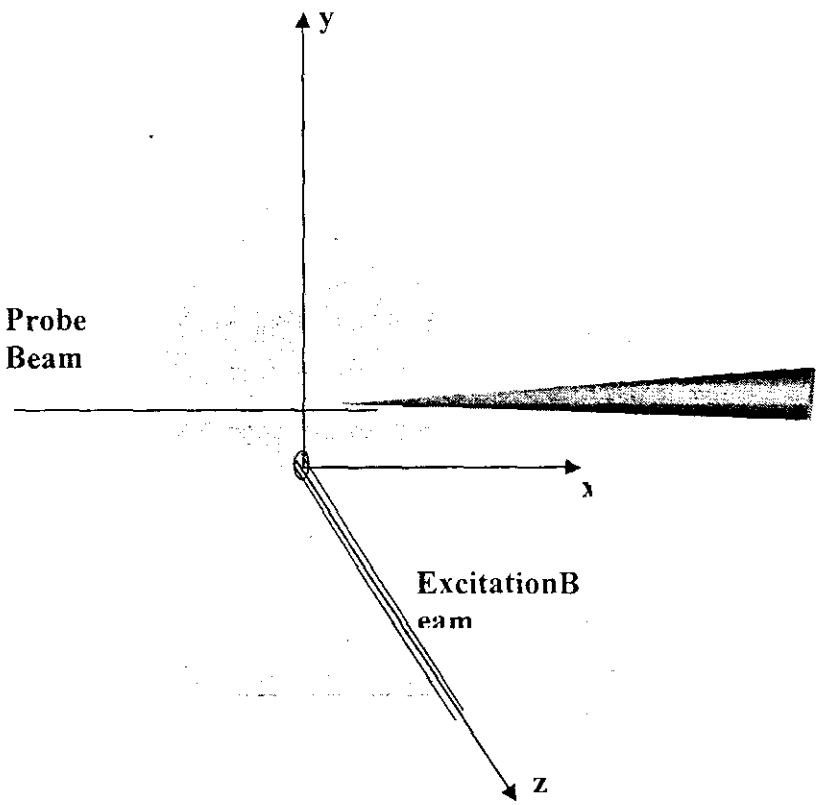

Figure 5: Geometry for 'mirage' deflection. The probe beam is along x direction and excitation beam or pump beam is along z direction.

$$\int_{-\infty}^{\infty} T_s(x)dx = 2\int_{0}^{\infty} \overline{T_s}(\lambda)\cos(\lambda y)d\lambda \qquad \text{.....(47)}$$

Hence substituting for the integral in eq (34)

$$\theta_n = \frac{2}{n}\frac{dn}{dT}\exp(j\omega t)\int_{0}^{\infty} \overline{T_s(\lambda)}\beta_g \exp(-\beta_g z)\cos(\lambda y)d\lambda\hat{j} \qquad \text{.....} \quad (48)$$

Similar treatment of the integral in eq (35) results in

$$\theta_t = \frac{2}{n}\frac{dn}{dT}e^{jwt}\int_{0}^{\infty} \overline{T_s(\lambda)}\lambda \exp(-\beta_g z)\sin(\lambda y)d\lambda\hat{k} \qquad \text{.....(49)}$$

Substituting the value of $T_s(\lambda)$ from eq. (30) in the above equation the general expression for θ_t and θ_n can be obtained. θ_n is related to the heat diffusion process perpendicular to the surface whereas θ_t represents the heat diffusion process parallel to the sample surface.

Depending upon the optical absorption co-efficient, sample can be divided into optically opaque and optically transparent. According to the thermal properties, each are subdivided into thermally thick and thermally thin. Equation (30) will be modified accordingly for each of these special cases [42]. The basic assumption is that the thermal diffusivity of the sample is greater than that of fluid as well as backing i.e. $b = g \sim 0$

Case I: Optically Opaque ($\alpha l >> 1$)

In these materials, the optical absorption length is much smaller than the sample thickness. $\qquad \frac{r}{1+r} = \frac{\alpha}{\beta_s + \alpha} \approx 1$

$$\frac{r}{1-r} = \frac{\alpha}{\beta_s - \alpha} \approx -1$$

Then the expression for the tangential component of deflection

$$\theta_t = -\frac{1}{n}\frac{dn}{dT}\frac{P}{2k_s\pi} e^{j\omega t} \int_0^\infty \lambda \sin(\lambda y) e^{-\beta_g z} e^{-\lambda^2 a^2/4} \frac{1}{\beta_s} \left[\frac{1+e^{-2\beta_s l}}{1-e^{-2\beta_s l}}\right] d\lambda \hat{k}$$

.....(50)

and that of normal component is given by

$$\theta_n = \frac{1}{n}\frac{dn}{dT}\frac{P}{2\pi k_s} \exp(j\omega t) \int_0^\infty \beta_g \cos(\lambda y) \exp\left(\frac{-\lambda^2 a^2}{4}\right) \frac{1}{\beta_s}\left(\frac{1+\exp(-2\beta_s l)}{1-\exp(-2\beta_s l)}\right) \exp(-\beta_z z) d\lambda \hat{j}$$

.....(51)

For thermally thick solids, l>μ. Hence $\exp(-\beta_s l) \sim 0$ and the integrands are further reduced. For thermally thin solids, l<μ. And the equations are suitably modified.

Case II Optically Transparent solids (αl <<1)

$\frac{r}{1+r} \approx \frac{r}{1-r} \approx \frac{\alpha}{\beta_s}$ Now the tangential component and normal components are given by (52)

$$\theta_t = -\frac{1}{n}\frac{dn}{dT}\frac{P}{2\pi k_s} \exp(j\omega t) \int_0^\infty \lambda \mathrm{Sin}(\lambda y) e^{\frac{-\lambda^2 a^2}{4}} \frac{\alpha}{\beta_s^2} e^{-\beta_g z} d\lambda \hat{k} \quad .....(52)$$

$$\theta_n = -\frac{1}{n}\frac{dn}{dT}\frac{P}{2\pi k_s} \exp(j\omega t) \int_0^\infty \beta_g \cos(\lambda y) \exp\left(\frac{-\lambda^2 a^2}{4}\right) \frac{\alpha}{\beta_s^2} \exp(-\beta_g z) d\lambda \hat{j} \quad ....(53)$$

According to their thermal properties for thermally thick solids, $l > \mu$. Hence $\exp(-\beta_s l) \sim 0$ and the integrands are further reduced. For thermally thin solids, $l < \mu$, and the equations are suitably modified.

In conclusion,this opening chapter gives an account of various photothermal techniques that can be suitably applied to various materials for the optical as well as thermal characterisation non-destructively. A review on the applicability of these techniques ,namely PA and PTD technique,on the class of materials under investigation is also presented.

References

1 P.E.Nordal Jeffrey A.Sell, Photothermal Investigations of Solids and Liquids, Academic Press Inc, New York(1988)

2. Stephen E.Bialkowski, Photothermal Spectroscopy Methods for Chemical Analysis, John Wiley &Sons, Newyork.1996.

3. Yu. G. Gurevich, G. Gonzalez de la Cruz, G. Logvinov and M.N. Kasyanchuk, Semiconductors, 32 (11), 1179 (1998).

4. A. Mandelis Physics Today, August,29-34 (2000).

5 . George Biranbaum and Bert A Auld (Ed.) Sensing for materials Characterisation, processing and manufacturing,(TheAmerican Society for Nondestructive Testing, Inc., Columbus) 1998

6. A. Mandelis (Edit.)Principles and Perspectives of Photothermal and Photoacoustic Phenomena (Elsvier, Oxford) 1992.

7 .H. Vargas and L.C.M. Miranda, phys. Rep. 161(2), 43-101 (1988).

8 D.Fournier, A.c. Boccara, A, Skumanich and N.M. Amer, J. Appl. Phys. 59 (3), 787 (1986).

9 I A. Vitkin, C. Christofields and A. Mandelis, Appl. Phys. Lett., 54, 2392 (1989)

10 Madelis and M.M. Zver, J. Appl. Phys., 57, 4421 (1985).11

11 H.Coufal, Appl. Phys. Lettt., 45, 516 (1984)

12 A. Mandelis, Nondesturctive Evaluation (PTR Prentice Hall, Englewood Cliffs New Jersy) 1994.

13. R.L. Thomas, Anal. Sciences, 17, April, (2001).

14. H. Shinoda, T. Nakajima, K. Ueno and N. Koshida, Nature, 400, August (1999).

15 .H. Vargas and L.C.M. Miranda, Review of Scientific Instruments, 74 (1), 794, (2003).

16 P. Helander, J. Phtooacoust 1, 103 (1982).

17 Achamma Kurian, K.P. Unnikrishnan, Sajan. D. George, Pramod Gopinath, V.P. N. Nampoori and C.P. G. Vallabhan Spec trochimica Acta Part A, 59, 487 –491 (2003).

18 . P.R. Bajra, Revista Phsyicae, I, 1 (2000)

19. 3J.C. Krapez, J. of Appl. Phys. 87 (9), 2003).

20. J.R.D. Pereira, A.M. Mansanares, E.C. de Silva, J. Palangana, m.L. Bi
Molecular Crystals and Liquid Crystals, 332, 569 (1999).

21. Scudieri and M. Bertolotti, Proce. 10th Conference of Phtooacoustic and Photothermal Phenomena (AIP,New York) 1999.

22. A Fukuyama, Y. Akashi, K. Yoshino. K. Madea and T.Ikari, Phys. Rev. B, 58 (19), (1998).

23. J.A. Balderas Lopez, A. Mandelis and J.A. Gracia, J. Appl. Phys., 92 (6), (2002).

24. W.Y. Zhou, S.S. Xie, S.F. Qian, G. Wang, L.X. Qian, D.S. Tang and Z. Q. Liu, J. of Phys. Chem. Of Solids 61 (7) 1165 (2000).

25 B.X. Shi, C.W. Ong. And K.L. Tam, Journal of Material Science 34 (210 5169 (1999).

26 Q.E. Khuen, W. Faubel, H.J. Ache Journal de Physique 4 (C7), 361 (1994).

27 M. Bertolotti, G.L. Liakhou, A. Ferrari, V. Ralchenko, A.A. Smolin E. Obraztova, Korotoushenko, S.M. Pimenov and V.I. Konov J. of Appl. Phys 75 (12) 7795 (1994).

28 Sajan D. George, C.P. G. Vallabhan, M. Heck, P. Radhakrishnan, and V.P. N. Nam Journal of Nondestructive Testing and Evaluation Vol. 1,2,75, (2002).

29 R. CastroRodriguez, M. Zapata-Torres, V. Rejon Moo, P. Bartolo-Perez and J.L. Pe Phys. D: Appl. Phys., 32, 1194 (1999).

30 .N.F. Leite and L.C.M. Miranda, Rev. Sci. Instru. 63 4398 (1992).

31 .P. Charpentier, F. Lepoutre and L. Bertrand, J. Appl. Phys. 53, 608 (1982).

32 X. Quelin, B. Perrin, G. Louis and P. Peretti, Phys. Rev. B, 48, 3677 (1993).

33 .JA Balderas – Lopez and A. Mandelis, J. Appl Phys. 88 (11) 6815 (2000).

34. B.C. Li, R. Gupta, J. Appl Phys 89 (2) 859 (2001).

35. Bertolotti, A. Falabella, R. Li Voti, S. Paoloni, C. Sibilia, G.L. Liakhou, High Temp – High Pressures 31 (2) 235 (1999).

36. Sajan D. George, P. Radhakrishnan, V.P.N. Nampoori and C.P.G. Vallabhan, J. of P Appl. Phys. 36(8), 990 (2003).

37 .Z. Bozoki, J. Sneider A. Mikols, Acoustica 82 (1) 118 (1996).

38 .Achamma Kurian, K.P. Unnikrishnan, Sajan D George, Pramod Gopinath, V.P.N. Nampoori and C.P.G. Vallabhan.Spectrochimica Acta Part A. 59, 487 – 491 (2003).

39 .Ristovski Z D and M.D Dramicanin, Appl. Opt. 36(3) 648 (1997).

40 .A. Fukuyama, T. Ikari, K. Miyazaki, K. Maeda and K. Futagami, Jpn. J. Appl. Phys. Suppl. 31, 20 (1992).

41 .A. Fukuyama, T. Ikari, K. Maeda and K. Futagami, Jpn. J. Appl. Phys. Part 1, 32, 2567 (1993).

42 .S.E. Bialkowski Photothermal Spectroscopy Methods for Chemical Analysis (John Wiley and Sons, New York), 1996.

43 .G.H. Brilmyer, A.Fujishima, K.S.V. Santhanam, A. J.Bard, Anal.Chem.49, (1977) 2057

44 .M.Bass, L.Liou, J.appl.Phys56 (1984)184

45 .Christofies, A. Mandelis, A. Engel, M. Bisson and G. Harling, Can. J. Phys 69, 317 (1991).

46 . A. Mandelis, J. Vanniasinkam, S. Budhudhu, A. Orthonos and Kokta M, Phys. Rev. B, 48, 6808 (1993).

47 .J. Shen and A. Mandelis, Rev. Sci. Instrum., 66, 4999 (1995).

48 .D. Bicanic, M. Chirtoc, V. Tosa and P. Torfs, Ber Bunsenges, Phys. Chem. 95, 766 (1991).

49 J..R.D. Pereira, E.C. da Silva, A.M. Manasanares. and L.C.M. Miranda, Anal. Sci., 17, April S 172 (2001).

50 . Jacob Philip, Ravindran Rajesh and Preethy C Menon, Anal. Sci., 17, April (2001).

51 P.E.Nordal and S.O. Kanstad ,Pysica Scripta 20,59 (1979).

52 .S.O.Kanstad and P.E.Nordal, Can.Phy 64, 1155 P.E.(1986).

53 53A.Rosencwaig, Photoacoustics and Photoacoustic spectroscopy, Wiley, NewYork (1980).

54 .A.Rosencwaig, J.B.Willis, J.Appl.Phys. 51(8), (1980) 4361

55 .David A.Hutchins, Andrew C.Tam, IEEE Transactions on Ultrasonics, Ferroelectrics and Frequency Control, Vol.UFFC-33 (5) (1986) 429

56 R.C.Leite, R.S.Moore, J.R.Whinnery, Appl.Phys.Lett5, (1964) 141

57 R.L.Swofford, M.E.Long, A.C.Albrecht, J.Chem.Phys65 (1976)179 .

58 Howard L.Fang, Robert L.Swofford, J.Appl.Phys50(11) (1979) 6609.

59 A.C.Boccara, D.Fournier, J.Badoz, Appl.Phys.Lett36, (1979)130.

60 J.C.Murphy, L.C.Aamodt, J.Appl.Phys 51(9) (1980) 4580 .

61 L.C.Aamodt, J.C.Murphy, J.Appl.Phys. 52(8) (1981)4903.

62 J.C.Murphy, L.C.Aamodt, Appl.Phys.Lett 39(7) (1981) 519.

63 .A.C.Boccara, D.Fournier, W.Jackson, D.Fournier, Opt. Lett 5(9) (1980) 377.

64 .N.J.Dovichi, T.G.Nolan, W.A.Weimer, Anal.Chem. 56 (1984) 1700 .

65 J.F.Power, M.A.Schweitzer, Opt.Eng.36(2), (1997) 521.

66 S.E.Bialkowski, A. Chartier, Appl.Opt.36(27), (1997) 6711

67 M.A.Olmstead, N.M.Amer, Phy.Rev.Lett, 52, (1984) 1148 .

68 J.-C. Cheng and S.-Y. Zhang, J. Appl. Phys. 70, (1991) 7007 .

69 G.L.Bennis, R.Vyas, R.Gupta, S.Ang, W.D.Brown, J.Appl.Phys.84 (1998) 3602.

70 .P.E.Nordal, S.O.Kanstad, Phy.Scr.20, (1979) 659

71 A.Rosenwaig, J.Opsal, W.L.Smith, D.L.Willenborg, Appl.Phys.Lett. 46, (1985) 1013 .

72 A.Rosenwaig, J.Opsal, W.L.Smith, D.L.Willenborg,, J.Appl.Phys. 59 (1986)1392

73 W.Zapka, A.C.Tam, Opt.Lett. 7, (1982) 86.

74 C.J.Dasch, J.A.Sell, Opt.Lett. 11, (1986) 603.

75 W.A.Weimer, N.J.Dovichi, Appl.Opt. 24, (1985) 2981.

76 P.Hess, Photoacoustic, Photothermal and Photochemical processes in gases, Springer- Verlag, New York (1989).

77 P.Hess, Photoacoustic, Photothermal and Photochemical processes at surfaces and Thin films, Springer-Verlag, New York (1989).

78 .H.B.Lin, A.J.Campillo, Appl.Opt.24, (1985) 222, .

79 D.Fournier, A.C.Boccara, A.Skumanich, N.Amer, J.Appl.Phys.59, (1986) 787.

80 Nibu A.George, C.P.G.Vallabhan, V.P.N Nampoori, A.K.George, P.RadhakrishnanD:Appl.Phys.33 (2000) 3228 .

81 N.Mikoshiba, H.Nakamura, K.Tsubouchi, Proceedings of the IEEE ultrasonic symposium , Diego, San Diego, CA (1982).

82 H.S. Carslaw and J.C. Jaeger, Conduction of heat in solids, Oxford, Clarendon (1959)

CHAPTER II

ANALYSIS OF PHOTOTHERMAL DEFELECTION SIGNAL FOR DETERMINING THERMAL DIFFUSIVITY OF CERTAIN ORGANIC MOLECULES

2.1 EXPERIMENTAL CONFIGURATIONS

Photothermal deflection technique is one of the Photothermal techniques [1] employed for the thermal and optical characterization of a material by analyzing the effects of temperature distribution caused by absorption of an intensity modulated light beam(usually laser beam).In the Photothermal deflection technique,the modulated refractive index gradient produced as a result of the modulated temperature gradient is probed.This technique uses two laser beams, one for heating the sample (pump) and the other to detect the produced refractive index gradient (probe). The pump and probe beams can be aligned with respect to each other in two configurations. Transverse PBD: In this case, the pump and probe beams are perpendicular to each other. Collinear PBD: Here the pump and probe beams are parallel to each other. Moreover, the probe beam can be directed to the sample surface in two ways [2,3,4] 1) Skimming configuration: In this configuration, the probe beam just grazes the sample surface. This implies that the probe beam travels at a certain height above the sample surface, which is determined by the size

of the probe beam. The main problems that can occur in the skimming configuration is thus related to the size of the probe beam.

Though the probe beam is focused tightly it has a definite size and it passes through the coupling medium which could influence the photothermal deflection signal,unless it is very small compared to the sample.2) Bouncing configuration or surface reflection scheme: The probe beam impinges on the sample surface at a certain angle and the deflection of the reflected beam is noted. Hence, the height of the probe beam above the sample surface is zero. In the bouncing configuration, the probe beam deflection is obtained as a result of two different mechanisms, the thermal gradient in the areas near to the heated sample (mirage) and the sample deformation due to thermal expansion. The bouncing scheme however cannot be applied to samples with no relevant probe reflection i.e. absorbing, rough or non-reflecting samples. This problem can be overcome by covering the surface with a thin reflecting layer.the use of this layer can cause the pump beam reflection too.Hence it is betterto apply bouncing configurations to samples which are reflecting and which has very low thermal expansion coefficient.The effects introduced in both the configurations by the finite size of the heating beam, finite height of the probe beam above the sample surface, the secondary effects like finite size of the probe beam, sample temperature, optical misalignment, diffusivity of the deflecting medium are discussed in detail by Salazar et a l [2]

There are two methods for making the optical beam deflection measurements [5].

Method 1:-The Standard Method:

The separation between the pump and probe beams (transverse offset 'y') is fixed (usually y=0 when the two beams intersect). The signal amplitude and phase are measured as some physical or operational parameter of the system is changed. Thus when an infinitesimal probe beam skims the sample surface and when there is no heat diffusion in the gas, this method measures the normalized surface temperature τ along a line passing through the excitation beam axis. Although theoretically, this temperature is integrated along a line infinite in extent, it is effectively determined only by the temperature in the region of the sample significantly heated by the absorbed light. Thus as the pump and probe beams are moved across the sample surface, the localized area contributes effectively to the OBD signal changes, whereby the optical and thermal properties of the sample can be measured as a function of the beam position.

Method 2:The Transverse Scan Method:

Here the pump beam is fixed to a particular position on to the sample surface. The probe beam is then scanned across the sample surface perpendicular to the pump beam. Hence, the separation between the pump and the probe beams (transverse offset 'y') is a variable. Thus, the normal and tangential beam deflection profiles are measured about the center position of the exciting laser beam.

In all the above mentioned methods and configurations of the probe beam deflection, one condition is strict which is regarding the size of the probe beam. This is so because the basic equations dealing with the normal and

tangential component of the deflection requires that the size of the probe beam must be small compared to the gas thermal diffusion length. Large probe beams can be treated as a bundle of infinitesimal light filament each satisfying these basic equations and hence each of them will be deflected differently and the finite probe beam will have no well-defined deflection. In addition, the beam spreads and its cross sectional shape will be distorted. Thus in short if the ratio of the probe beam radius R_p to the thermal diffusion length (μ_g) of the deflecting medium 'g', R_p/μ_g is small enough, then the different parts or rays of the probe beam are submitted to approximately the same thermal gradients and they undergo almost the same deflection. On the contrary when this ratio is large enough, then each individual ray of the beam is deflected in a particular direction with given amplitude and phase. Under high excitation power, it was proved that there was deformation in the probe beam shape due to constant heat gradient [6]. In the collinear configuration, the effect of absorption of the probe beam must be taken into account. An absorption change is always present when there is an increase in thermal refractive index induced by the pump beam, which is of the same order as that of magnitude of the refractive index change.

It has been theoretically analysed by Bertolotti etal [7] to extract the expression for the deflection signal eliminating the probe beam absorption effects from the experimental data.

2.2 ANALYSIS OF EXPERIMENTAL DATA

PTD experiment consists of a pump source for excitation of the sample, which is modulated using a chopper and a probe source to probe the refractive

index gradient. The deflection of the probe beam is detected using a position sensitive detector. The vectorial nature of the deflection implies that the magnitude has two spatial components. The components are referred to as the normal component φ_n and tangential component φ_t [1,8]. Different methods are developed by many workers to analyze the amplitude and phase data for determination of thermal diffusivity. Some of the important methods of analysis are given below.

a) Zero crossing technique:

The theory of the technique has been developed by Kuo et al[9,10]. In this technique, the transverse scan method is used and amplitude of the tangential component of the deflection signal (A_t) is measured using the lock-in-amplifier. A graph is plotted between A_t and the transverse offset 'y' as shown in figure. The antisymmetric plot is explained on the fact that the probe beam deflection switches from left to right as one passes from one side of the heated region to the other. The two points at which the plot of real part of A_t just goes to zero on either side of the central zero corresponds to points that are shifted in phase by $\pm \pi/2$ relative to the central position. It is to be noted that these points do not correspond to quarter wavelength distance on each side of the center. However, this is not so for two reasons.

1) The effect of finite heating beam size is such as to effectively add a constant to this distance.
2) Cylindrical waves are not exactly periodic and first zero do not occur precisely at $\pm\pi/2$ radians from the origin. It was later proved that the distance x_0 between two ninety degree phase points on either side of the origin is given by

$x_0 = d + \sqrt{\gamma}\,\lambda/2 = d + \sqrt{\gamma\pi\frac{\alpha}{f}}$, where γ is a parameter which depends on the kind of material, 'd' is the distance on the order of the heating beam diameter and 'f' is the modulation frequency.

γ=1.4 when the sample is optically opaque and thermally thick.

γ=1, for optically opaque thermally thin solids and optically transparent ones.

Thus, a plot of x_0 vs $1/f^{1/2}$ gives a straight line with a slope $\sqrt{1.4\pi\alpha}$, where α is the thermal diffusivity of the sample.

Though this method of determination is direct and simple, it cannot be applied to materials whose thermal diffusivity is lower than that of the surrounding fluid medium. If the thermal diffusivity of the fluid is higher than that of the sample, then the mirage signal will be dominated by the thermal properties of the fluid. Thus, when the thermal diffusivity of the specimen is much lower than that of the surrounding fluid, the applicability of the zero crossing method becomes complicated as either no zero-crossing exists or the signal level at the zero-crossing point is so small that noise makes its accurate determination impossible.

b) Multiparameter fitting [11,12]:

This method has been suggested as a new method to determine the anisotropic thermal diffusivities parallel to the surface of a solid sample. Moreover, this method can be employed for the determination of low thermal diffusivity. The thermal diffusivity of specimen has to be calculated from entire mirage measurement data, which contains information on the thermal properties of both the specimen and gas, the size of both heating beam and probe beams and their alignment as well as the modulation frequency of heating. Initially a possible data analysis method for this kind of problem is

the multiparameter least square regression fitting developed by Anthony et al [13]. It was applied for the determination of thermal diffusivity of diamonds. Later this method was extended by Rantala et al [12] for determination of low thermal diffusivity of materials like polymers, ceramics etc. The severe thermal expansion of polymer samples, which causes difficulties in the case of optical measurement, has been taken into account. The sensitivity of the multiparameter to the sample diffusivity is studied by calculating the variance of the fitting when the sample thermal diffusivity is held as fixed. Other variables whose values are unknown are fitted. For example the height of the probe beam, thermal diffusivity of the coating and the phase shift and the amplitude of the signal. However, the thickness of the sample affects the accuracy of measurement. The method is reliable only for samples with thickness exceeding 100 μm. When applied to a polyvinyl film of thickness 50 μm, the thermal diffusivity obtained was double that of expected value.

c) Thermal wave coupling method [14,15]:

Photothermal measurements on thin films are not easy. While dealing with thin films, it is to be noted that they are always coated on to a substrate. If the film is very thin then a significant portion of the pump power will be absorbed by the substrate. Thus the true sample is a film-substrate composite. Wong et al derived explicit expressions for the thermal diffusivity for film substrate composites by including contributions from the thin film as well as the substrate to the temperature field at the probe beam position. This method requires the measurement of the phase of deflection at two positions (y_0) over a range of pumping frequency from which the thermal diffusivity of the film can be found out. From the regression line of the phase - $f^{1/2}$ plot, the thermal diffusivity of the substrate can be determined. The measurements are made

with probe beam well beyond the pump spot so that the influence of the pump beam profile is negligible and also the frequency range used is very high. Hence, measurable signal results only if the sample is a highly absorbing one.

d) Phase Method [16,17]:

This method utilizes the phase of the tangential component of deflection signal (φ_t).

Theoretically,

$$\varphi_t = \varphi_0 \exp\left[-j\left(y/l_t + \phi\right) - j\omega t\right] \qquad (1)$$

This implies that the phase varies linearly with the pump-probe offset 'y'. l_t is the characteristic length , which is the distance corresponding to one radian phase shift.

From the slope of plot of phase vs. 'y', s, thermal diffusivity of the sample can be determined using the relation

$$D = \frac{\pi f}{s^2} \qquad (2)$$

This direct determination is possible only if the thermal diffusivity of the sample is greater than that of the coupling medium. On the contrary, if the thermal diffusivity of the sample is lower than that of the coupling medium, modified phase method must be applied. In such a case, slope 's' is determined

for various modulation frequencies 'f' and a graph is plotted between $1/s$ and $1/\sqrt{f}$. The slope of this straight line graph, s', gives the thermal diffusivity using the relation

$$D = \pi s'^2 \qquad (3)$$

e) Amplitude Method:

The method developed by Quelin et al took into account the linear variation of logarithm of amplitude of the tangential component of the deflection signal with the pump-probe offset. The three-dimensional thermal conductivity tensor of a polymer crystal is determined in the front configuration where the pump and probe runs on the same side of the sample [18]. This is similar to the Phase method and the thermal diffusivity is obtained from the relation $D = \pi f / s'^2$ where s' is the slope of graph between ln $[A_t]$ and 'y'. Further they observed that only a numerical simulation led to the thermal conductivity co-efficient perpendicular to the sample surface. Hence in order to determine the thermal conductivity coefficient in the normal direction, they used amplitude of normal component of deflection in the rear configuration, which means that the pump and probe are running on either side of the sample [19].

2.3 Laser based measurement of Thermal diffusivity of liquids by Probe Beam Deflection method :

The spacial variation of a heated material's refractive index, of that of a gas or fluid in contact with it will deflect a laser beam.This deflection can be monitored and used as a means of detecting thermal waves generated in a sample Probe beam deflections as explained in chapter11 can be monitored

by a bi-cell photodetector.Hence photothermal refractive index modulation provides highly sensitive,localized and non contact detection techniques.Thermoptical properties of liquids ,such as thermal conductivity and thermal diffusivity, are fundamental parameters in heat transfer and thermal processing.[20-21] A variety of techniques have been developed to measure thermal conductivity and thermal diffusivity .Flippov in 1968 discusses not less than nine experimental investigations developed in the 1950'sand 1960's in his review paper on liquid thermal conductivity. A typical conventional technique,the hot wire method has been employed by many researchers like Nagasakaand Nagashima in1981.[22-24]

The accurate measurements of thermal diffusivity and thermal conductivity for liquids is vital not only for practical engineering ,but also for theoretical studies and analysis. Photothermal refraction is a part of a family of thermooptical techniques for absorbance measurements . In Photothermal refraction ,a modulated pump beam illuminates the sample .Absorption of the pump laser beam results in the formation of a cylindrically symmetric temperature rise within the sample. A coplanar CW probe laser beam intersects the pump laser beam at right angles. The heated sample acts as a cylindrical lens to defocus the probe beam along the axis perpendicular to the to the plane containing the two laser beams.The effect of the heated sample upon the probe beam is measured as a change in far-field probe beam center intensity and is detected in phase with the pump laser modulation function. Since the refraction signal is generated only at the intersection region of the twolaser beams ,a measure of sample absorbance may be made with high spatial resolution.[20-21]

In photothermal refraction techniques , an optical element is formed within the sample from a temperature rise generated by absorption of

a pump laser beam.This optical element perturbs the propagation properties of either the pump beam or a second probe laser beam. Thermooptical elements include a change of optical path length in interferometric techniques a lens in Thermal lens,a prism in photothermal deflection ,and a grating in thermal diffractionand we add a cylindrical lens in photothermal refraction. Photothermal refraction is experimentally related to photothermal deflection.

REFERENCES:

1. Jeffrey A.Sell, Photothermal Investigations of Solids and Liquids, Academic Press Inc, New York (1988)
2. A.Salazar, A.Sanchez-Lavega, J.Fernandez, *J.Appl.Phys.* **69**(3), (1991)1216
3. M.Bertolotti, G.L.Liakhou,R.Li Voti, S.Paoloni, C.Sibilia, *J.Appl.Phys.* **83** (2) (1998) 966.
4. M.Bertolotti, G.L.Liakhou, R.Li Voti, S.Paoloni, C.Sibilia, *Appl.Phys B* **67** (1998) 641
5. L.C.Aamodt, J.C.Murphy, *J.Appl.Phys.* **52**(8) (1981) 4903
6. E.Legal Lasalle, F.Lepoutre, J.P.Roger, J.Appl.Phys. **64** (1) (1988)1
7. Norman J Dovichi,Thomas G.Nolan and Wayne A Weimer (Anal.Chem 1984 ,56 1700-1704)have
8. M.Bertolotti, L.Fabbri, E.Fazio, R.Li Voti, C.Sibilia, G.Leakhou, A.Ferrari, **69**(6) (1991) 3421
9. J.C.Murphy, L.C.Aamodt, *Appl.Phys.Lett*, **39**(7) (1981) 519
10. P.K.Kuo, M.J.Lin, C.B.Reyes, L.D.Favro, R.L.Thomas, D.S.Kim, Shu-yi Zhang, L.J.Inglehart, D.Fournier, A.C.Boccara, N.Yacoubi, Can.J.Phys. 64 (1986)1165
11. P.K.Kuo, E.D.Sendler, L.D.Favro, R.L.Thomas, Can.J.Phys. 64 (1986)1168
12. J.Rantala, J.Jaarinen, P.K.Kuo, Appl.Phys. A. 55(1992) 586
13. J.Ranatala, Lanhua Wei, P.K.Kuo, J.Jaarinen, M.Luukkala, R.L.Thomas, J.Appl.Phys. 73 (6) (1993) 2714
14. T.R.Anthony,W.F. Benholzer, J.F.Fleischer, lanhua Wei, P.K.Kuo, R.L.Thomas,R.W.Pryor Phy.Rev.B. 42, (1990) 1104
15. P.K.Wong, P.C.W.Fung, H.L.Tam, J.Gao, Phys.Rev.B 51(1) (1995) 523
16. P.K.Wong, P.C.W.Fung, H.L.Tam, J.Appl.Phys 84(12) (1998) 6623
17. M.Bertolotti, R.Li Voti, G.Liakhou, C.Sibilia, Rev.Sci.Instrum 64(6) (1993)1576

18. M.Bertolotti, R.Li Voti, G.Liakhou, C.Sibilia, Rev.Sci.instrum 66 (1) (1995) 277

19. X.Quelin,B.Perrin, G.Louis, P.Peretti, Phys.revB 48 (6) (1993) 3677

20 Norman.Dovichi,ThomasG.Nolan,andWayne.aWeimer Anal.chem,56, (1984), 1700.

21J.Sun,J.P.Longtin and T.F.Irvine,Jr Proceedings of the 33rd National Heat Transfer Conference Aug 15-17,1999,Albuqerque,New Mexico

22 Y.Nagasaka and A. Nagashima J.Phys E : Sci.Instrum.,Vol.14.1981.Printed in Great Britain.

23 Y.Nagasaka and A. Nagashima.Review of Scietific instruments Vol 52 , No 2 ,February 1981. PP 2-

24 .Nagasaka and A. Nagashima.Review of Scietific instruments Vol 56 No.9, September 1985. PP 2-

CHAPTER III

PREPARATION AND OPTICAL CHARACTERIZATION OF CERTAIN R.F. PLASMA POLYMERIZED THIN FILMS

3.1 INTRODUCTION

The Plasma polymerized materials gained recognition since they are significantly different from conventional polymers. Initially they were an insoluable deposit which were very difficult in cleaning.In modern technology of thin films this undesiarable deposit has extremely important characteristics like excellent adhesion to substrate materials and strong resistance to most chemicals.

Electric discharge, controlled nuclear reactions, shocks and other means generate plasma in laboratories.. Since plasma loses energy to its surroundings mainly by radiation and conduction to the walls in order to maintain plasma state continuously in a laboratory apparatus, energy must be supplied as fast as it is lost. In order to maintain plasma state for a relatively long period of time, the most obvious and most common method is the use of electric discharge. Most experimental work in the study of polymerization is carried out using some kind of electric discharge. There are many types of electric discharges, all characterized by the presence of free electrons and or an electric field. Among the many types of electric discharge, all are characterized by the presence of free electrons and or an electric field. Among these, glow discharge is by far the most frequently used in plasma polymerization.

Plasma polymerization refers to formation of polymeric materials under the influence of plasma (partially ionized gas), which is generated by some kind of

electric discharge. However, little attention was paid either to the properties of these materials or to the process as a means of forming useful materials as these materials were initially regarded undesirable. At the earlier stages of the discovery, the plasma polymerization technique was not treated as standard method for preparation of polymers[1-4] . These methods gained importance when they were used to make special coatings on metals and began to be recognized as techniques for synthesizing polymers.

Polymers formed by plasma polymerization are in most cases highly branched , crosslinked and resistant to physical and chemical treatment[5-11]. Although a great number of research studies have been published and numerous potential application and uniqueness of polymer formation process have been demonstrated, the subject has not drawn much academic interest as a new subject area of polymer science. This is largely due to the fact that the very unique and advantageous feature of forming insoluble, infusible polymers has hampered the basic study of the process at the molecular level. The well recognized concept of conventional polymerization is based on molecular processes by which the size of the molecule increases. The arrangement of atoms that constitute the molecules of a monomer is accomplished during the organic synthesis of the monomer. During the polymerization of a monomer rearrangement of atoms within a molecule seldom occurs. However, polymer formation in plasma is recognized as an atomic process in contrast to the above molecular process.

In short, plasma polymerization was dealt with in the 1960's and 1970's as a new and exotic method of polymerization. Plasma polymers have no repeating monomer units unlike the conventional polymers processed through ionic or radical mechanisms. They are composed of a mixture of molecules cross-linked or fragmented and rearranged from monomer molecules. Thus, the technique can be

considered as a method for forming new types of materials rather than a method of preparation of conventional polymers. Certain molecules, which cannot be polymerized conventionally because of the absence of active species to propagate the polymer chain can be plasma polymerized. There are various steps involved in obtaining a good coating by conventional methods while with the plasma polymerization technique, a single step can produce a good polymer coating. Thus, simplicity also favours plasma polymerization technique.

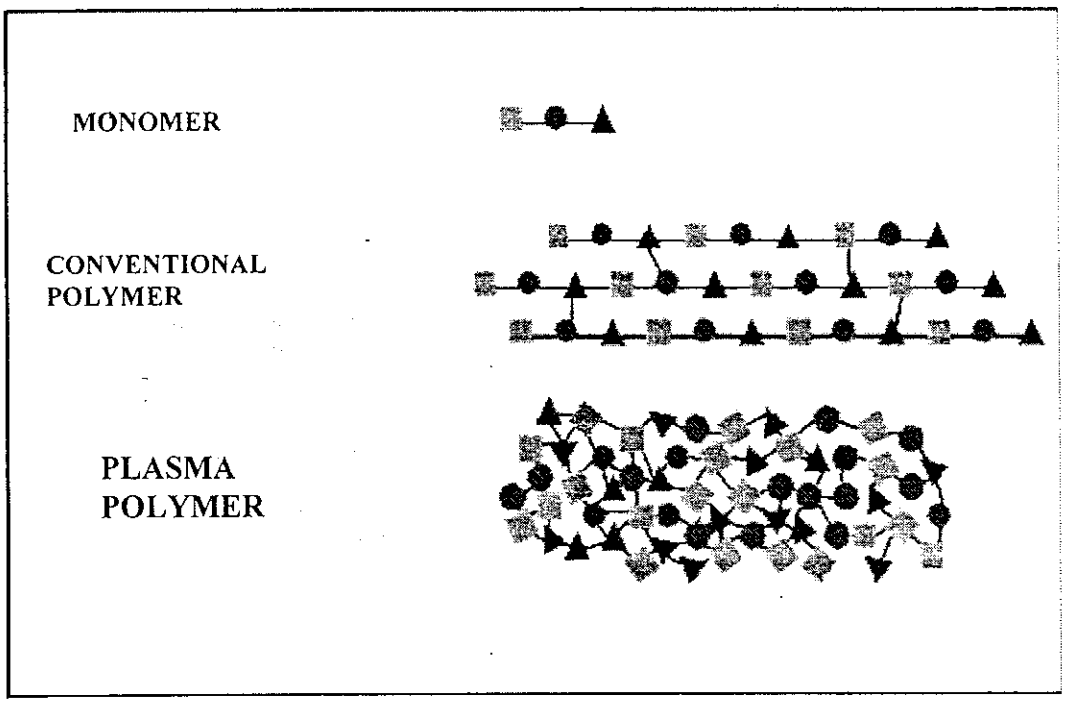

Figure 1: differentiates the plasma polymer from a conventional polymer of the same monomer

Figure 1 gives a general idea of conventional polymerization and plasma polymerization. The plasma polymerized thin films are highly adhesive, pinhole free, dielectric, hydrophobic, cross-linked, highly branched and highly resistant to physical and chemical treatment.

The most important forms of plasma polymers are ultra thin films which require special attention.Chemical reactions occurring under the plasma conditions are generally very complex and consequently are non-specific in nature. These polymerization techniques are advantageous when special excited states are required as intermediate states. This cannot be achieved using other conventional polymerization techniques. Thus, plasma polymerization is recognized as special means of preparing unique polymers that cannot be made by other methods.

Many bulk properties of polymer films such as permeability, electric volume, resistivity and dielectric constant can be considered as characteristic material constants. The parameters do not change as the thickness of the film varies. This is true for a film as its thickness is above a certain critical value i.e. 0.05 - 0.1μm depending upon the parameters under consideration. As the thickness of the film is below a critical value, the constancy of the parameters is no longer observed. This might be probably due to the increased contribution of flaws to the total film. As the thickness of the film decreases the contribution from the flaws to the film increases. It is difficult to prepare flawless films with thickness below a critical value. However, with plasma polymerization, we can obtain ultra thin film containing minimum amount of flaws, which is a valuable asset in material characterization [1].

According to the growth mechanisms, polymerization is classified into two. a) **step-growth polymerization** and b) **chain-growth polymerization** [12, 13].

3.1.1 STEP GROWTH POLYMERIZATION

In **step-growth polymerization**, a polymer is formed by the step-wise repetition of the same reaction. If the monomer is represented by M, and the growing molecules by M_l, step growth polymerization can be represented by

$$M_1+M=M_2+H_2O$$

$$M_2+M=M_3+H_2O$$

$$M_m+M_n=M_{n+m}+H_2O$$

It is seen that the reaction at each step is identical to the first reaction. Since the overall polymerization is the multiplication of the same reaction, the enthalpy change ΔH, entropy change ΔS and the Gibb's free energy change ΔG for overall polymerization are nearly identical to those in each step as long as the condition that the reactivities of the functional groups are independent of the size of the reacting molecules.

3.1.2 CHAIN GROWTH POLYMERIZATION

In **chain-growth polymerization,** a long chain molecule is formed by a series of consecutive steps that is completed in a very short time. In this case, products are only final polymers. Unlike the case of step growth polymerization, intermediate size molecules cannot be isolated. Consequently, entire polymer formation can be

essentially considered a one step process, as long as the concept of chemical reaction that relies on the identification of reactants and products is concerned.

If the chain carrying species is indicated by M* and the monomer by M, the chain growth mechanism can be shown by

$$M^* + M = M_2^*$$

$$M_2^* + M = M_3^*$$

$$M_n^* + M = M_{n+1}^*$$

&

$$M_m^* \rightarrow M_m \text{ (Polymer)}$$

The first three reactions represent the propagation reaction and the last reaction in which the chain carrying species is lost is the termination reaction. In short, in the step growth polymerization, each growth step is a chemical reaction between two molecules whereas in chain growth polymerization, each individual growth step is a chemical reaction between a chain carrying species and a molecule.

A typical example of the chain growth polymerization is the **addition polymerization**. Depending on the nature of the reactive species, the addition polymerization can be classified as *free radical polymerization, cationic polymerization, anionic polymerization* and so on.

Free radical polymerization:

Since most of the studies of plasma polymerization suggests that free radicals are the most likely reactive species in the formation of polymers under plasma

conditions, it is necessary to review the fundamental aspects of free radical polymerization. The reactions of the free radical polymerization can be looked upon in four steps.

Step 1: Initiation

$$I \xrightarrow{K_d} 2R$$

$$R.+M \xrightarrow{K_f} M.$$

Step 2: Propagation

$$M.+M \xrightarrow{K_p} MM.$$

$$M_n.+M \xrightarrow{K_p} M_{n+1}$$

Step 3: Termination

Recombination $$M_m.+M_n \xrightarrow{K_{t,c}} P_{m+n}$$

Disproportionation $$M_m.+M_n. \xrightarrow{K_{t,d}} P_m+P_n$$

Step 4: Chain Transfer

$$M_n\cdot + A \xrightarrow{K_{tr}} P_n + A$$

$$A\cdot + M \xrightarrow{K_{tr}} M\cdot + A$$

The important aspects of free radical polymerization are 1) The rate of polymerizatio is proportional to the square root of the initiator concentration or the square root of th rate of initiation. 2) The degree of polymerization is inversely proportional to th square root of the square root of the initiator concentration or the square root of th rate of initiation.

Hence, faster polymerization leads to shorter chain length of the resulting polymer.

Ionic polymerization

Depending on whether the chain carrying reactive species is electrophilic initiator o nucleophilic initiator they are classified into *cationic polymerization* or *anioni polymerization* respectively. In the following schematic representations, electron use in the A-B bond are represented by 'dot' and the electron in monomer double bond i expressed by 'colon'.

Electrophilic Initiator:

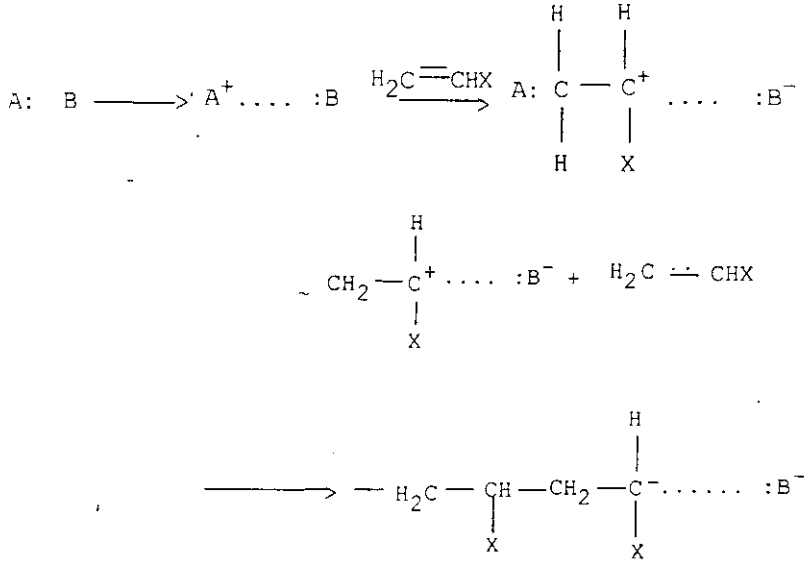

This is also referred to as cationic polymerization.

Nucleophilic Initiator:

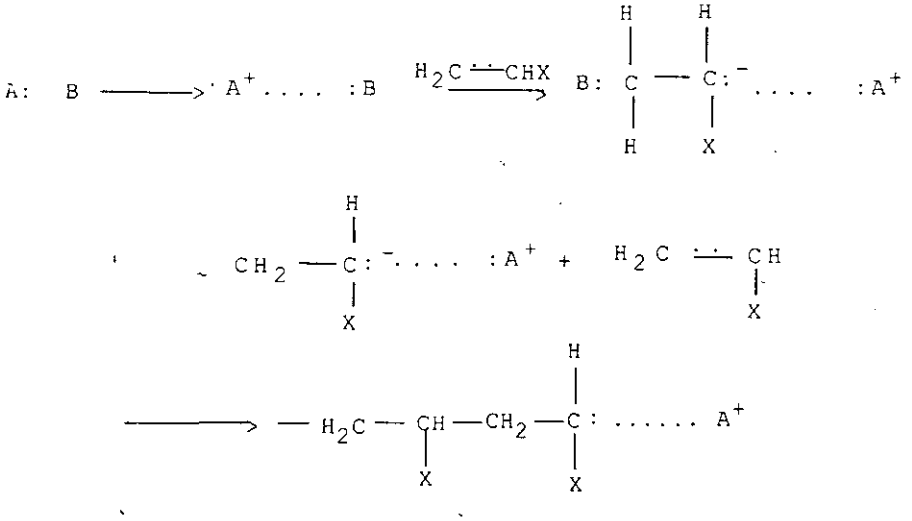

This is referred to as anionic polymerization.

The difference between ionic polymerization and free radical polymerization is the fact that the growing chains in ionic polymerization are accompanied by corresponding counter ions. Therefore in ionic polymerization, chain propagation is highly dependent on the type of initiation (which determines the counter ion) and the nature (particularly the dielectric constant) of the solvent used in the polymerization. In the case of free radical polymerization, the reactivity of growing chain is nearly independent of the nature of R or of the type of solvent. The initiator moiety R remains at the non- reactive end of the growing chain. Another notable difference is in the mode of chain termination. In ionic polymerization, the growing chain possesses the electric charge and two growing chains cannot react due to the coulombic repulsion of two similarly charged species. Hence, the termination by a molecular reaction of the growing chain is absent in the cationic and anionic polymerizations. Therefore, the termination occurs by other reactions such as chain transfer and reactions with impurities. On the contrary in free radical polymerization, the chain termination occurs by reaction between two free radicals (growing chains). Consequently, the termination is an apparent monomolecular reaction (first-order reaction).

3.1.3 RADIATION POLYMERIZATION:

Polymerization initiated by ionizing radiation such as γ rays from ^{60}Co or high-energy beams is somewhat similar to Plasma polymerization. For elucidating the mechanism of plasma polymerization, an understanding of radiation polymerization is helpful.

The significant difference between radiation polymerization and the polymerizations discussed so far is that no initiator is employed in radiation polymerization. The chain carrying species are created by ionization of a monomer molecule. It is this aspect of radiation-induced polymerization, which is similar to plasma polymerization.

Under irradiation, the monomer is ionized ejecting an electron forming a cation radical M^+

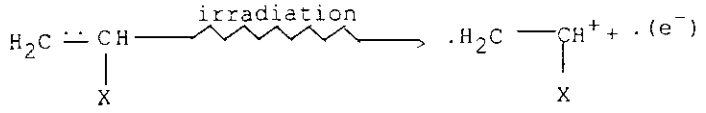

The cation radical and the ejected electron may either recombine or separate depending upon the distance of the initial separation. A cation radical that is sufficiently separated from electron will then proceed with the polymerization procedures.

The cation radical first adds to another monomer forming a dimer structure that has a free radical at one end (expressed by.) and a cation site at the other end.

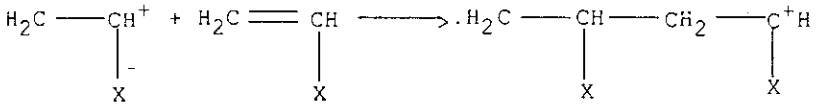

Propagation then proceeds independently at each site according to the respective characteristic rate constant of the particular active site.

At the same time, some of the ejected electrons from the initial ionization are captured by monomers to form anionic radicals $\underline{M^{-\cdot}}$. The anionic radicals also then add to another monomer to form dimeric structure with free radical at one end and an anionic site at the other. Propagation again proceeds independently at each active site according to the respective rate constants of the anionic and free radical polymerization.

Radiation induced polymerization differs from the polymerization by an initiator in that (i) free radical and ionic polymerization co-exist, (ii) ion radicals contribute to the initiator reaction and (iii) ionic sites have no counter ions.

3.1.4 PARYLENE POLYMERIZATION:

This kind of polymerization can be described as a rapid step- growth polymerization by polycombination of difunctional active species. The reactive species, hence do not add onto the monomer but they react with each other to form polymer. In this sense, this kind of polymerization differs from the classes of polymerization discussed in the preceding sections.

Parylene polymerization utilizes a dimer of p-xylylene or p-xyleylene derivatives. Unsubstituted p-Xylene dimer is designated as Parylene N where as monochloro substituted dimer is designated as Parylene C. Various other kinds of substitution are also possible.

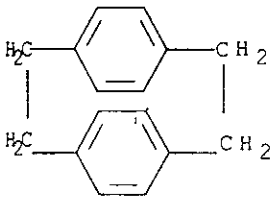

Parylene

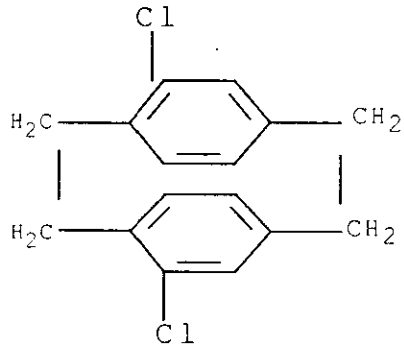

Parylene C

Parylene C is used industrially and in research applications whereas Parylene N is used in the study of Parylene polymerization and characterization of polymer properties. In Parylene polymerization process, the system is first evacuated to the level of 10^{-3} to 10^{-2} Torr with a known amount of dimer charged in the sublimation chamber. Then the sublimation chamber is heated to 120-160 ^{0} C and the cracking chamber is heated to 600-650 ^{0} C respectively. The sublimated dimer molecules dissociate into p-Xylene at the cracking temperature.

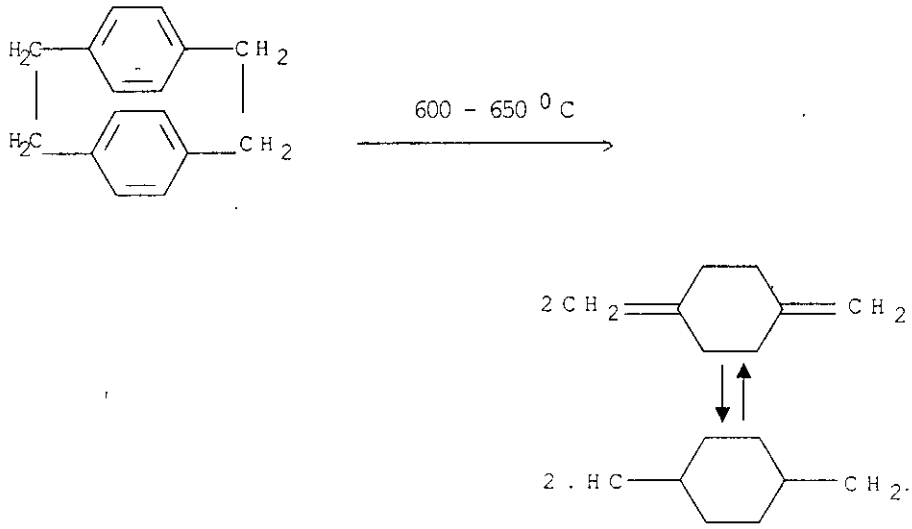

The cracked species reach the deposition chamber, which is at room temperature and the polymer is deposited on the surface, including the wall of the reaction chamber. The polymer formed is often highly crystalline and insoluble in organic solvents.

Hence among the polymerizations described, plasma polymerization is close to radiation polymerization and parylene polymerization. The radiation polymerization is similar to plasma polymerization in that the primary step is the ionization of monomers. However, radiation polymerization does not yield polymers in vacuum. The similarity between plasma polymerization and parylene polymerization is in the formation of polymer deposits in vacuum and differ in that parylene polymerization does not involve the ionization process. In short, plasma polymerization can be viewed as a hybrid of these two polymerization mechanisms.

3.2 PLASMA SOURCES

In the plasma polymerization, plasma of the monomer vapour is generated by different sources like

a) ***Direct current (DC) Glow Discharge:*** This can be established by passing a D.C. electric current through gas under low pressure. The cathode is bombarded with positive ions, which results in the generation of secondary electrons. These electrons are accelerated away from cathode until they gain sufficient energy to ionize the gas molecules or atoms that collide with the electrons.

b) ***Alternating Current Glow Discharges:*** The polymerization mechanism depends upon the frequency of alternation. Some of the AC discharges are given below.

Silent Discharge: In the typical arrangement, the discharge tube consists of a co-axial section and the linear and outer surfaces of the co-axial sections are connected to high ac voltage of 1000V and a frequency of 50 to 60 Hz. The polymerization takes place near the electrodes.

Low Frequency Discharge: Two metal electrodes are placed inside a reactor and is connected to a variable high voltage source. The required voltage depends upon the pressure, the nature of the substance and the distance between the electrodes.

Microwave discharge: Plasma can be produced using microwave generators of few kW powers and is found to be successful with inorganic compounds.

R.F. Discharge: At frequencies above 1MHz., no direct contact between electrodes and plasma is necessary. Hence in r.f plasma polymerization, the energy can be fed to plasma by inductive or capacitative coupling. Hence r.f plasma can be initiated and sustained by external electrodes at a much lower voltage than it is required for maintaining DC glow discharges.

This chapter describes the method of preparation of plasma polymerized thin films and investigations on their structural and optical characteristics, which include the analysis of FTIR spectra, absorption spectra and transmission spectra. The IR spectra give information about possible bond linkages, whereas the optical parameters like direct and indirect band gaps and refractive indices are evaluated from the absorption and transmission spectra.

3.3 PREPARATION OF PLASMA POLYMERIZED THIN FILMS

Three different polymers namely poly o-toluidine, poly m-toluidine and poly diethyl aniline are prepared in a plasma deposition system comprising of an r.f. generator source that uses four 807 RCA tetrode valves. The tuned plate, tuned grid r.f. source oscillates in the frequency range 4.5 to 13 MHz and has an output power of 35 Watts. Poly- DiEthyleneTriamine, poly- Phenyl Hydrazine,poly- Furfuryl Amine and poly-Propyl Amine are prepared at a frequency of 6-7 MHz The deposition chamber is a long tube of length 35cms and diameter of 3.5 cms. The energy is fed to the deposition chamber by capacitative coupling using aluminum foils for maintaining plasma. The tube is connected to a rotary pump and is evacuated to a pressure of 10^{-2}

Torr. The monomer flow into the tube is regulated using a manually operated needle valve.

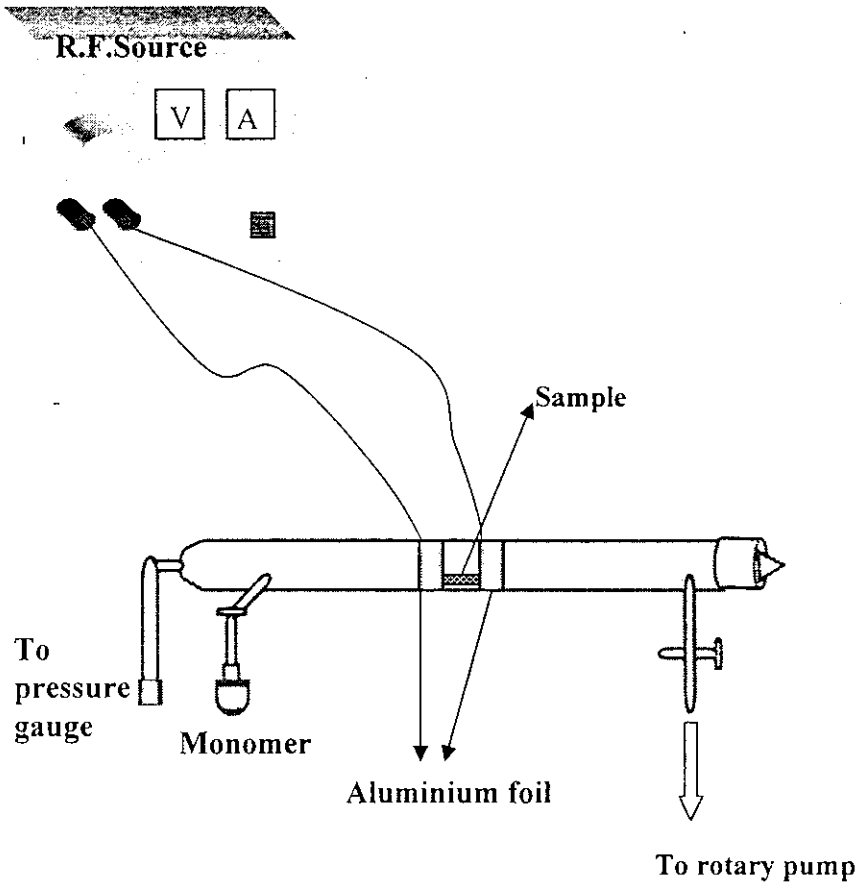

Figure (5): Schematic of the plasma polymerization unit.

The polymer thin films are prepared on optically flat glass slides of dimensions 75 x 25 x 1.4 mm. The glass plates are first cleaned in running water and are immersed in chromic acid for about 1-2 hours in order to remove alkaline impurities. The slides are then washed in distilled water and are cleaned ultrasonically. The microscopic impurities are stripped off by ultrasonic agitation in water. The glass slides are then dried and placed in the deposition chamber. The chamber is evacuated to a pressure of approximately 10^{-2} Torr keeping the monomer needle valve closed. The r.f. power is switched on and a bluish glow appears in between the electrodes. The monomer needle valve is opened gradually. After a deposition time of about 25-30 minutes, a thin film of the corresponding polymer is coated on to the glass plate.

3.4 OPTICAL CHARACTERISATION

3.4.1 BANDGAP MEASUREMENTS:

Optical absorption in solids occurs by various mechanisms. In all cases photon energy will be absorbed by the lattice or by electrons and transferred energy will be conserved. The lattice absorption, which occurs in the infrared region of the spectrum, gives information about the atomic vibrations involved. The higher energy parts of the spectrum associated with the inter-band electronic transition, provides information about the electron states. In such process, the electrons are excited from a filled band to empty band by the absorption of photons. This results in a sharp increase in the absorption coefficient and the onset of this rapid change in absorption coefficient is called the *fundamental absorption edge*. The corresponding energy is referred to as the *optical energy-gap* or the *band gap energy*. There are two kinds of

optical transitions at the fundamental absorption edge of crystalline and amorphous solids- *direct absorption (*or *transition) and Indirect absorption (*or *transition).*

a) DIRECT ABSORPTION

For a direct transition from the valence band to the conduction band, the wave vector of the electron must be conserved. This can be explained as follows: In any optical transition process, the total energy and momentum of the electron-photon system must be conserved. i.e.

$$E_f = E_i + h\nu; \quad k_f = k_i + q;$$

where E_i and E_f are the initial and final energies of the electron in the valence and conduction bands respectively and k_i and k_f are the corresponding electron momenta.

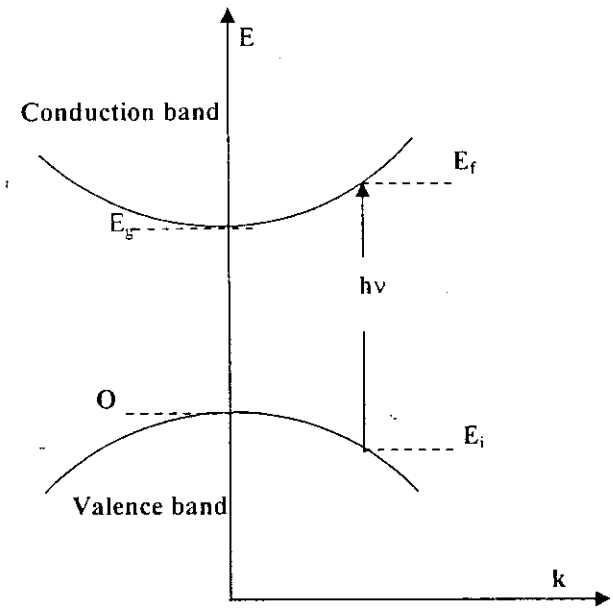

Figure 6: Direct Absorption

'q' is the wave vector of the absorbed photon. The wave vector of the photon in the optical region is usually small. The momentum condition therefore reduces to

$$\mathbf{k_f}=\mathbf{k_i}$$

Hence the momentum of electron alone is conserved. This selection rule indicates that only vertical transitions are allowed between the valence and conduction band. The bottom of conduction band and top of valence band lies at k=0 as shown in figure (6) so that electrons near the top of valence band can make direct transition to the states near the bottom of conduction band.

The density of states for a direct transition is given by [14]

$$N(E) = \frac{(2m_r)^{3/2}}{2\pi^2\hbar^3}(h\nu - E_g)^{1/2}$$

Theoretically by this equation, at $h\nu=E_g$, N (E) =0; In reality this is wrong. This means that the density of states is not nil in the band gap of the material and their presence is attributed to the *band tails*. Band tails are nothing but perturbation of the conduction and valence bands by the formation of tails of states extending the bands into the energy gap (figure (7)). These are referred to as localized states and are characteristic of amorphous solids or when defects, impurities etc are present.

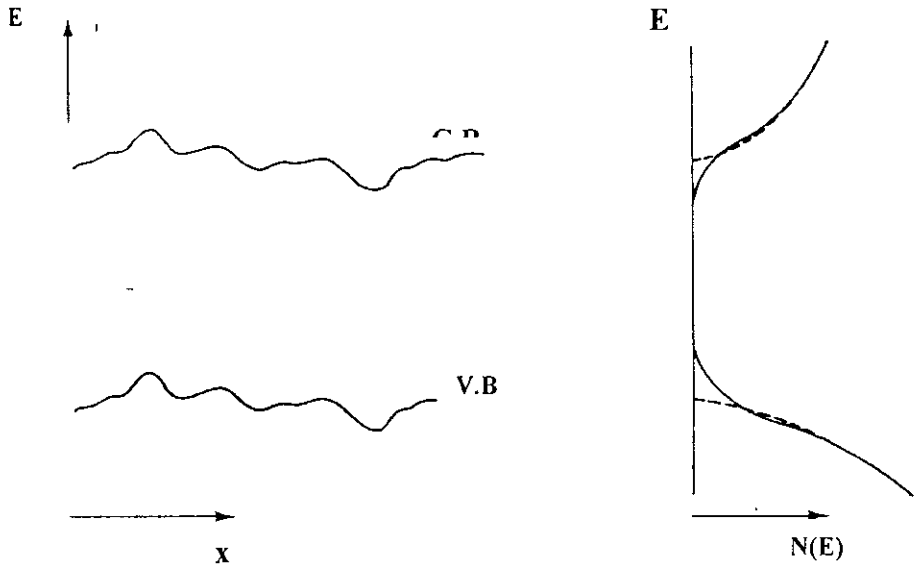

Figure (7): The left diagram shows the perturbation of the band edges by Coulomb interaction with inhomogeneously distributed impurities. This leads to the formation of tails of states shown on the right side. The dashed lines show the distribution of states in the unperturbed case.

The transition between the band tails causes an exponentially increasing absorption coefficient α, $(d(\ln\alpha)/d(E)=1/kT)$ and is known as **Urbach's rule.**

Hence in amorphous materials, three different types of optical transitions are to be dealt with as shown in figure (8). They are

1) ***Extended to extended transitions***:

The transitions from extended to extended states are very similar to the ones known from crystalline materials. The absorption coefficient in this case has the form [15,16]

$$\alpha h\nu = A\left(h\nu - E_g\right)^{1/2}$$

where 'α' is the absorption coefficient, 'hν' is the energy of absorbed light A is a constant for different transitions indicated by the different values of 'm'. $(\alpha h\nu)^2$ is to be plotted against hν in eV to determine the allowed direct transition energy band gap from the intercept of the extrapolation of $(\alpha h\nu)^2$ to zero on the photon energy axis.

2) ***Localized to extended and extended to localized transitions***:

In ideal crystalline materials, no transition takes place in the gap. However, in amorphous materials, there can be transitions from occupied extended states of valence band to empty tail states of conduction band and also from occupied tail states of valence band to empty extended states of conduction band. Both these transitions will have similar matrix elements. The density of states of localized states decays exponentially into the gap. Hence for transitions from localized to extended states and for extended to localized states, there is an exponential relation between absorption coefficient and frequency [17].

$$\alpha(\omega) \sim \exp\left(\frac{\hbar\omega}{E_u}\right)$$

where E_u is called the Urbach energy.

Since

$$\ln\alpha(\omega) = C + \frac{\hbar\omega}{E_u}$$

$$E_u = \frac{\hbar}{\frac{d}{d\omega}(\ln\alpha(\omega))}$$

Hence Urbach energy can be obtained from the inverse of the slope of plot between *ln* $\alpha(\omega)$ and frequency (ω).

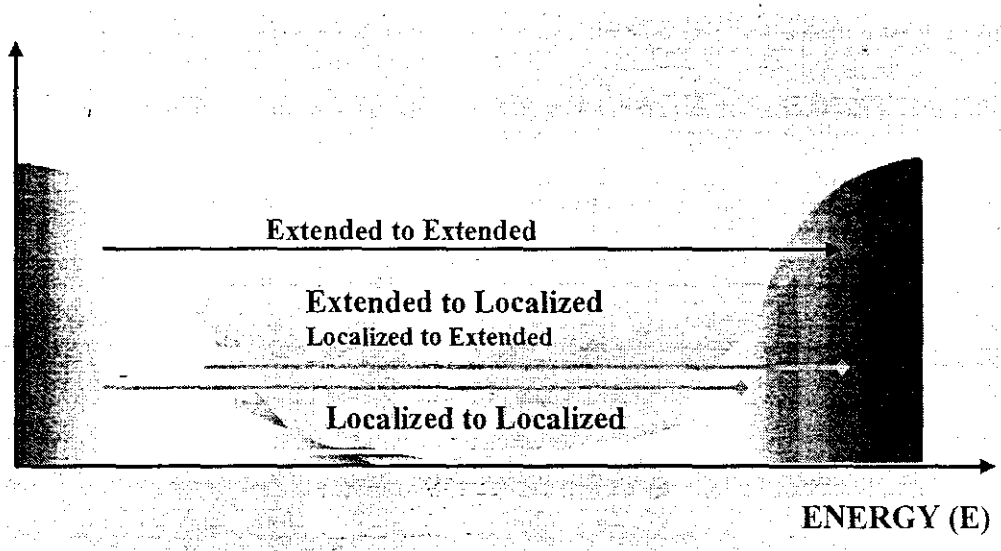

Figure (8): Different optical transitions involved in the direct absorption.

3) ***Localized to localized transitions***: These transitions usually are not very important since the number of states involved is low and the transition matrix elements are significantly smaller compared to those of the above-mentioned transitions. This is

due to the fact that the matrix elements are integrals over all space over the product of two functions (the initial and the derivative of the final state) which are separated in space and hence do exhibit almost no overlap. Transitions from localized to localized states would lead to absorption in the low energy regions of the spectrum which in most cases is the near to mid infrared region.

b) INDIRECT ABSORPTION:

As seen in direct absorption, if the bottom of conduction band and top of valence band lies at the same k (momentum) value then absorption process do not require change in k and hence direct transition is possible. However, if the bottom of conduction band and top of valence band has different k, then the absorption process requires a change in k. In order to conserve momentum in such indirect transition, participation of a phonon (lattice vibration, longitudinal or transverse) is required in the optical absorption process. The phonon is either created by the absorption process or thermally excited in the crystal, if the temperature is high enough. In the indirect absorption process, either electron transition from valence band absorbing a photon followed by electron transition within conduction band emitting or absorbing a phonon takes place or hole transition for conduction band to valence band followed by hole transition within the valence band emitting or absorbing a phonon takes place. It is not necessary that energy be conserved in the intermediate stages though energy must be conserved overall. Urbach's rule does not apply to indirect transitions.
The absorption coefficient is of the form

$$\alpha h\nu = A\left(h\nu - E_g\right)$$

Hence the intercept on x-axis of the plot of $(\alpha h\nu)^{1/2}$ vs. hν in eV gives the indirect band gap energy in eV.

3.4.2 REFRACTIVE INDEX MEAUSREMENTS

The refractive index of a dielectric film can be determined by the measurement of the transmission T of light through the film using a simple method suggested by J.C.Macifer etal [18].

Consider a thin film with a complex refractive index $\eta = n - ik$, bounded by two transparent media with refractive indices n_0 and n_1. Considering unit amplitude for the incident light, in the case of normal incidence, the amplitude of the transmitted wave is given by

$$A = \frac{t_1 t_2 \exp\left(-2\pi i \eta t / \lambda\right)}{1 + r_1 r_2 \exp\left(-4\pi i \eta t / \lambda\right)} \qquad (1)$$

in which t_1, t_2, r_1, r_2 are the transmission and reflection coefficients at the front and rear faces. The transmission of the layer is given by

$$T = \frac{n_1}{n_0}|A|^2 \qquad (2)$$

In the case of weak absorption with $k^2 << (n - n_0)^2$ and $k^2 >> (n - n_0)^2$

$$T = \frac{16 n_0 n_1 n^2 \alpha}{C_1^2 + C_2^2 \alpha^2 + 2 C_1 C_2 \alpha \cos\left(4\pi nt/\lambda\right)} \qquad (3)$$

where $C_1 = (n + n_0)(n_1 + n), C_2 = (n - n_0)(n_1 - n)$ and

$$\alpha = \exp\left(-4\pi kt/\lambda\right) = \exp(-Kt) \qquad (4)$$

K is the absorption coefficient of the thin film.

Generally outside the region of fundamental absorption ($h\nu > E_g$ thin film gap) or of the free carrier absorption (for higher wavelengths), the dispersion of n and k are not very large. The maxima and minima of T in equation (3) occurs for

$$4\pi nt/\lambda = m\pi \qquad (5)$$

where m is the order number. In the usual case ($n > n_1$, $C_2 < 0$), the extreme values of transmission are given by the formulae

$$T_{max} = 16 n_0 n_1 n^2 \alpha / (C_1 + C_2 \alpha)^2 \qquad (6)$$

$$T_{min} = 16 n_0 n_1 n^2 \alpha / (C_1 - C_2 \alpha)^2 \qquad (7)$$

By combining equations (6) & (7), Lyashenko and Miloslavskii developed an iterative method allowing the determination of n and α. J.C.Macifer etal proposed a simplification of this method by considering T_{min} and T_{max} as continuous functions of λ through n (λ) and α (λ). The ratio of equations (6) and (7) gives

$$\alpha = \frac{C_1\left[1-\left(T_{max}/T_{min}\right)^{1/2}\right]}{C_2\left[1-\left(T_{max}\,T_{min}\right)^{1/2}\right]}$$

Then from equation ()

$$n = \left[N + \left(N^2 - n_0^{\,2} n_1^{\,2}\right)^{1/2}\right]^{1/2}$$

where $N = \frac{n_0^{\,2} + n_1^{\,2}}{2} + 2n_0 n_1 \frac{T_{max} - T_{min}}{T_{max}\,T_{min}}$

The above equation shows that n is explicitly determined from T_{max}, T_{min}, n_1 and n_0 at the same wavelength.

A Hitachi model U-3410 UV-Vis-NIR spectrophotometer is used to record the absorption and transmission spectra of the plasma polymerized samples. The optical absorption and transmission of samples prepared on glass substrate is measured against a blank substrate as reference. Direct band gap, indirect band gap and Urbach energy of the three plasma polymerized samples are determined form the absorption spectra and refractive indices of the corresponding samples are determined from the transmissioh spectra.

Figure (9) shows the absorption spectrum of the poly DiEthyleneTriamine. The direct and indirect band gaps are determined from the plots (10) and (11)

respectively. From the graph (12), Urbach energy is calculated. The transmission spectrum of the thin film sample is as shown in figure (13).

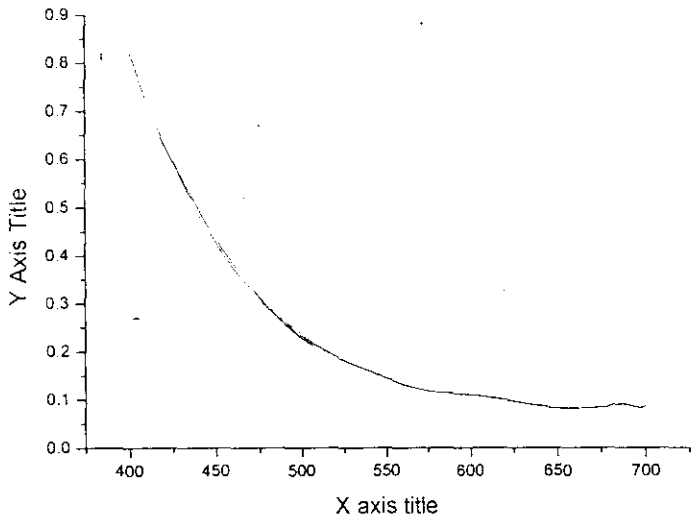

Figure(9) : Absorption spectrum of poly – DiEthyleneTriamine

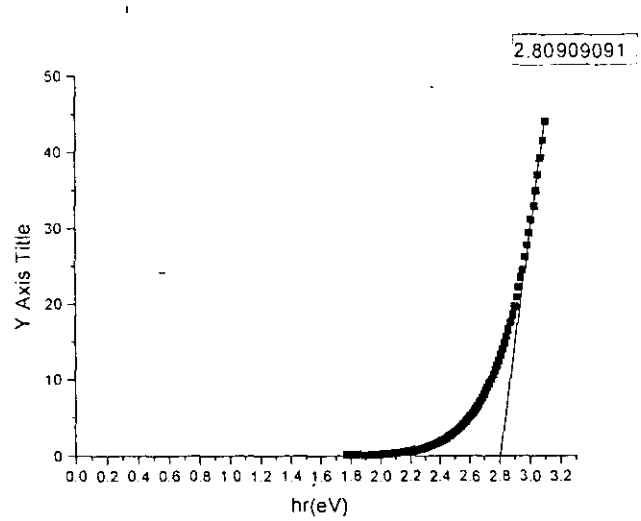

Figure 10. $(\alpha h\nu)^2$ vs $h\nu$ in eV for determining direct band gap Energy of pol DiEthylene TriAmine

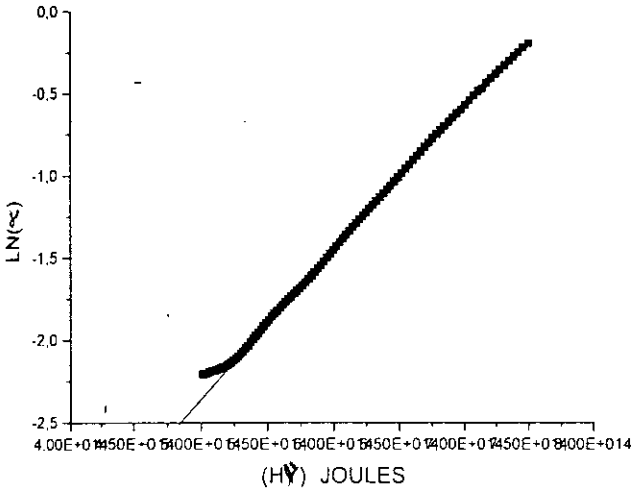

Figure11. ln(α) vs hν (Joules) plot for determining the Urbach Energy of poly-DiEthylene TriAmine

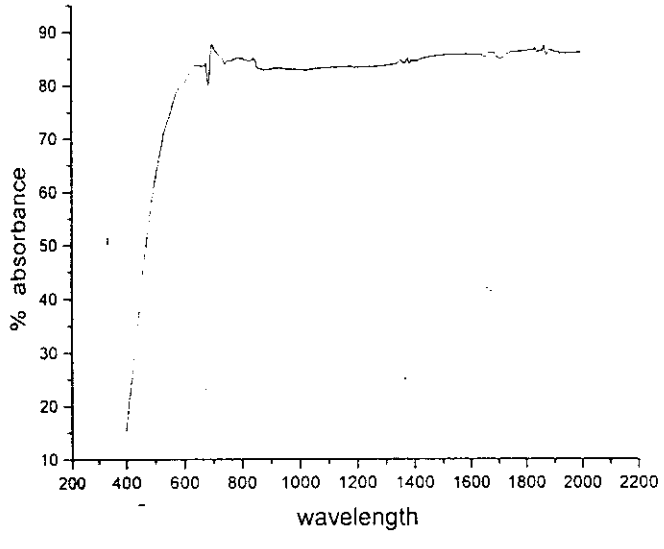

Figure12Transmissionspectrum of DiEthylene TriAmine

The absorption spectrum and transmission spectrum of poly -Phenyl Hydrazine thin film is as shown in figures (13) & (14). The direct band gap, indirect band gap and Urbach energy are determined from the plots .

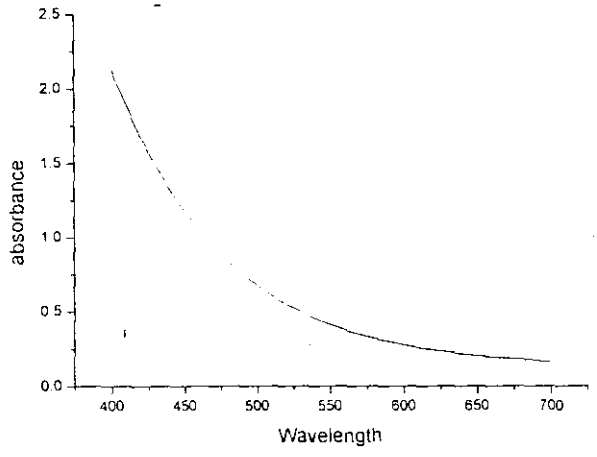

Figure (13) Absorption Spectrum of poly- Phenyl Hydrazine

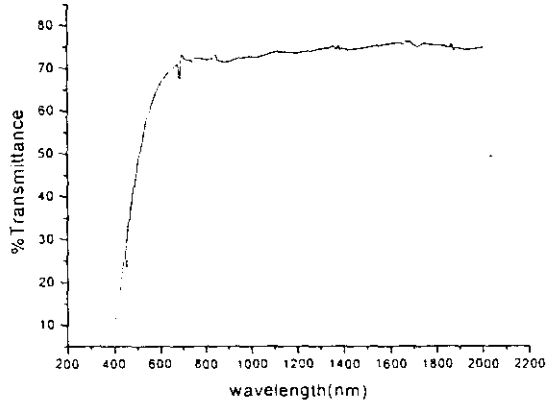

Figure 14 Transmission spectrum of poly- Phenyl Hydrazine

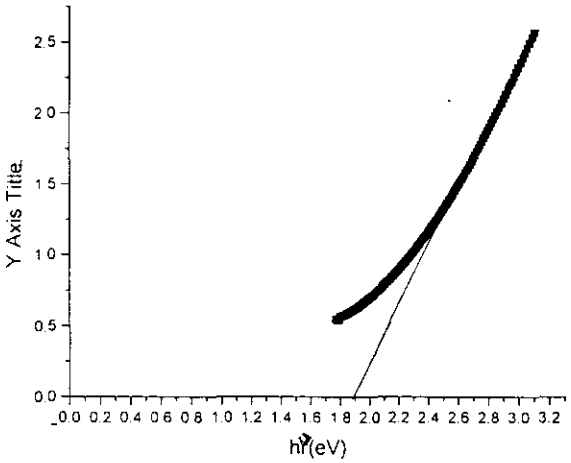

Figure (15) $(\alpha hr)^{1/2}$ vs hr for determining indirect band gap energy poly- Phenyl Hydrazine

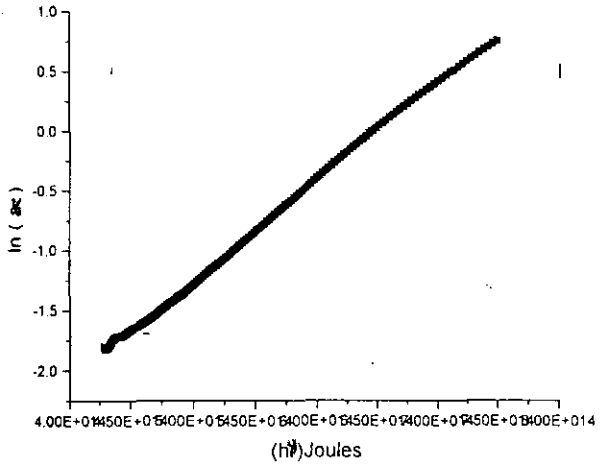

Fig (16) ln (a) vs hr for determining Urbach Energy of poly · Phenyl Hydrazine.

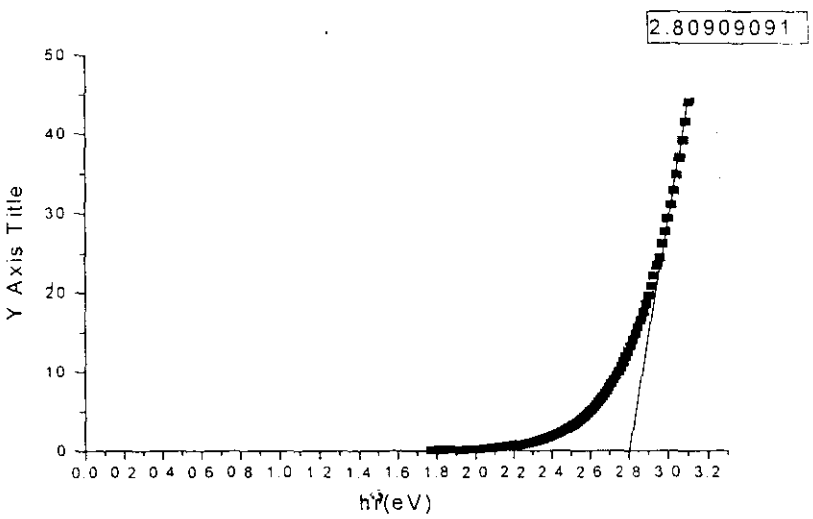

Figure 17. $(\alpha h\nu)^2$ vs $h\nu$ in eV for determining direct band gap Energy of poly-Phenyl Hydrazine

Similarly, from the absorption spectrum of poly –Furfuryl amine(figure (18)), direct band gap , indirect band gap energy and Urbach energy are determined. Refractive index of the thin film sample is determined from the transmission spectrum.Figure(19).

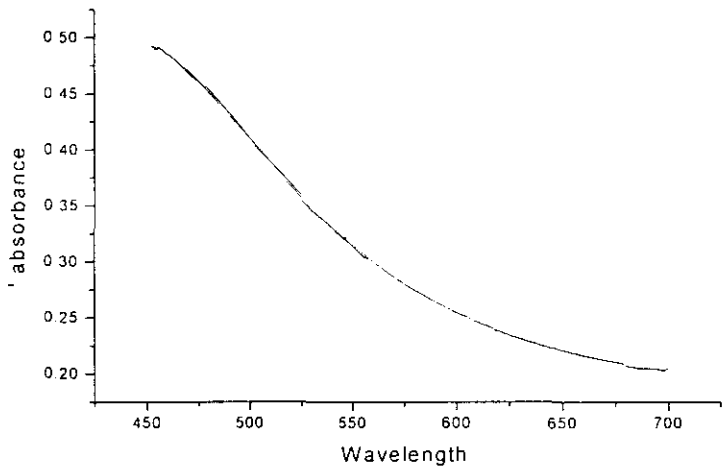

Figure (18) Absorption Spectrum of poly-- Furfuryl amine.

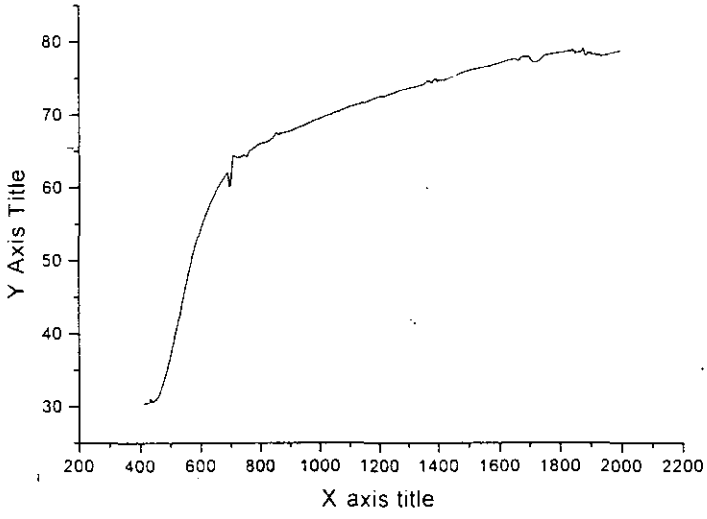

Figure. (19) Transmission spectrum of poly- Furfuryl amine.

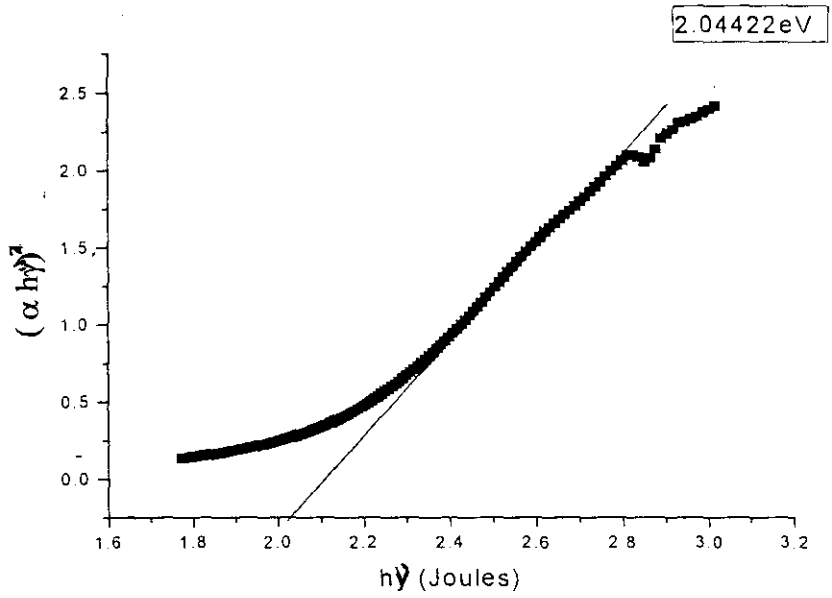

Figure 20: $(\alpha h\nu)^2$ vs hν in eV for determining direct bandgap energy of poly- Furfuryl amine

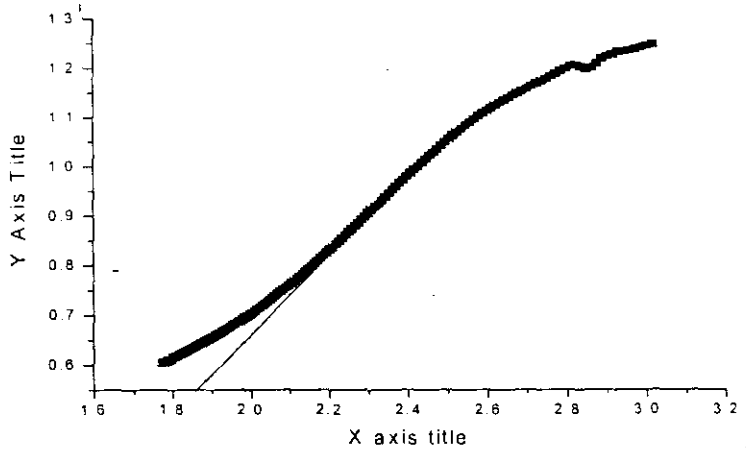

Figure (21): $(\alpha h\nu)^{1/2}$ vs hν plot for determining indirect band gap energy of poly Furfuryl amine

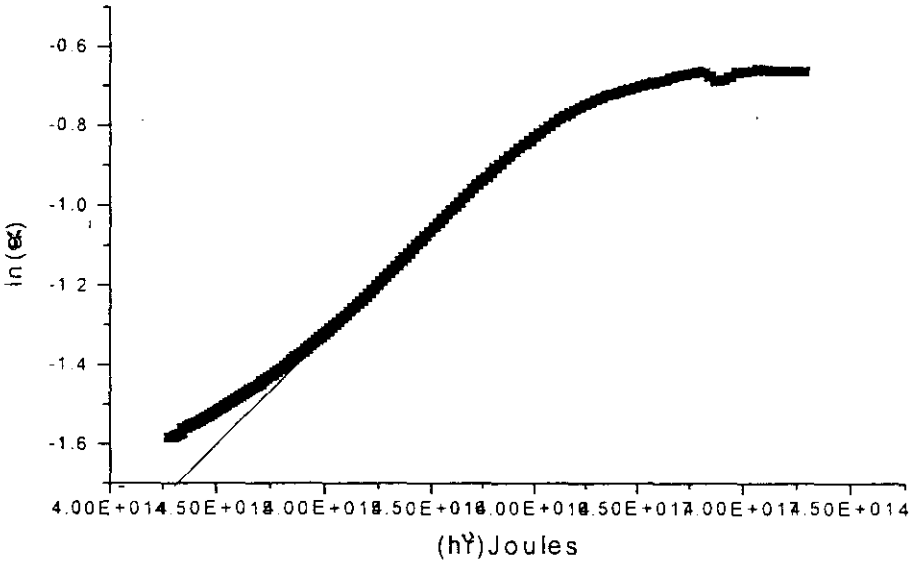

Figure(22) ln (a) vs hr for determining Urbach Energy of poly Furfuryl amine

From the absorption spectrum of poly–Propyl amine(figure (23), direct band gap , indirect band gap energy and Urbach energy are determined. Refractive index of the thin film sample is determined from the transmission spectrum (fig (24)

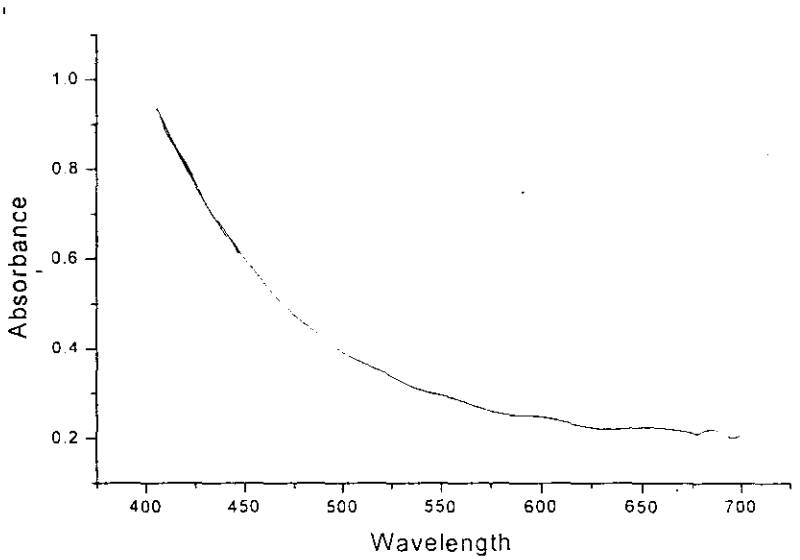

Figure (23) Absorption Spectrum of poly-- Propyl amine.

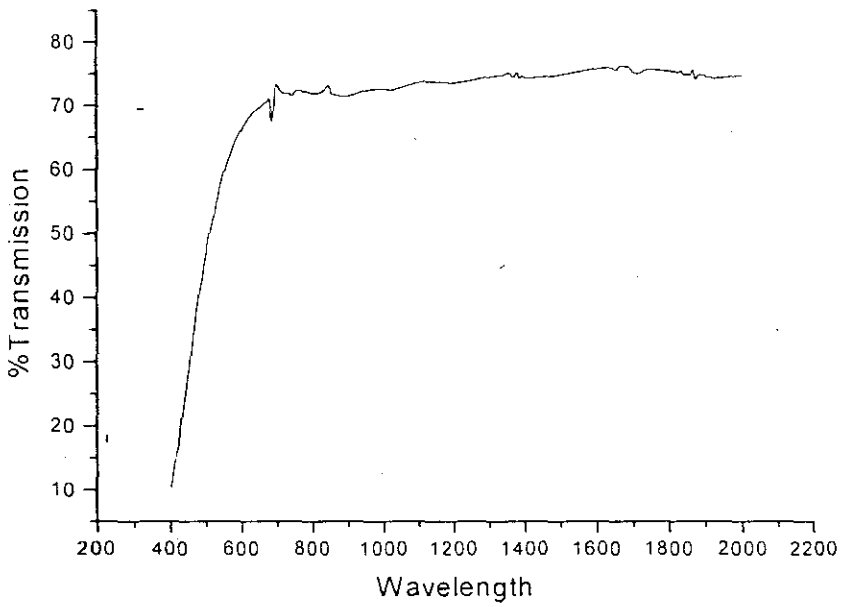

Figure. (24) Transmission spectrum of poly- Propyl amin

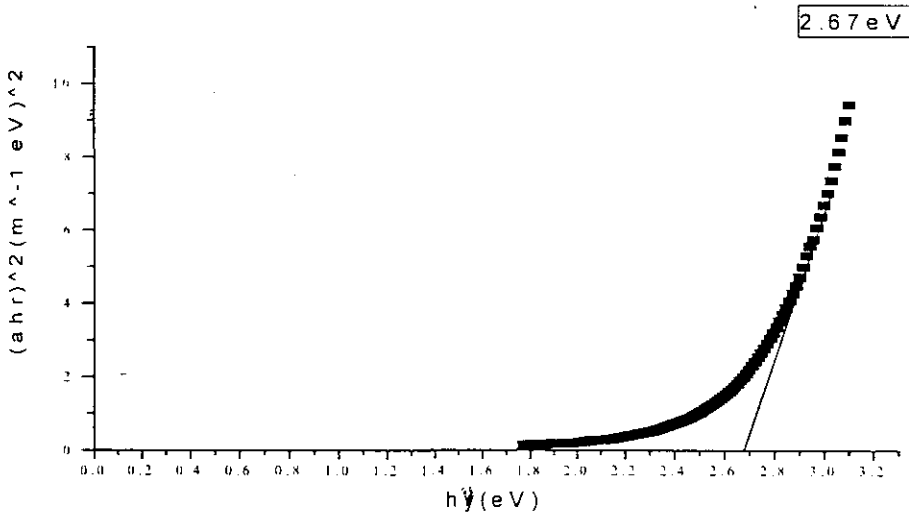

Figure(25) $(\alpha hr)^2$ vs hr for determining direct bandgap Energy of poly Propyl amine

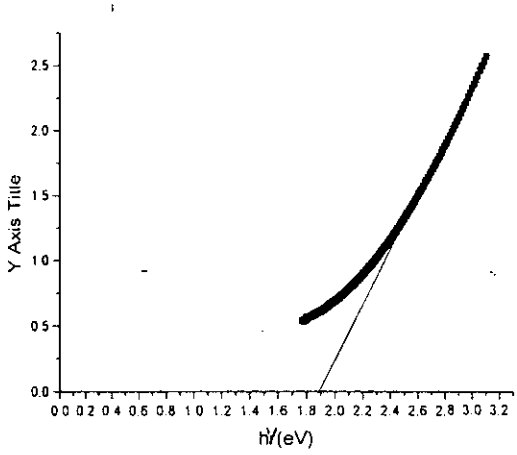

Figure(26) $(\alpha hr)^{1/2}$ vs hr for determining in direct bandgap Energy of poly Propyl amine

The direct bandgap energy, indirect bandgap energy, Urbach energy and the refractive index of the three samples are tabulated in Table I.

Sample	Direct energy bandgap (eV)	Indirect energy bandgap (eV)	Urbach energy (eV)	Refractive index
PolyDiEthyleneTriamine	2.8094	2.044	0.5131	1.552
Poly PhenylHydrazine	2.8090	1.8909	0.5211	1.65909
Poly Furfuryl amine	2.0448	1.862	0.8240	1.54327
Poly Propylamine	2.6772	1.872	.7701	1.60194

TABLE I showing the direct bandgap, indirect bandgap, Urbach energy and refractive index of the three plasma polymerized samples.

3.4.3 FTIR ANALYSIS

Michelson interferometer invented by Albert Abraham Michelson in 1880 forms the basis for the development of FTIR. Though originally, the Michelson interferometer was designed to test the existence of "luminiferous ether" a medium through which light

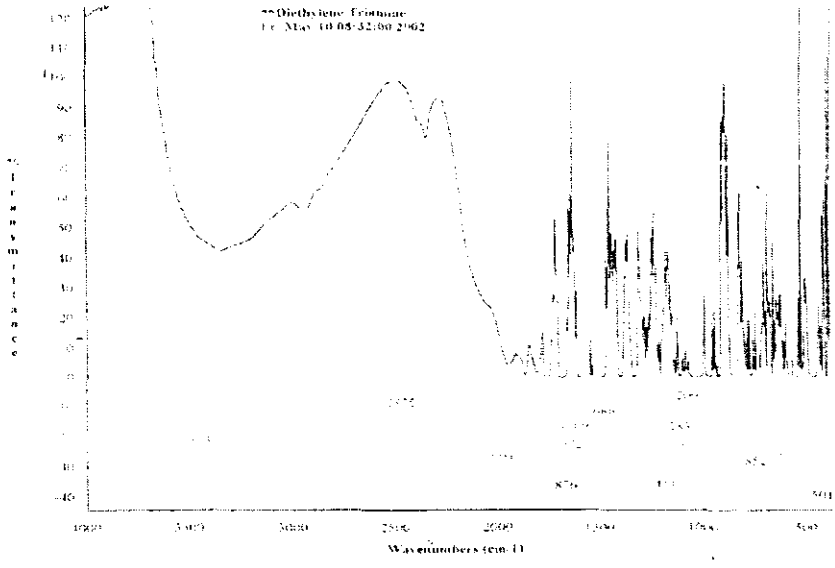

Figure(27) FTIR Spectrum of Di Ethylene Triamine

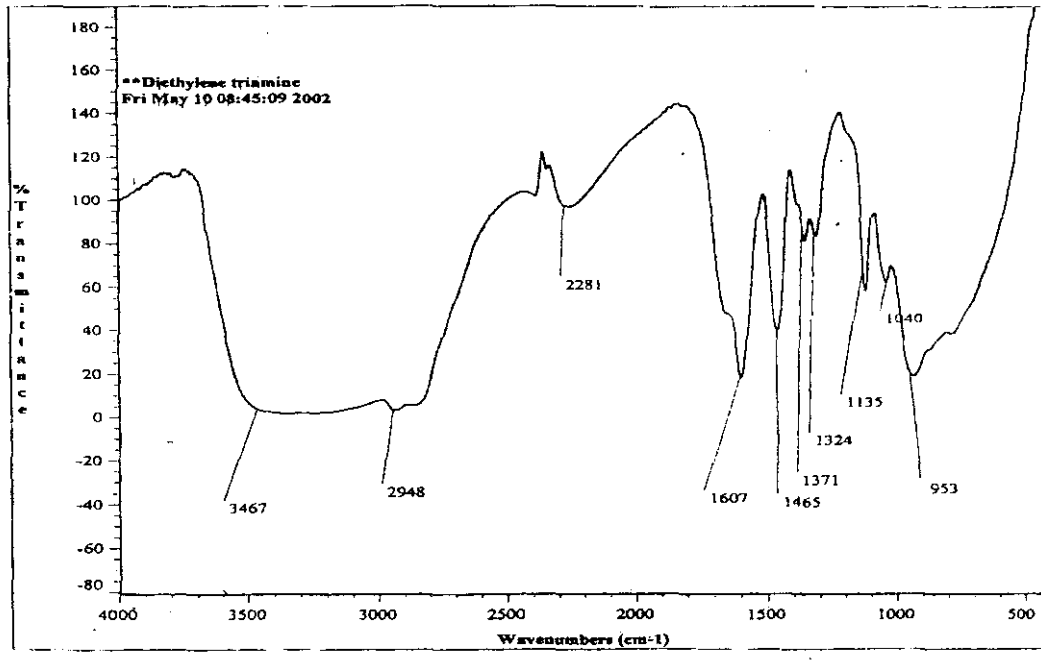

Figure(28) FTIR Spectrum of Poly-Di Ethylene Triamine

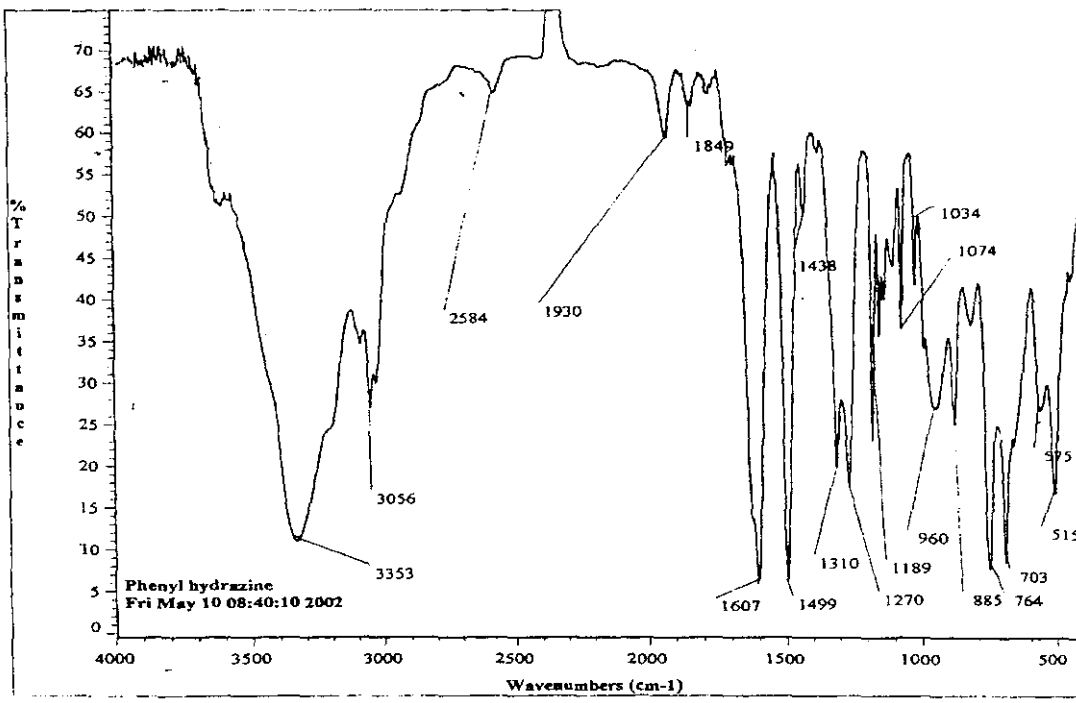

Figure(29) FTIR Spectrum of Phenyl Hydrazine

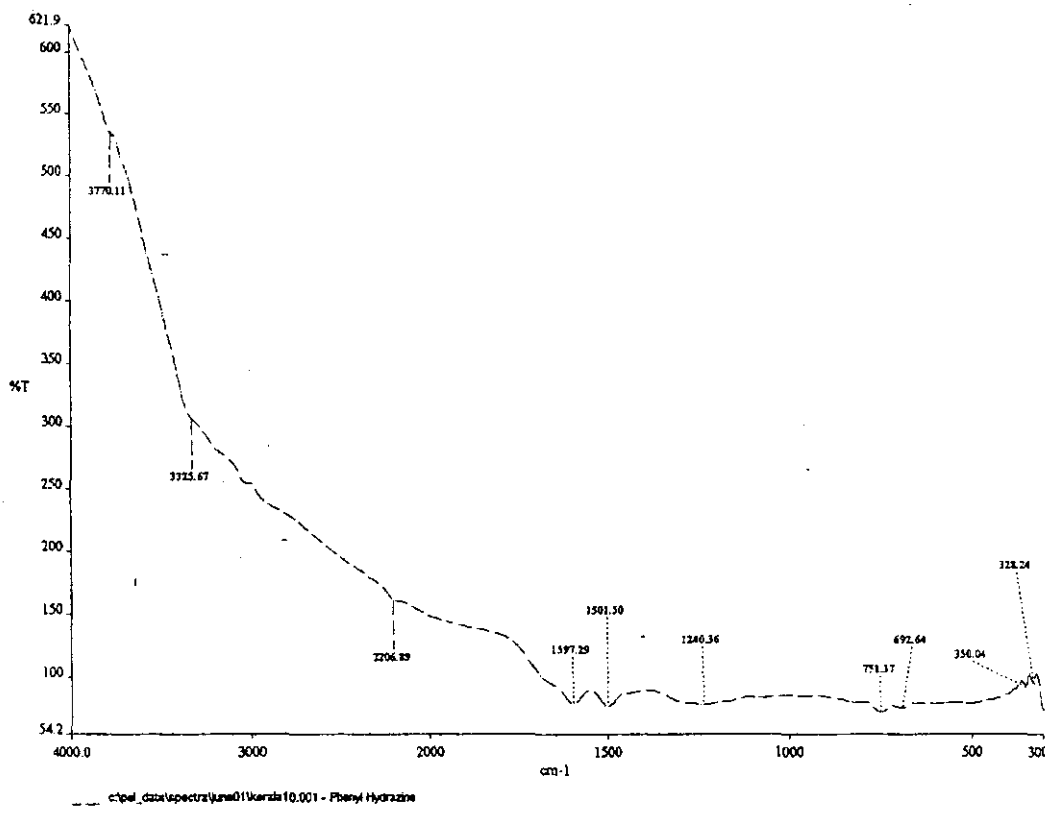

Figure(30) FTIR Spectrum of Poly Phenyl Hydrazine

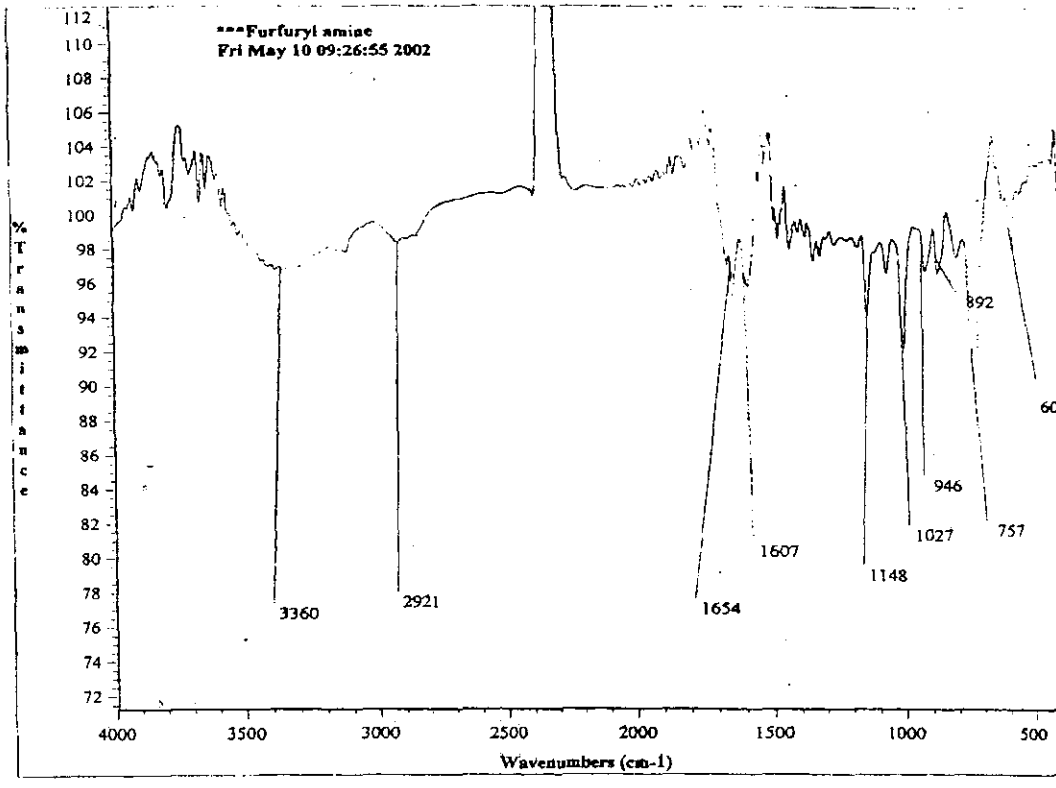

Figure(31) FTIR Spectrum of Furfuryl Amine

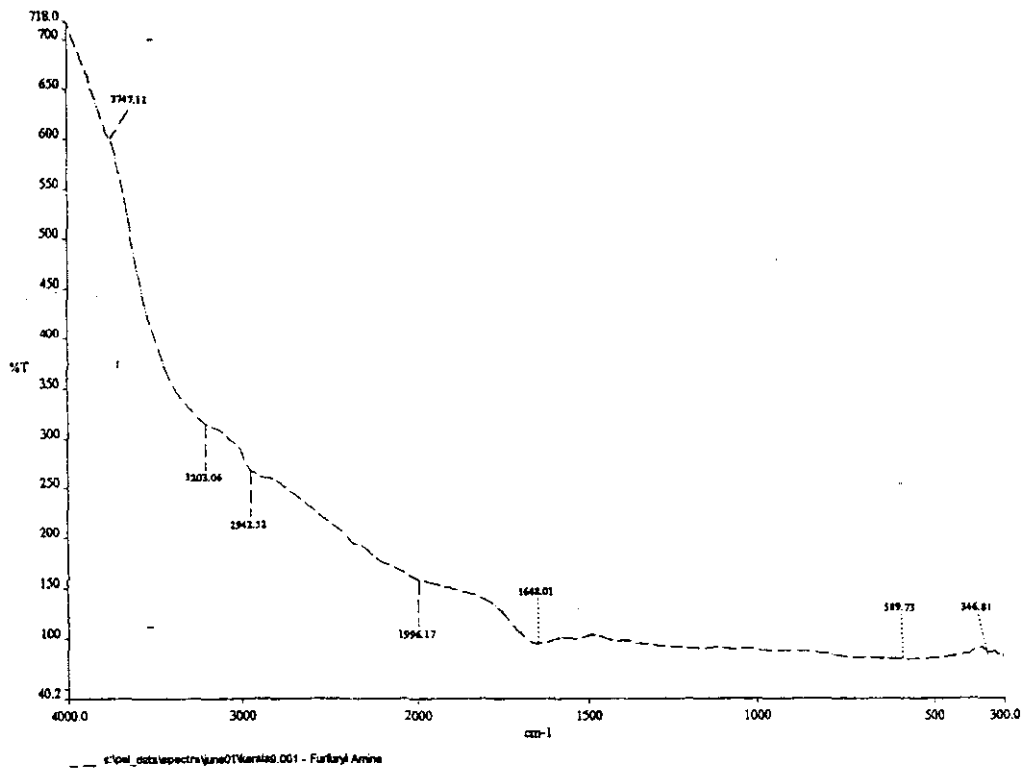

Figure(32) FTIR Spectrum of Poly Furfuryl Amine

waves were thought to propagate, Dr. Michelson was aware of the potential use of his interferometer in spectral analysis. He also manually measured many interferograms. Unfortunately the calculations required to convert an interferogram into a spectrum were time consuming and hence the use of an interferometer to obtain spectra was impractical. The invention of computers and advances in how computers perform

mathematical operations made FTIR a reality. J.W. Cooley and J.W. Tukey, at Bell Labs, made the major advance in this area when they invented "Fast Fourier Transform" (FFT), or "Cooley-Tukey Algorithm". This algorithm quickly performs Fourier transforms on a computer, and is still the basis for the transformation routines used in commercial FTIRs. The combination of the FFT algorithm and minicomputers was the breakthrough that made FTIR possible.

Infrared spectroscopy is the study of interaction of infrared light with matter. The infrared spectrum is generally regarded as one of the most characteristic properties of a compound. The range from 0.75 micron to 200 micron i.e. from just outside the visible region and extending up to the microwave region is called the infrared. The wavelength of infrared radiation is most frequently expressed in terms of wavenumbers, which are the reciprocal of wavelengths expressed in centimeter units. Two types of spectrophotometers are available, those linear in wavelengths and those linear in wavenumbers. The wavenumber unit is most widely used today. The majority of FTIRs operates in the mid infrared region of the spectrum, between 400-4000cm^{-1}. As the infrared radiation interacts with matter, it can be absorbed, causing chemical bonds in the material to vibrate. Since the vibrational energy levels of the molecules are quantized, only the infrared photon with a frequency exactly matching that required for a vibrational transition will be absorbed by the sample. When an infrared beam, whose frequency is changed continuously, irradiates the sample, the molecule will absorb certain frequencies as the energy is consumed in stretching or bending different bonds. The transmitted beam corresponding to the region of absorption will naturally be weakened and thus a recording of the intensity of the transmitted beam as a function of wavenumber gives the infrared spectrum. Hence, Fourier Transform Infrared Spectroscopy (FTIR) is a powerful tool for identifying

types of chemical bonds in a molecule by producing an infrared transmission spectrum that is like a molecular "fingerprint".

Samples for FTIR can be prepared in a number of ways. In the case of liquid samples, the easiest way is to place one drop of sample between two plates of sodium chloride (salt) so that the drop forms a thin film between the plates. Salt is transparent to infrared light. In the case of solid samples there are two ways: 1) Solid samples can be milled with potassium bromide (KBr) to form a very fine powder. This powder is then compressed into a thin pellet, which can be analyzed. KBr is also transparent in the IR. 2) Solid samples can be dissolved in a solvent such as methylene chloride, and the solution placed onto a single salt plate. The solvent is then evaporated off, leaving a thin film of the original material on the plate. This is called a cast film, and is frequently used for polymer identification. Solutions can also be analyzed in a liquid cell. This is a small container made from NaCl (or other IR-transparent material), which can be filled with liquid, such as the extract for EPA 418.1 analysis. This creates a longer path length for the sample, which leads to increased sensitivity. Sampling methods include making a mull of a powder with a hydrocarbon oil (Nujol) or pyrolyzing insoluble polymers and using the distilled pyrolyzate to cast a film. Films can be placed in an Attenuated Total Reflectance cell and gases in gas cells.

All molecules are made up of atoms linked by chemical bonds. The movement of atoms and chemical bonds can be likened to that of a system comprised of springs and balls in constant motion. Their motion can be regarded as being composed of two components, the stretching and bending vibrations. The frequencies of vibrations are not only dependent on the nature of particular bonds themselves, such as the C-H or C-O bonds, but are also affected by the entire molecule and its environment.

An infrared spectrum is usually studied under two regions:

a) The functional group region, 4000-1300 cm^{-1} (2.5-7.7 μm)

b) The finger print region, 1300-909 cm^{-1} (7.7-11.0 μm)

The high frequency portion (4000-1300 cm^{-1}) is called the functional group region. The characteristic stretching frequencies for important functional groups such as OH, NH, C=O etc occur in this portion of the spectrum. The absence of absorption in the assigned ranges for the various functional groups in is an evidence for the absence of such groups in the molecule. Overtones and combination tones of the lower frequency bands frequently appear in the high frequency region of the spectrum. In general, the high frequency region shows absorption arising from stretching vibrations and is useful for the identification of functional groups.

The region from 1400 cm^{-1} – 650 cm^{-1} is called the finger print region since the pattern of absorptions in the region is unique to any particular compound. The intermediate portion of the spectrum 1300 cm^{-1} -909 cm^{-1} region is usually complex since both the stretching and bending modes give rise to absorption in the region. The absorption bands in the finger print region are also complex with the bands originating in interacting vibrational modes. Each organic compound has its own absorption in the region. This region contains many absorption bands due to bending vibrations and the region is particularly rich in number of bands and shoulders. Aromatic compounds display numerous bands in the finger print region than their aliphatic counterparts. The Patterns of the infrared spectrum in the finger print region are very sensitive and change even with minor chemical or stereo chemical alternations in a molecule. The finger print region of the spectrum is extremely valuable when examined in reference to the other regions.

The bands in an infrared spectrum are generally classified by the intensity of the bands: strong, weak and variable. The relative strengths of the absorption bands in spectrum is changed by the number of similar groups in a molecule.

In the present work, the FTIR spectra of the monomer samples and the corresponding polymers are recorded in the range 400cm^{-1}-4000cm^{-1}. The pellets of the polymer samples mixed with KBr are used for the IR measurements.

In the present work, the FTIR spectra of the monomer samples and the corresponding polymers are recorded in the range 400cm^{-1}-4000cm^{-1}. The pellets of the polymer samples mixed with KBr are used for the IR measurements.

The FTIR spectra recorded in the range 400-4000cm^{-1} of the Diethylene Triamine monomer and polymer are shown in figures (27) & (28). The Diethylene Triamine molecule consists of two ethylene and three amino groups. IR spectra of monomer and polymer shows that the N-H stretch frequency present in the monomer is sustained in the polymer and is shifted from 3339 cm^{-1} to 3467 cm^{-1} in polymer form. The peak at 1964 cm^{-1} in monomer corresponds to the C = C asymmetric stretching of Aliphatic compounds and is absent in polymer. The C-H bend overtone frequencis corresponding to 1876cm^{-1},and 1822cm^{-1}, ,and 1769cm^{-1} present in the monomer are abstracted during polymerization. A peak at 1688 cm^{-1} shows the presence of CH stretching which is absent in the polymer.Most of the peaks appeared in the monomer in the region 1209cm^{-1} - 501 cm^{-1} indicates the presence of C-N groupwhich is absent in Polymer.1040 cm^{-1} skeltal stretching of Aliphatic compounds in present in polymer.Also the signature of ketonic group (1135)cm^{-1} is observed in the polymer. This can be attributed to the formation of ketonic group during the process of polymerisation in the presence of oxygen..

IR spectra of Phenyl hydrazine monomer and polymer is shown in figures(29,30)

The 3353^{-1} peak of monomer which is the characteristic of aromati amine group is shifted to 3325cm^{-1} which indicates the dislocation of the amino group in the polymer form .

The 1930cm^{-1} peak of C-H out of plane band of aromatic compound is found shifted to1957cm^{-1} in the polymer.1607cm^{-1} in monomer indicates the C-C skeletal vibrations of aromatic ring is absent in polymer . 1499cm^{-1} peak characterising the Benzene ring is also present in polymer which indicates the existence of Benzene ring in polymer.In the fingerprint region of the spectrum1189cm^{-1} peak characteristic of C-N stretching of Aliphatic amine is shifted to1220cm^{-1} in the polymer.

1. Figures(31,32) shows the IR spectra of Furfuryl amine monomer and polymer. The monomer peak of N-H stretching of aromatic Amine in monomer is shifted to 3203.06 in polymer. 1654 cm^{-1} peak present in the monomer indicates C=C stretching is present in polymer also.1607cm^{-1} characterizes the C-H out of plane stretching which may characterize the cyclic compound and is absent in polymer.In the finger print region (1300 cm^{-1} -900 cm^{-1}) most of peaks in monomer Is absent in polymer which indicates the abstraction of such groups in polymer.

FTIR Spectra of monomer and polymer of Propyl amine is shown in figures (33,34) Propyl Amine is a linear molecule in Mononer form .(CH_3 - CH_3 - CH_2 – NH_2)The characteristic peak of NH stretching frequency 3373 cm^{-1} is observed both in monomer and polymer.Frequencies corresponding to 2402cm^{-1}, 1897 cm^{-1}, 1822cm^{-1} which characterize N-H and C-H stretching which is present in the monomer disappears in polymer.An additional peak appear at 1573cm^{-1} which characterises the cumulative linkage C-C-C-O of single bonds of having more or less same bond strengths. . A peak at 1148 cm^{-1}shows the presence of skeletal stretching of aliphatic amine and is

shifted to 1135 in the polymer.885cm^{-1} Freqencies Corrponding to 987cm^{-1} 885cm $^{-1}$ 811 cm^{-1} of 622cm^{-1}, 545cm^{-1} indicates the presence of C-H bending which is also present in the polymer at 1130 cm^{-1}, 879 cm^{-1},616cm^{-1}.

The exact structure of the monomer and polymer molecules cannot be obtained only from FTIR analysis due to the the highly branched and cross-linked nature of the r.f. plasma polymers. Due to the variable extent of fragmentation and rearrangement of atoms during the process of plasma polymerization in plasma, the IR spectra also will vary with the conditions of the plasma polymerization [1]. Thus the IR analysis alone cannot give complete information on on branching and cross-linking .

Diethylene triamine,Phenyl Hydrazine,Furfuryl amine and Propyl amine plasma polymerized thin films of four monomers are prepared using excitation by an r.f. source. The direct band gap, indirect band gap and Urbach energy are determined from optical absorption spectral studies. It is observed that the band gap values lie in the range of other plasma-polymerized samples [23]. Similarly the Urbach energies obtained for the three samples also lie in the expected range [24]. The approximate values of the refractive indices are estimated from the transmission spectra.

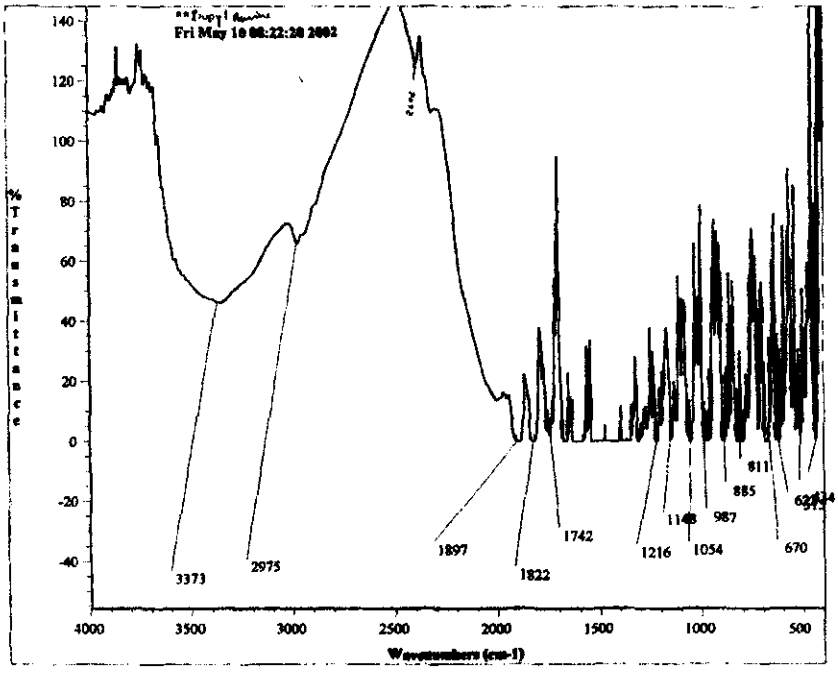

Figure 33 FTIR Spectra of Propyl amine

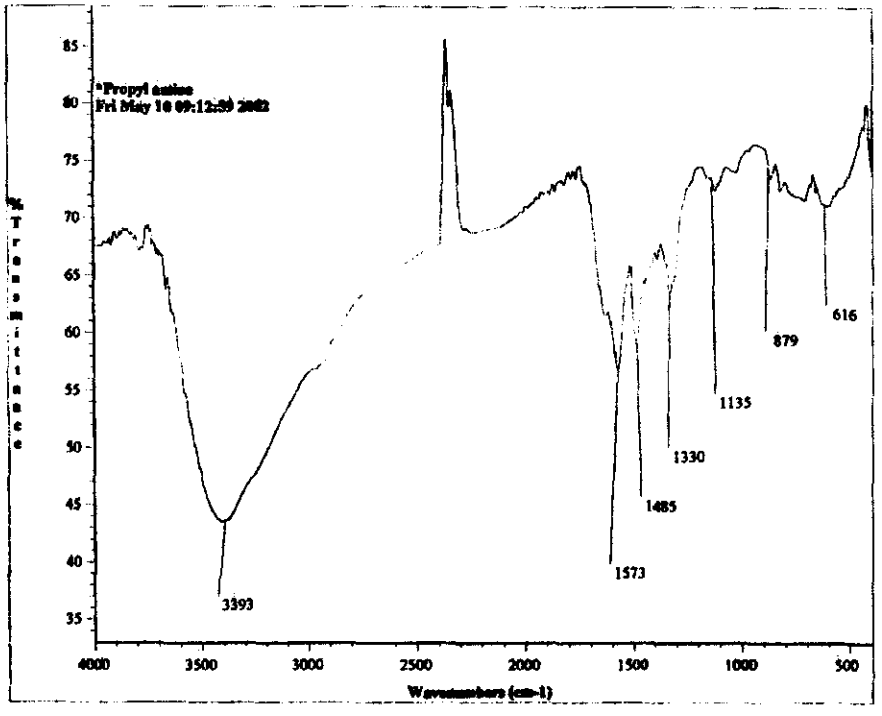

Figure 34 FTIR Spectra of [redacted] polyPropyl amine

References :-

1. H.Yasuda, Plasma Polymerization, academic Press, New York, 1985
2. Alfred Gill, Cold Plasma in Materials Fabrication, IEEE press, New York, 1994
3. H. Biederman and Y.Osada, Plasma Polymerization Processes, Elsevier, New York, 1970.
4. R.D. Agostino Plasma Deposition, Treatment and Etchhing of Polymers, Academic Press 1990.
5. J. Reecee Roth, Industrial Plasma Engineering, Volume 1 &2, IOP, Philadelphia, USA 2001.
6. R.H Turner, I.Segall, F.J.Boerio, G.D Davis, J.Adhesion 62 1, 1997
7. S.Kurosawa, N. Kamo, D. Matsui, Y.Kobtake, Anal.Chem. 62 (1990) 353
8. S. Kurosawa, J. Jpn. Oil Chem. Soc. 47 (1998) 1133.
9. L. O'Toole, R.D. Short, A.P. Ameen, F.R. Jones, J.Chem.Soc., Faraday Trans 91(9) (1995)1363.
10. P.W. Kramer, Y-S Yeh, H.Yasuda. J Membr Sci 46(1) (1989) 1.
11. H. Yasuda. J Membr Sci 18 (1984) 273.
12. Yoshinori Matsumoto, Makoto Ishida, Sensors and Actuators A 83 (2000) 179
13. F. W Billmayer Jr., text Book of Polymer science, John Wiley and Sons, New York, 1970.
14. P.S.Kireev, Ssemiconductor Physics, Mir Publishers, Moscow,(1978)
15. J.Tauc, Optical Propeties of solids, North Holand, Amsterdam, (1972)
16. J.Tauc, Amorphous and Liquid Semiconductors, Plenum, London, (1974).
17. F.Urbach, Phy.Rev. 92 (1953) 1324.

18. J.C Manifacier, J.Gasiot and J.P Fillard, J.Phys E: Sci.Instr. 9, (1976) 1002
19. B.K.Sharma, Spectroscopy, 11th and enlarged edition, Goel Publishing House, Meerut (1995-96).
20. Brian C. Smith, Fundamentals of Fourier Transform Infrared Spectroscopy, CRC Press, New York, 1996.
21. K.Nakanishi, P.H. Solomon, Infrared Absorption Spectroscopy, II edition, Holden- Day, Inc. Sanfrancisco(1977).
22. C.JosephMathai,S.Saravanan,M.R.Anantharaman,S.Venkatachalam.S .Jaya Lekshmi JphysD:Appl Phys.35(2002)240.
23. F.U.Z Chowdhury, A.H.Bhuiyan Thin Solid Films, 360 (2000) 69.
24. J.D.Dow, D. Redfield, Phy.Rev. B 5 (1972), 594.

CHAPTER IV

THE MEASUREMENT OF THERMAL DIFFUSIVITY OF ORGANIC MOLECULES AND THEIR PLASMA POLYMERIZED THIN FILMS

4.1 INTRODUCTION

Today there is an undiminishing demand for reliable measurements of the basic thermal properties of the vast range of materials in use .For the past two and a half decades, there has been a rapid increase in the development and application of new and improved materials for a broad range of applications in physics, chemistry, biology, medicine and in microelectronics. Thermal property measurement techniques include Differential Scanning Calorimetry, Contact Transient Methods etc. Above all these techniques either require large samples or are too complex and time consuming. In these conventional measuring methods the sample must be kept in contact with the detector, which produces fluctuations in the thermal field to be measured. The magnitudes of the thermal conductivity,specific heat etc of materials subjected to all conditions are required to feed computer models that has become a bed-rock of the modern design process .Meanwhile another set of non destructive and non contact techniques, commonly known as the Photothermal techniques [1]detailed in Chapter I, have

been developed and applied to study matter.The techniques have proved attractive for thermal property measurement because they combine the non-contactive application of well defined amounts of thermal energy with methods,mostly non-contactive,for the determination of the resulting temperature changesThe temperature changes employed in a property determination can be very small because of the very high sensitivitydetection techniques that have been developed in the photothermal sciences.This attribute is particularly important where measurements are required of a material whose thermal properties vary significantly with temperature.The study of phase transitions,at which thermal properties vary very rapidly with temperature,is a good example of such a situation and one in which photothemal science have proved successful.Another attribute is the possibility of focusing the photothermal probe and detection system to perform measurements on far smaller samples than would be needed by rival methods and to offer a means of studying the spatial variation of thermal properties across an inhomogeneous sample..Another most interesting applications of thermal wave physics is the measurement of thermal diffusivity of solids, liquids and gases. Different methods have been proposed for particular cases depending upon the thermo-optical properties and structure of samples: Photoacoustic [2-7], mirage or photothermal beam deflection [8-13], photopyroelectric [10-13]. All these techniques can be viewed, as alternatives to classical non-contact tools like Flash method [13]. Tthe design and fabrication of a compact photothermal probe beam deflection (PBD) experimental setup and its application to the determination of thermal diffusivity of certain organic

molecules and the corresponding plasma polymerized thin film samples are described in this Chapter.

4.2 Thermal Waves generation and propagation.

When ever temperature difference exists in a medium,or between bodies,heat transfer occurs.Heat transfer from or to a material can occur by a combination of conduction,convection and radiation.Out of the three modes of heat transfer, convection is altogether absent in solids. The conductive heat flow in certain solid samples, under conditions of negligible radiation losses is outlined in the present work. Thermal conduction is a process by which heat is transferred from one part of the sample to another as a result of the temperature gradient. Both electrons and phonons are instrumental in transferring energy from one place to another in a solid. Electrons are primary carriers in metals and these materials have fairly large thermal conductivities. For example at room temperature the thermal conductivity of aluminium is about 235 W/mK and that copper is about 400W/mK. Heat conduction in insulators can be considered as the diffusion of phonons from the hot to the cold end. Radiative heat transfer is a characteristic of all matter at a non-zero temperature and occurs by emission of electromagnetic energy.,which require no medium in contrast to the conductiveand convective mechanisms of heat transfer.The radiated energy is transported by electromagnetic energy(phonons).

For one diamentional heat flow Jean Fourier derived a basic law defining the propagation of heat as

$$\partial Q/\partial t = -kA\partial T/\partial x$$

This equation is known as the Fourier equation. The above equation implies that the quantity of heat conducted in the x-direction of a uniform solid in time dt is equal to the product of the conducting area A normal to the flow path, the temperature gradient ($\partial T/\partial x$) along the path and the thermal conductivity k of the conducting material.

The formal definition of thermal diffusivity arises from the expression for a transient temperature field in a conducting solid, which is given by

$\nabla^2 T = 1 / \propto \partial T/\partial x$.

where the thermal diffusivity α is given by $\propto = k /\rho c$,is the thermal diffusivity($m^2 s^{-1}$) 'k' is the thermal conductivity, 'ρ' is the density and 'C' is the specific heat.This important thermophysical property indicates rate at which heat is distributed in a material and depends not only on thermal conductivity but also on the rate at which energy can be stored.

It is evident from the units that, α represents the rate of heat flow. The reciprocal of thermal diffusivity ($1/\alpha$) expressed in sm^{-2} is a measure of the time required to heat-up a conducting material to a particular temperature level. Obviously, 'α' is a significant thermo physical parameter that determines heat diffusion in bulk as well as thin film samples.

4.3 Instumentation and detection techniques of a Transverse PBD setup for Thermal diffusivity measurements.

Photothermal deflection methods are based on the detection of thermal waves generated in the specimen after illumination with achopped or pulsed optical

radiatiation. Efforts have been made by several workers are still going on to make the experimental setup compact, economic, sensitive and error free. For designing any experimental setup,a thorough knowledge of the basic principle of the experiment and all the equipment including the cost (to make the setup economical) used in the measurement is a necessity. The main components for the mirage (PBD) technique are: 1) Excitation Source 2) Probe Source 3) Modulater 4) sample cell 5) Detection & Data acquisition assembly consisting of the position sensitive detector (bi-cell, quadrant cell etc.), preamplifier and Lock-in amplifier.

1) Excitation Source: Lasers are widely used because they provide the well-defined localized region of heating required for thermal wave probing techniques. The monochromatic spectral brightness enjoy significant advantageous over the lamp/monochromator combinations which account for their wide acceptance as light sources in Photothermal experiments. In addition, the laser output is highly collimated with cylindrical beam symmetry. The basic theory of the probe beam refraction treats the excitation beam as Gaussian. The strength or amplitude of the photothermal signal is directly proportional to the amount of laser light absorbed and to the laser power. However the high excitation power is found to cause deformation of the probe beam []. In the present work, a He-Ne laser (λ=6328 A^0, power 20mW) with geometrical dimensions of length 50 cm and diameter 5 cm is used as the excitation source. The beam diameter is 0.7mm and the divergence is 1.2.milliradians Compared to the Argon ion laser which is the commonly used excitation source, the present source is compact and economical. It also meets the

requirements of the pump source to be used in mirage experiments, in terms of coherence and directional properties and also the important condition that the sample absorbs at least a small portion of the energy of the pump source.

2) Probe Source,: The probe source used is a diode laser instead of the traditional setups use He-Ne laser as the probe source. However, the availability of cheap and compact semiconductor lasers operating in the visible region prompted us to use diode laser (λ=6328 A^0, 5mW) as the probe beam. Since the power required for the probe source in mirage experiment is small, only a low power semiconductor laser is required. The size of the laser is about7cm long and 1.5cm diameter. Easy power stabilization and absence of high frequency pointing noise are the other advantages of semiconductor lasers .

3) Modulator: Light from the excitation source should be modulated for observing the photothermal signal. The two main types of modulation are amplitude modulation and frequency modulation of which the former one is the most common technique. There are several ways for obtaining the amplitude modulation.

i) Mechanical Chopper: A rotating sectored blade provides an efficient modulator of light beam. This is the most inexpensive, efficient and easy way to modulate with the depth of modulation being 100%. High quality, variable speed and low vibration noise chopper are available commercially. However modulation up to a few kHz can be obtained with a mechanical chopper.

ii) Electrical: Gas lasers and semiconducting lasers can be modulated by varying the electrical drive current.The output of electrically excited CW gas lasers such as CO_2 laser can be modulated by varying the discharge tube current. However

this method suffers a serious setback in that the depth of modulation is cannot approach 100%. Moreover, the electrical circuits in the commercial ion lasers are not designed for high frequency modulation (f>100 Hz). The only advantage of overcoming the vibrations associated with the mechanical chopper does not favor this kind of a modulation being used from practical point of view.

iii) Electro optic: This method is superior to electrical and mechanical modulation methods with a modulation frequency range 0-20 MHz. The modulation depth can be as high as 100% and produces three times lower noise than the mechanical choppers under identical conditions. However these modulators are expensive and require wavelength specific half wave voltages.

Iv) Acousto optic: Extra dense flint glass, lead molybdenate and tellurium oxideare some of the crystals used in acousto optic modulation. Power in the diffractedlaser beam can be as high as 75% of the input laser beam.

A mechanical chopper (Stanford Model SR 540) can chop light beam at rates of 4Hz-4 kHz.. The whole frequency range operation requires two blades: a 6-slot blade for operation in the frequency range 4Hz-400 Hz and 30-slot blade for 400 Hz 4 kHz.

The modulation frequency has a major role in determining the whether the sample thermally thick or thermally thin. This is due to the fact that the thermal diffusion length follows an inverse relation with the square root of modulation frequency. As mentioned earlier in Chapter I, the sample is classified into thermally thick or thermally thin according to whether the thermal diffusion length is less than or greater than the thickness of the sample. Hence by controlling the modulation

frequency, the sample can be changed from thermally thick to thermally thin or vice versa. However, in the mirage measurements for thermal diffusivity, the technique can be applied irrespective of whether the sample is thermally thin or thermally thick.

4) Sample cell: The specimens under investigations are placed in a quartz cuvette of dimensions 10 mm x 10 mm x 5 mm. High purity carbon tetrachloride is used as the coupling fluid surrounding the sample, mainly due to the high value of dn/dT (6.12×10^{-4} K^{-1}) compared to air. This implies that for each degree temperature rise there will be considerable change in the refractive index, which will lead to an appreciable beam deflection. The comparatively low values of thermal conductivity ($k=0.099$ $Wm^{-1}K^{-1}$), specific heat capacity ($C_p= 0.85$ $Jg^{-1}K^{-1}$) and thermal diffusivity ($7.31 \times 10^{4} cm^{2}$ s^{-1}) also make carbon tetrachloride an ideal coupling fluid for thermal diffusivity measurements.The choice of carbon tetra chloride in most photothermal experiments is aqdue to its low value of thermal conductivity and high rate of change of refractive index with temperature.

5) Detector and data assembly: The position sensitive detector, a preamplifier and Lock-in-amplifier forms the assembly of detector.For light power measurements Silicon photodetectors are widely used in applications such as spectroscopy, photography, optical remote control, optical switches, analytical instrumentation, medical imaging, laser printers, bar code readers and many more. Another application that utilizes the photodetectors as optical position sensors and hence are referred to as Position Sensitive detectors (PSD). Under this head they are widely used in ultra fast, accurate auto focusing schemes for a variety of

optical systems, human eye movement monitoring etc. They are conveniently used in beam deflection or mirage experiments since the position of beam with fractions of microns can be obtained using PSD's. The PSD's are broadly classified into segmented PSD's and lateral effect PSD's.

Segmented PSD's are common substrate photodiodes divided into either two or four segments or photodiode elements separated by a gap or dead region and are referred to a s bi-cell and quadrant cell respectively. The photodiode elements are generally masked on to a common substrate so that their cathode is shared. A symmetrical optical beam generates equal photocurrents on all segments, if positioned at the centre. The relative position is obtained by measuring the output current of each segment. The bi-cell is used for one-dimensional measurement where as the quadrant cell is used for two dimensional measurements. The light spot diameter should be larger than the gap between the photodiode elements.

In the case of a quadrant cell, X and Y displacements of the light spot can be obtained using the simple relationships given below. If the segments of the quadrant cell are designated as A, B,C and D then

$$X= [(A+D)-(B+C)]/ [A+B+C+D]$$

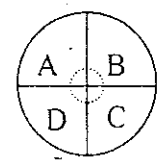

$$Y= [(A+B)-(C+D)]/[A+B+C+D]$$

However, in the case of a bi-cell, there are only two segments say A & B and can measure only displacement in one direction, then

$$X= (A-B)/(A+B).$$

Lateral effect PSD's are continuous single element planar diffused photodiodes with no gaps or dead areas. Though Schottky discovered lateral photo effect in 1930, devices using this principle became available only in the last decade or so. These detectors consist of only a single active element. Dividing photon-generated electrons within the substrate of the device rather than profiling the intensity distribution on the surface derives position. In fact the lateral effect detectors are not perfectly linear. Most devices exhibit $\pm$ 0.5% linearity over the central 25% of their area, $\pm$ 3% out to 75 % and $\pm$ 5% out to the periphery. The major contribution to this nonlinearity is the sheet resistance of the device. At the centre of the detector where the light spot is equidistant from all contacts these non-uniformities will tend to average out to a greater extent than at out lying areas on the detector.

In the present work we used a bi-cell (SPOT 2D from M/s UDT Sensors Inc) as the position sensitive detector for the probe beam deflection measurements. The important features of this bi-cell include high accuracy, excellent resolution, high-speed response, ultra low dark current and excellent response match. Spectral response range is from 350-1100 nm and excellent stability over time and temperature. They have fast response times necessary for high speed or pulsed operation and position resolutions of better than 0.1 μm. Though the signal output can be directly read from each segment, electronic modules can be used in order to perform the task. We have constructed a preamplifier to obtain the amplified output since the deflection signal is usually small.

Preamplifier:

The block diagram of the preamplifier circuit used in the present setup is as shown in figure (1). Giving common signal from a function generator to the two different inputs initially tests the preamplifier and it is ensured that the output is zero. Furthermore, two different inputs are fed to obtain the same result as expected theoretically.

Lock-in-Amplifier:

The out put of the quadrant detector is converted into electric signal using an I toV convertor ,and is fed to the lock-in amplifier.The Lock-in Amplifier is used to detect and measure very small a.c signals using a technique known as phase-sensitive detection in order to single out the component of the signal at a specific reference frequency and phase.Noise at other frequencies are rejected and do not affect the measurement. Lock-in-amplifiers use a phase locked loop (PLL) to generate the reference signal. The PLL locks the internal reference oscillator to the external reference signal provided to the lock-in-amplifier resulting in a reference sine wave of a particular frequency and a fixed phase shift. In the present work, SR830 (Stanford Research Model) is used. The SR 830 operates from 100V, 120V, 220V or 240V nominal a.c. power source having line frequency 50 Hz or 60Hz and can measure voltage from 2nV to 1 V.

The schematic diagram of the experimental setup used for the measurement of thermal diffusivity is as shown in figure (2). In the present work, we employed the transverse scan method The measurements are performed by varying the distance between the pump and probe

beams, and hence requires that either of these two beams be fixed. We chose to fix the pump beam and scan the probe beam across the sample surface, since our pump source is bulky compared to the probe source. In traditional mirage experimental setups, usually the probe beam is fixed

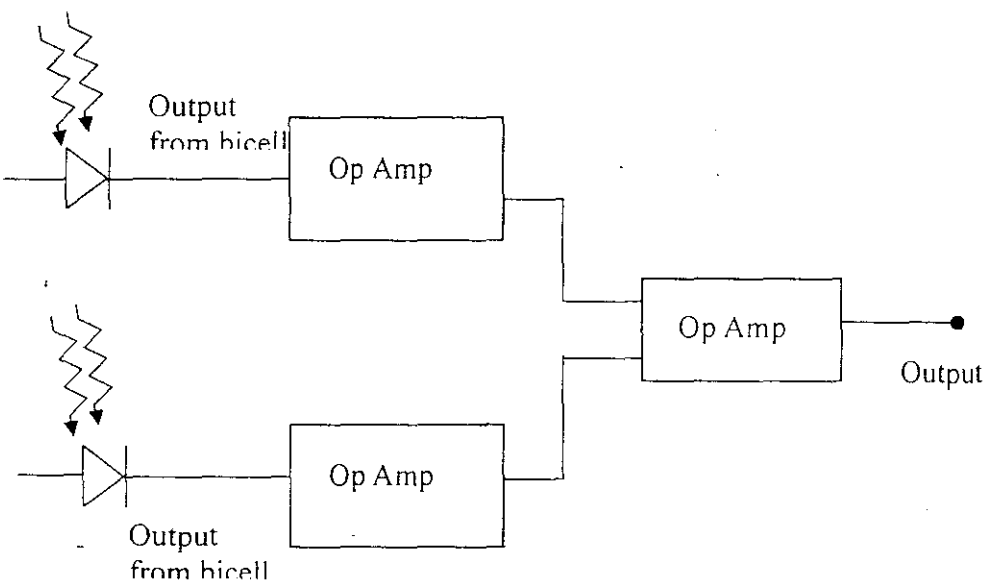

Figure(1):Block diagram of the pre-amplifier

and the pump beam scans across the sample surface with the help of a mirror arrangement. This is because probe beam scanning requires a synchronous movement of the lens focusing the probe beam and the

detector, which makes the system complex, especially when the probe source is bulky.

. In our experiment, the probe laser is of small size that, it together with the focusing lens and detector could be fixed on an aluminium flat of length 30 cm and width 1cm, which in turn is fixed onto an XYZ translation stage, so that all the three move in synchrony.

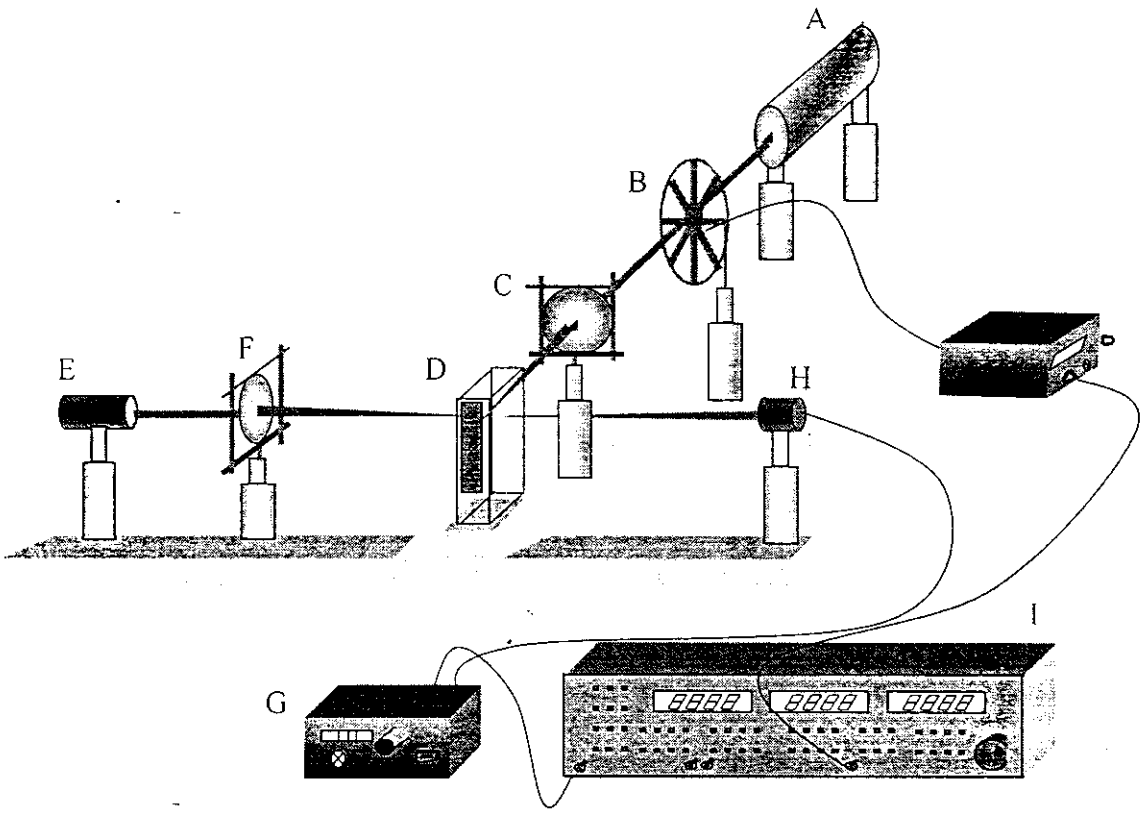

Figure 2: Schematic diagram of the experimental setup

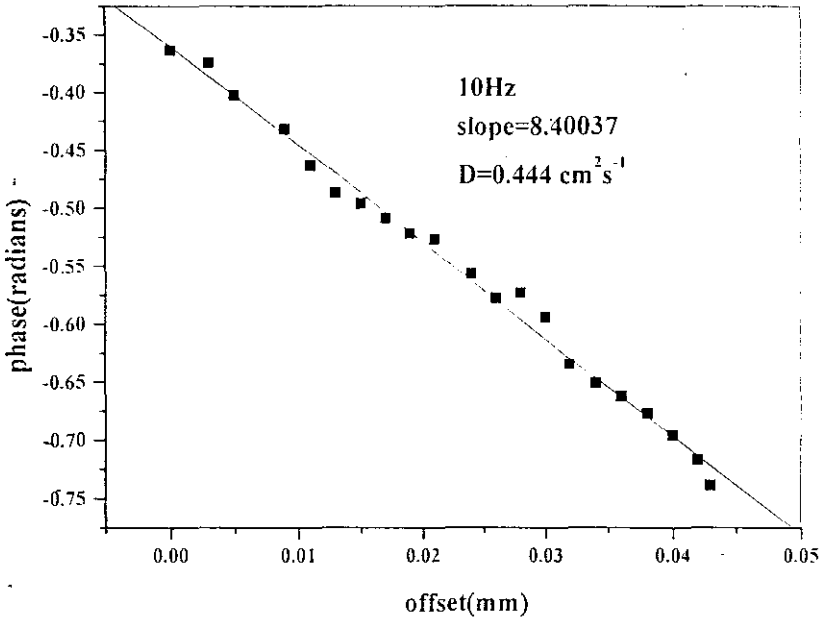

Figure (3) shows. the plot of phase vs. transverse offset of InP at 10 Hz.

The sample fixed in the cuvette is also fixed on a translation stage. The pump laser and these two translation stages are fixed on an optical breadboard with honeycomb structure, placed on a granite table so as to minimize the errors due to mechanical vibrations. The experimental setup is standardized for thermal diffusivity using InP wafer of thickness 350μm using the Phase Method as described in Chapter II. Figure (3) shows the plot of phase vs. transverse offset at a modulation frequency 10 Hz. The thermal diffusivity value calculated from the slope of graph is 0.444 cm^2s^{-1} and is in good agreement with the literature value (14).

4.4 THERMAL DIFFUSIVITY OF ORGANIC MOLECULES.

Periodic photothermal heating produces modulations in the refractive index of a medium because of the temperature dependence of the refractive index.The basis of the PBD is to measure the deflection of a probe beam passing through the coupling liquid just above the surface heated at a point by a focused pump beam. At small distances above the surface the temperature distribution in the medium will match that in the solid and enabling probe beam deflection measurements to be used to obtain information about the thermal distribution in the solid. Experimentally,the transverse probe beam deflection component is monitered as the probe beam is scanned to vary. its distance x away from the heated spot,keeping its height abovethe surface constant.

Figures (4,6,8,10,11,12,14) show the phase vs offset plot for Diethylene triamine.Phenyl Hydrazine and Propyl amine.All graphs are linear as expected in the phase method.slope is evaluated from these graphs are inverse of the characteristic length and thermal diffusivity values are tabulated.The results are confirmed using amplitude method for the same set of modulation frequencies.The graphs showing the ln(Amplitude) and offset are shown in Figures(5,7,9,10,13,15).

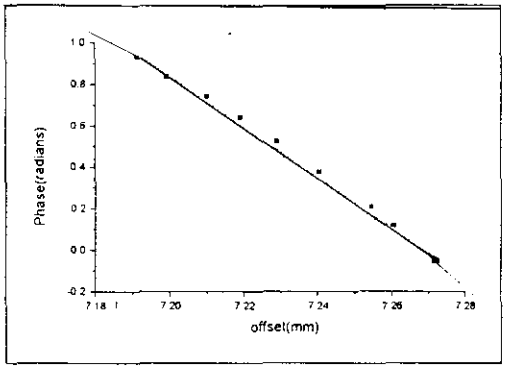

Figure (4) phase vs. the pump-probe offset for 12 Hz for Diethylene Triamine

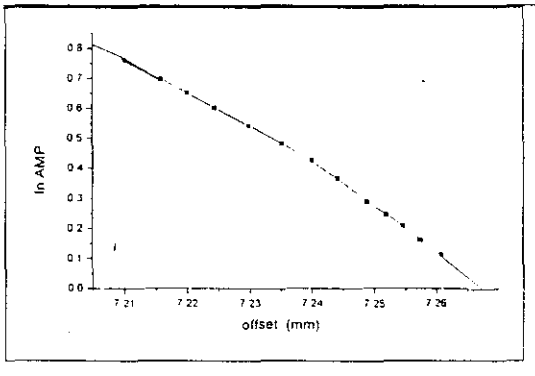

Figure (5)ln Amp phase vs. the pump-probe offset for 12 Hz for Diethylene Triamine

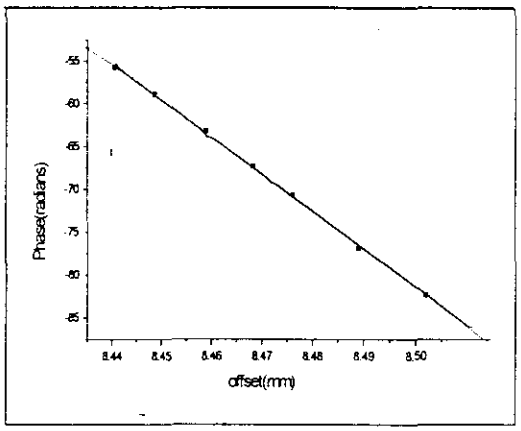

Figure (6) phase vs. the pump-probe offset for 8 Hz for Diethylene Triamine

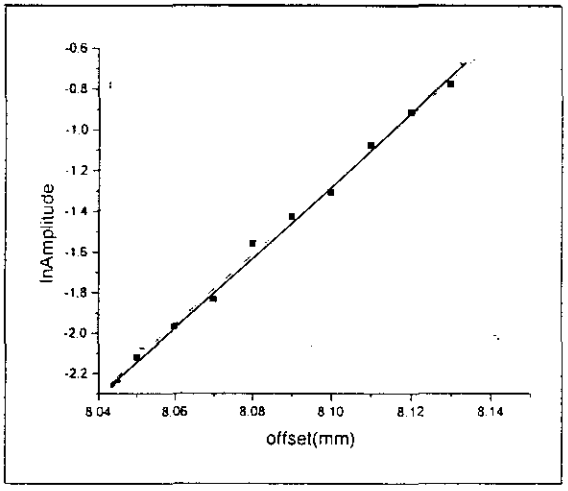

Figure (7)ln Amp vs. the pump-probe offset for 8 Hz for Diethylene Triamine

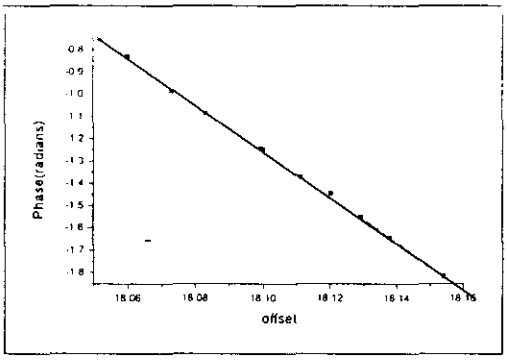

Figure (8) phase vs. the pump-probe offset for 12 Hz for Phenyl hydrazine

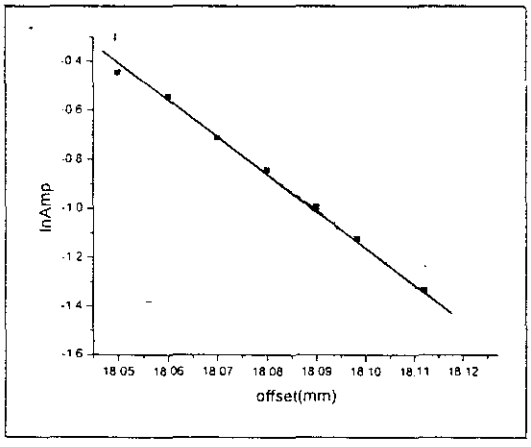

Figure (9)ln Ampe vs. the pump-probe offset for 12Hz for Phenyl hydrazine

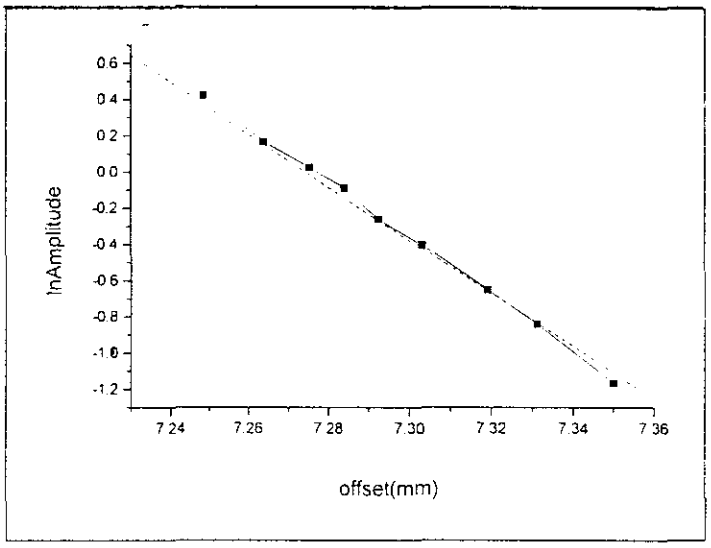

Figure (10) ln Ampe vs. the pump-probe offset for 8Hz for Phenyl hydrazine

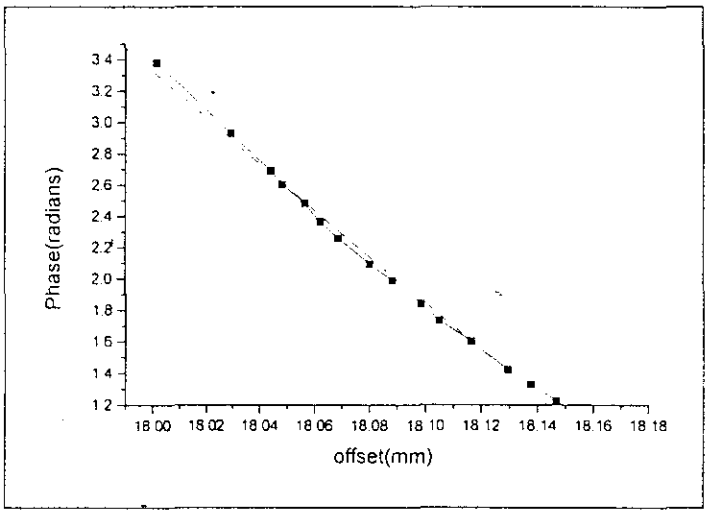

Figure (11) phase vs. the pump-probe offset for 8 Hz for Phenyl hydrazine

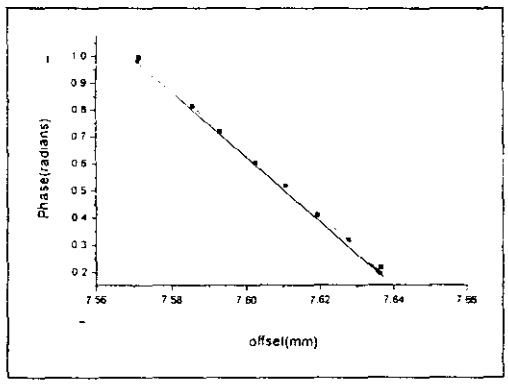

Figure (12) phase vs. the pump-probe offset for12 Hz for Furfuryl Amine

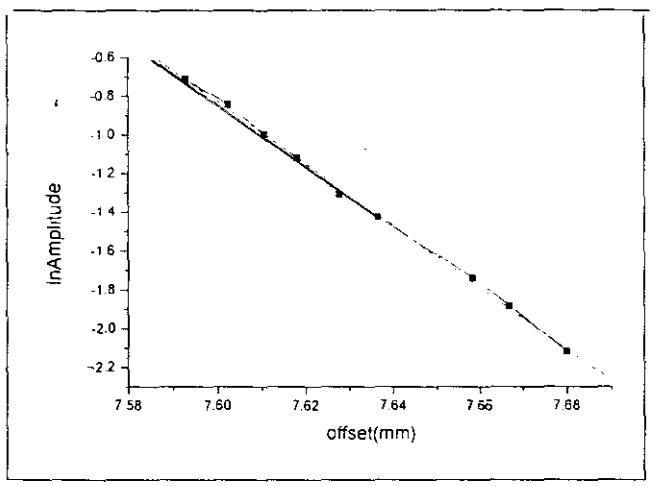

Figure (13) ln Ampe vs. the pump-probe offset for12 Hz for Furfuryl Amine

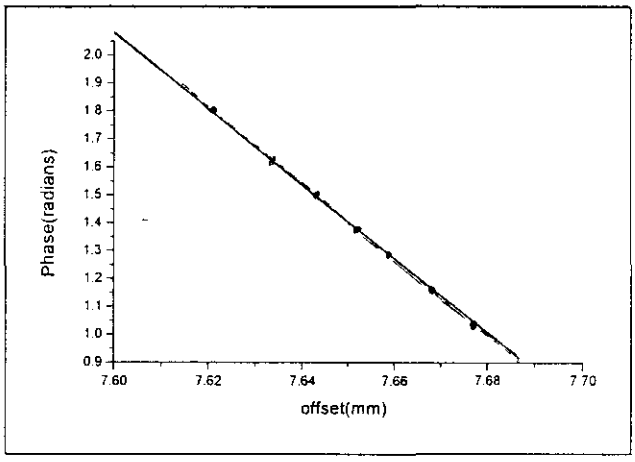

Figure (14) phase vs. the pump-probe offset for 8 Hz for Furfuryl Amine

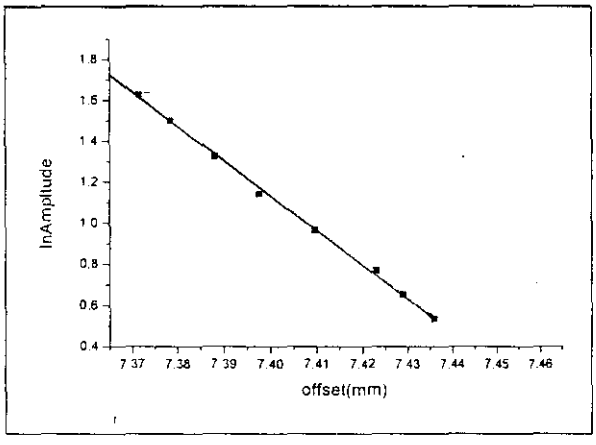

Figure (15)ln Ampe vs. the pump-probe offset for8 Hz for Furfuryl Amine

Table.1 shows the thermal diffusivity values calculated from the slopes of graphs

Sample	Method of Analysis	Frequency (Hz)	Thermal Diffusivity (cm^2s^{-1})
Diethlene Triamine	Phase Method	12	0.001643
		8	0.00166
	Amplitude Method	12	0.001628
		8	0.001652
Phenyl Hydrazine	Phase Method	12	0.001569
		8	0.001526
	Amplitude method	12	0.0016846
		8	0.001873
Furfuryl Amine	Phase Method	12	0.001882
		8	0.001879
	Amplitude Method	12	0.001879
		8	0.001862

4.5. Determination of Thermal diffusivity of Plasma polymerized films:

Polymer films are of great importance for the past decades due to its increased industrial applications. Plasma polymerized thin films find innumerable applications ranging from corrosion free adhesive coating materials to sensor technology and microelectronics The thermal diffusivity is an equally important parameter like electrical conductivity, which is to be known for the effectively applying these materials for different purposes. The thermal conduction parameters of polymers are very low whose determination is really challenging and the sample being in thin film form adds to the difficulty. Photothermal Beam deflection technique or mirage technique can accurately determine the thermal diffusivity of thin film samples of low thermal diffusivity. To the best of our knowledge, the present work determined the thermal diffusivity values of R.F. plasma polymerized thin films poly Diethylene Triamine, poly Phenyl Hydrazine, and poly Furfurylamine Hence we have used two different methods of analysis namely Phase method and Amplitude method ( ), which are described in detail in Chapter II. Carbon tetrachloride is used as the coupling medium. The measurements were performed at two different modulation frequencies in each case.

Figures (16,17)(20,21)and (24,25) show the phase vs. offset plot for poly – DiethyleneTriamine, poly PhenylHydrazine and,poly Furfurylamine respectively for different modulation frequencies (which are indicated in the corresponding graphs). All the graphs are linear as expected in the phase method. The slopes

evaluated from these graphs are the inverse of the characteristic length and thermal diffusivity values obtained from the slopes is tabulated in Table II. For confirmation, the analysis was done using the amplitude method for the same set of modulation frequencies as done in the case of Phase Method. The graphs between ln [amplitude] and offset are shown in figures which are also linear as expected. The thermal diffusivity values are calculated from the slope and are tabulated in Table II.

Heat transfer from or to a material can occur by a combination of conduction,convection and radiation.Heat diffusion in solids can take place either through the lattice vibration, carrier diffusion and carrier recombination. The latter two mechanisms are mainly characteristic of the semiconductors ( ). However, the thin film samples prepared by the r.f plasma polymerization techniques are highly crosslinked, exhibit exceptional dielectric properties( )and are basically insulators. The high direct and indirect band gap compared to the pump beam energy (1.95eV since a He-Ne laser having wavelength 632.8 nm is used) rules out the possibility of photo-excited carrier generation. Hence any heat diffusion in these samples are solely due to the lattice vibrations without any contribution from electron diffusion or carrier recombination.

The criteria for classification of the samples possessing high or low thermal diffusivity depends on whether the thermal diffusivity of the sample is higher or lower than that of the coupling medium.Two basic factors that need to

be considered in the photothermal beam deflection technique are the effects of coupling media and substrate on which the samples are coated. Earlier

experiments performed reveal that liquid paraffin can also be used as the coupling medium instead of carbon tetrachloridein order to have an idea about the influence of the thermal properties of coupling media to the deflection signal.The results in both cases yielded the same result.Contribution from the coupling fluid to the photothermal signal becomes dominant in the skimming configuration only when the thermal diffusivity of the coupling fluid is greater than that of the sample. In the present work, although the thermal diffusivity of the samples under study are low, the coupling media chosen in our measurements carbon tetrachloride ($D_{CCl4} \sim 0.731 \times 10^{-3}$ cm^2s^{-1}) have still lower diffusivity values. In conclusion, the thermal properties of the coupling media do not influence the photothermal measurements.

Fig. 16

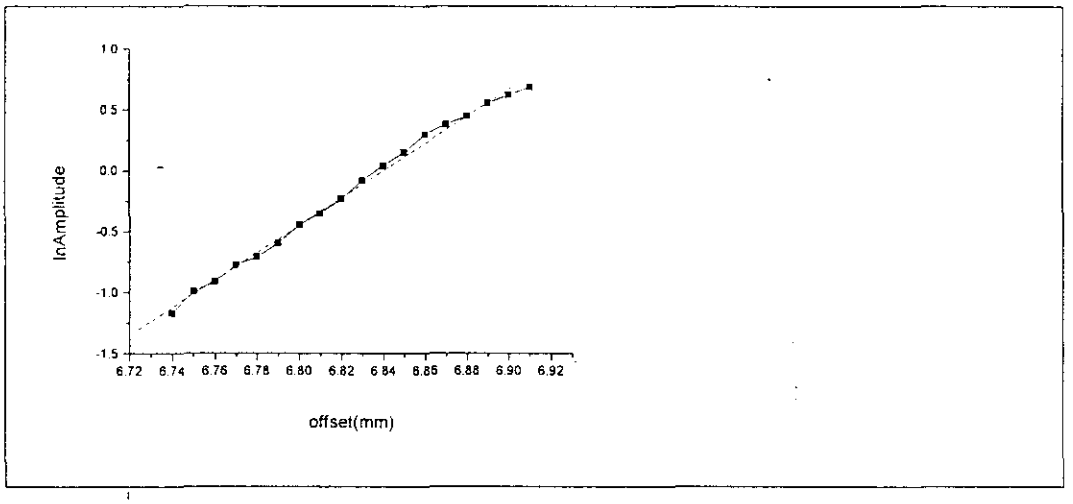

Figure[16] showing the lnAmplitude vs offset 8Hz of poly DiethyleneTriamine

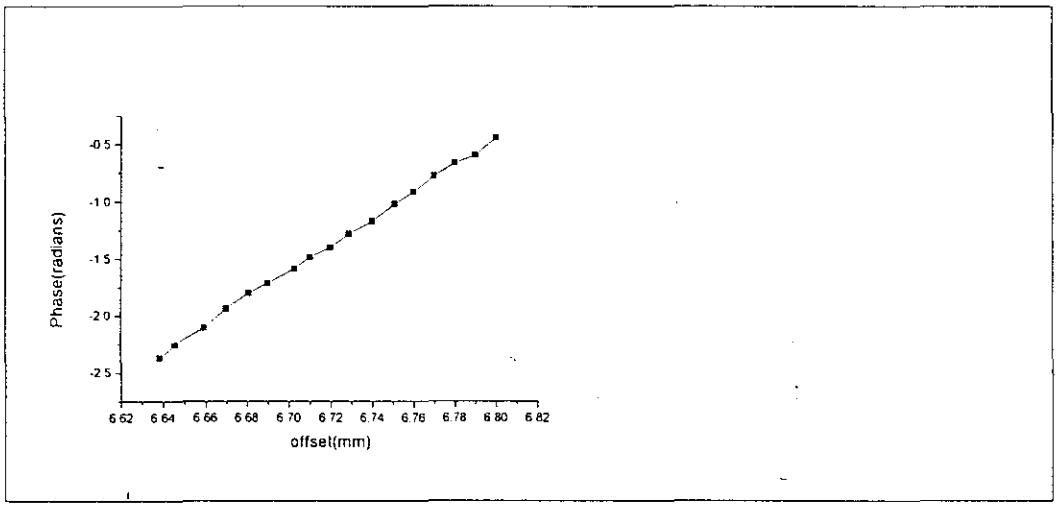

Figure[17] showing thephase vs offset 8Hz of poly DiethyleneTriamine

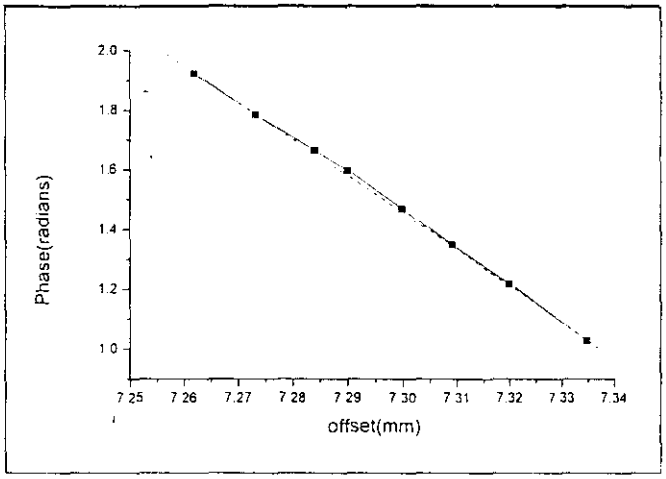

Figure[18] showing thephase vs offset 12Hz of poly DiethyleneTriamine

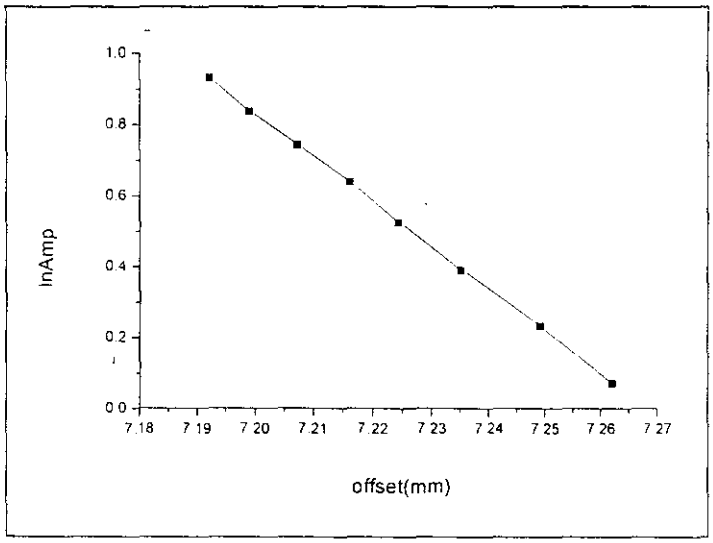

Figure[19] showing theAmplitude vs offset 12Hz of poly DiethyleneTriamine

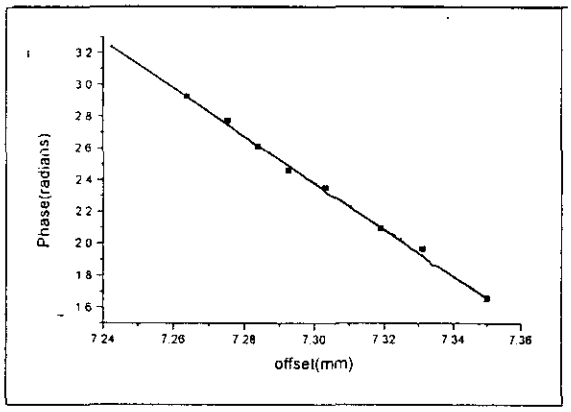

Figure[20] showing Amplitude vs offset 8 Hz of poly Phenyl Hydrazine

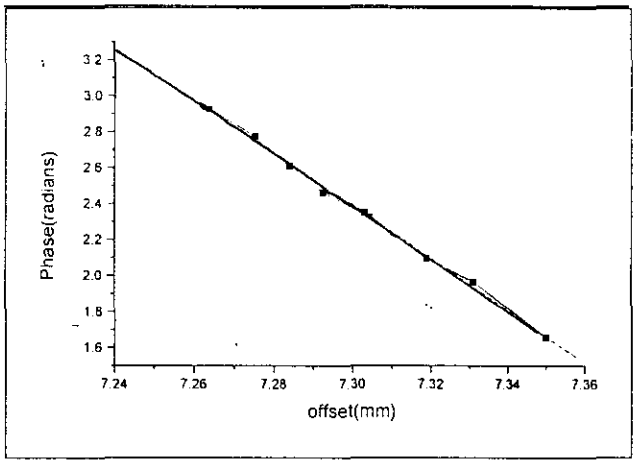

Figure[21] showing Phase vs offset 8 Hz of poly Phenyl Hydrazine

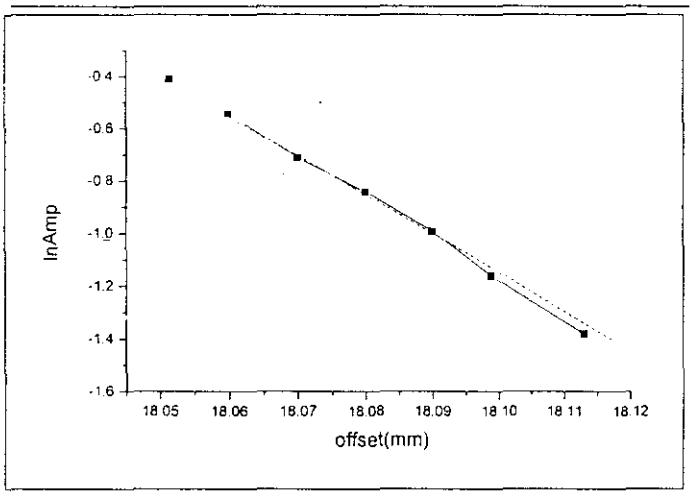

Figure[22] showing Ampltude vs offset 12 Hz of poly Phenyl Hydrazine

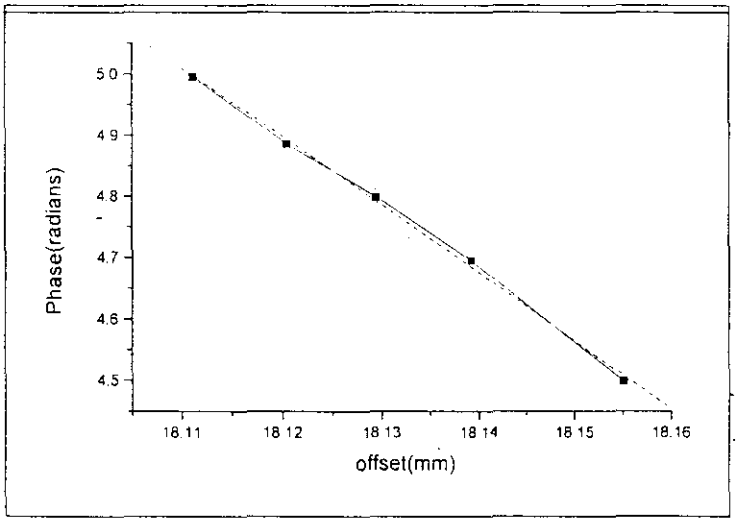

Figure[23]showingPhase vs offset12 Hz of poly Phenyl Hydrazine

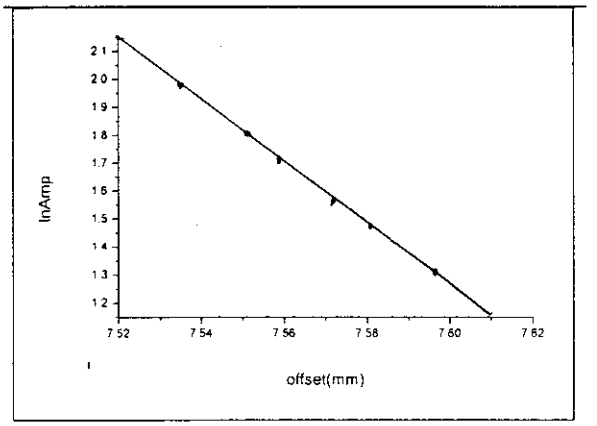

Figure[24] showing Ampitude vs offset 8 Hz of polyFurfurylAmine

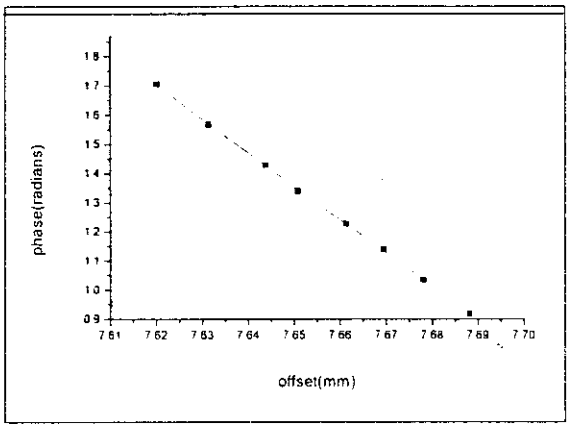

Figure[25] showing Phase vs offset 8 Hz of polyFurfurylAmine

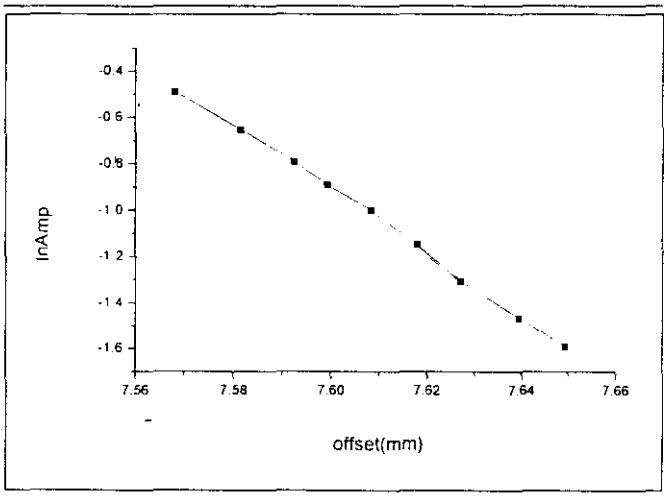

Figure[26] showing lnAmp vs offset 12 Hz of polyFurfurylAmine

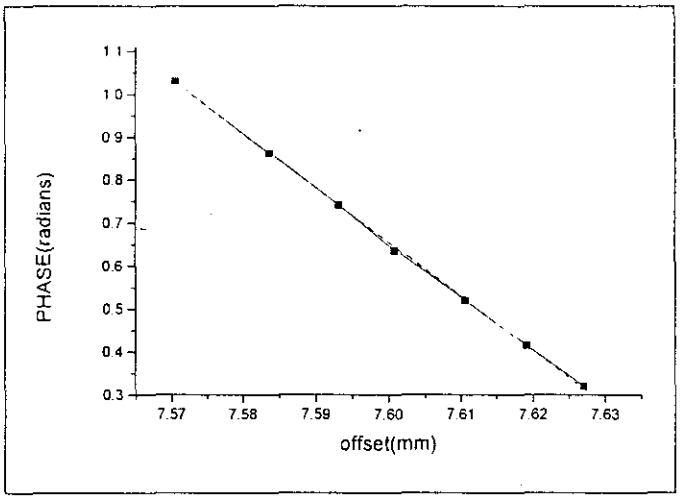

Figure[27] showing Phase vs offset 12Hz of Poly Furfurylamine

Table11 showing the Thermal diffusivity values determined from slope of graphs.

Sample	Method of Analysis	Frequency (Hz)	Thermal Diffusivity (cm^2s^{-1})
Poly Diethylene Triamine	Phase Method	8	0.002256
		12	0.002306
	Amplitude Method	8	0.002287
		12	0.002114
Poly Phenyl Hydrazine	Phase Method	8	0.002054
		12	0.002290
	Amplitude method	8	0.002076
		12	0.002118
Poly FurfurylAmine	Phase Method	8	0.002409
		12	0.002306
	Amplitude Method	8	0.00211
		12	0.002306

All the graphs are linear and thermal diffusivity values are calculated from the slopes, which are tabulated in Table II. It is observed that the thermal diffusivity values of the organic liquids under study shows a reduced value compared to their corresponding plasma polymerized thin film samples. This can be explained on the basis of the difference in the heat conduction mechanism in liquids and solids since thermal diffusivity is a measure of the rate of heat flow. In the case of liquids, the heat transport mainly takes place through convection which involves actual motion of molecules (atoms). However, in the case of thin films there is a definite lattice and heat conduction is mainly due to phonons (lattice vibrations) provided there is no contribution from the charge carriers (carrier diffusion and carrier recombination). In the present case, the plasma polymerized thin films have only a slight absorption at the excitation wavelength (632.8 nm) as observed from the absorption spectra of the thin film samples under study and hence the possibility of occurrence of photogenerated carriers is negligible. Thus the contribution to heat conduction from the carriers is neglected. Therefore, the heat transportation in solids takes place at a faster rate than the liquids thereby increasing the thermal diffusivity of solids.

From their absorption spectra, all the samples shows very low absorption at the pump laser wavelength, and are thermally thin at the modulation frequencies used in the experiment. In such circumstances, substrate absorption can play non-negligible role in the photothermal measurements. As a result, the samples must now be treated as layered one and we have to relax the assumption that the backing or substrate is non-absorbing. However, in the present work, the samples

are coated on to a glass substrate, which is perfectly non-absorbing at the pump beam wavelength. Hence the effect of substrate on the photothermal measurements can be neglected.

While dealing with the polymer samples, another important factor to be dealt with is the effect of the temperature rise on the expansion of the samples. However, the temperature rise in the heated area is estimated to be approximately 1 degree, which can cause a surface deformation of only <1nm. This expansion can affect the photothermal measurements only when the bouncing configuration is employed. In the present work skimming configuration is used where the probe beam skims the sample surface and the height of the probe beam above the sample surface is limited by the spot size of the probe beam. Due to the large spot size of the probe beam compared to the surface deformation, any error in the photothermal measurements caused by the thermal expansion of polymers is completely eliminated.

In conclusion, the thermal diffusivity values organic molecules and that of of r.f plasma polymerized poly diethyleneTriamine poly Phenyl hydrazine,poly Furfuryl amine thin films are measured using a compact and simple photothermal beam deflection experimental setup. The analysis of the deflection signal for thermal diffusivity is done using the Phase method and is verified using the Amplitude method. The measurements are repeated for different modulation frequencies , all of which are found to lead to similar results.

REFERENCES:

1) Jeffrey A Sell, Photothermal Investigations on Solids and Fluids, Academic Press Inc, New York (1989)

2) A.Rosencwaig, A.Gersho, J.Appl.Phys. 47, 64 (1976)

3) A. Rosencwaig, Photoacoustics and Photoacoustic Spectroscopy, John Wiley & Sons, New York, (1980)

4) C. Garcia-Segundo, M.Villagran-Muniz, S.Muhi, J.Phys.D: Appl.Phys 31, (1988) 165.

5) J.A.Balderas lopez, D.Acosta-Avalos, J.J.Alvarado, O.Zelaya-Angel, F.Sanchez-Sinencio, C.Falcony, A.Cruz-Orea, H.Vargas, Meas.Sci.Technol. 6 (1995) 1163

6) A.Rosencwaig, T.W.Hindley, Appl.Opt. 20(4) (1981) 606.

7) E.Marin, H.Vargas, P.Diaz, I.Riech Phys.stat.sol (a) 179 (2000) 387.

8) J.C.Murphy, L.C.Aamodt, J.Appl.Phys. 51(9) (1980) 4580.

9) L.C.Aamodt, J.C.Murphy, J.appl.Phys. 52(8) (1981) 4903.

10) M.A.Schweitzer, J.F.Power, Appl.Spectro., 48(9) (1994) 1054.

11) M.A.Schweitzer, J.F.Power, Appl.Spectro., 48(9) (1994) 1076

12) P.K.Kuo, M.J.Lin, C.B.Reyes, L.D.Favro, R.L.Thomas, D.S.Kim, Shu-Yi-Zhang, L.J.Inglehart, D.Fournier, A.C.Bocarra, N.Yacoubi, Can.J.Phys., 64 (1986) 1165.

13) P.K.Kuo, E.D.Sendler, L.D.Favro, R.L.Thomas, Can.J.Phys. 64 (1986) 1168.

14). M.Bertolotti, V.Dorogan,G.Liakhou, R.Li Voti,S.Paoloni,C.Sibilia, Rev.Sci.Instrum 68 (3), 1521 (1997)

CHAPTER V

THERMAL DIFFUSIVITY MEASUREMENT USING PHOTOACOUSTIC TECHNIQUE.

5.1 Introduction:

Many of the applications of the photothermal phenomena depend on a clear undertanding of the ways in which thermophysical properties or sub-surface structures affect heat flow. Thermal diffusivity is a thermal transport parameter which determines the rate of heat diffusion in a medium.Thermal wave physics has emerged as an effective research and analytical tool in all branches of science and technology [1].Invention of photoacoustic effect and the subsequent emergence of various photothermal methods have revolutionized the applicability of thermal waves for the detection and evaluation of material properties and processes.[2])

Substances exhibiting high electrical conductivity, optical transparency and than can be efficiently grown into thin films are essential for the next generation photovoltaics, energy efficient windows, flat panel displays, organic LED's and other optoelectronic applications. Advanced lithium ion batteries have a wide range of application in portable electronic devices and in the future electric vehicle systems. The high temperature behavior of these batteries is a vital issue, since elevated temperature can be used to enhance the battery performance or arise as an unwelcome complication. Being a widely used and important cathode

material in the present day battery technology, measurement of the thermal diffusivity of $LiNio_2$ has great practical significance.More recent innovations are the photoelecto-chemical or photo regenerative cells which convert solar energy into electrical energy. Fuel cells are now fully operational in space satellites while lithium batteries are commonly used in many devices.Most of today's exotic rechargeable battery systems such as nickel-cadmim,nickel metal hydride and the variety of lithium-based cells are twentieth centuary developments.In the present work the structural characterisation and thermal properties of $LiNIo_2$ is studied using photoacoutic technique.

5.2 HEAT CONDUCTION IN SOLIDS.

Heat conduction is a process in which heat is transferred from one part of the sample to another as a result of a temperature gradient. Mainly there are two mechanisms by which thermal transport is taking place in a solid.

1.The heat conduction due to charge carrier motion which is termed as electron or hole heat conductivity $(k_c)_1$ and

2 The heat conduction due to lattice vibration or phonons(k_L)

When a temperature gradient is built up in a substance the energy gradient is transmitted in such a manner that energy is transmitted from an atom which oscillates with more intensity to an atom which oscillates with less intensity .

The total heat conductivity $k = k_c + k_L$.

In this k_L is related to elastic properties of the solid and k_c to the charge carrier concentration.In metals $k_c >> k_L$ and in dielectrics $k_L >> k_c$. In semiconductors k_c strongly depends on the composition and on the temperature.

When a semiconductor is irradiated with an optical radiation of suitable energy, in addition, photo generated carrier recombination will also contribute to the heat transport. Free carrier generation resulting from the light absorption occurs when the incident photon energy is greater than the band gap energy. The photon is absorbed in this process and excess energy Eph-Eg is added to the electron and hole in the form of kinetic energy.Now the non – radiative recombination of these carries will result in the form of heat to the lattice [3]. Another ,form of non-radiative recombination process is the surface recombination ..Surfaces and interfaces of semiconductors usually contain a large number of recombination centres because of the abrupt termination of the crystal,which leaves a large number of electrically active dangling bonds.

In addition, surfaces and interfaces are likely to contain more impurities. The surface recombination is also an interband recombination process and excess energy is ultimately transferred to the lattice as heat. Trap assisted recombination is also one among the recombination mechanisms. Apart from this there exists an instantaneous thermalisation component which arises from intra band interaction of excited electrons with the lattice. This process is an after effect of excitation of electrons of the higher levels in the conduction band. Such hot electrons will come back to the minimum of the conduction band by the imparting the excess energy to the lattice. This thermalisation takes place in pico seconds and hence known as instantaneous thermalisation.

5.3 THERMAL CONDUCTION BY PHONONS

The transmission of heat can be conveniently explained by considering phonon gas transport. In every region of space there are phonons traveling in all directions, much like the molecules in gas. The advantage of using this gas model is that many of the concepts of the kinetic theory of gases can also be applied here. The thermal conductivity is given by

$$k=cvL/3$$

Where c is the specific heat per unit volume [4,5]) v is the speed of the particle and L its mean free path. The only difference in solids is that phonons replace the molecules so that the velocity and mean free path now refer to phonons instead of gas molecules. The thermal conductivity k will be determined by the nature of the mean free path, since c is constant at high temperature and varies as T^3 at low temperatures and v is almost a constant.Here L is the average distance the phonon travels between two successive collisions. This in turn is determined by the scattering mechanisms. The important scattering mechanisms are (1) scattering due to phonon-phonon interactions (2) scattering by the imperfections such as impurities and dislocations and (3) boundary scattering caused by collision of phonons with the external boundaries of the sample.

The phonon-phonon collision becomes more pronounced at high temperatures, at which the atomic displacements are large and this give rise to harmonic coupling between phonons, causing their mutual scattering. In this

region the mean free path is inversely proportional to the temperature ($L \propto 1/T$). This is reasonable, since the larger the value of T, greater is the number of phonons participating in the collision process.

Crystal imperfections such as impurities and defects also can scatter phonons because they partially destroy the perfect periodicity, which is the very basic concept of a freely propagating lattice wave. The scattering may be due to (1) point defects and/or due to (2) dislocations. Thus the random distribution of the different isotopes leads to a decrease in thermal conductivity. For instance a substitutional point impurity having a mass different from that of the host atom causes scattering of the wave at the impurity. The greater the difference in mass and density of the impurities, the greater is the scattering and the shorter the means free path. This gives rise to a decrease in the value of thermal conductivity there by reducing the thermal diffusivity of the sample.

Though various techniques are available for the measurement, the photo acoustic technique has proved to be the most efficient and convenient tool for the measurement of the thermal diffusivity. The detected signal is strongly depend upon the interplay of the sample's optical absorption coefficient for the incident radiation, the light into heat conversion efficiency, as well as how heat diffuses through the samples. The dependence of the photons acoustic signal on the absorption coefficient allows one to perform spectroscopic studies, where as the signal is proportional to the light into heat conversion efficiency means that it is complementary to other photo induced energy conversion processes. Thus the photos acoustic signal can be used for obtaining the information concerning the non-radiative de-excitation processes.

5.4 SIGNIFICANCE OF THERMAL DIFFUSIVITY

The photoacoustic process depends not only on the optical properties of the sample but also on its thermal and geometric properties and in some cases on its eleastic properties as well. The thermal diffusivity α is of direct importance in heat flow studies as it determines the rate of periodic or transient heat propagation through a medium.

Jean Fourier has derived the basic low defining the propagation of heat in a onedimensional homogenous solid as [6])

$$\partial Q/\partial t = -kA\partial T/\partial x$$ this is known as Fourier equation.

This equation implies that the quantity of heat ∂Q conducted in the X-direction of a uniform solid in time ∂t is equal; to the product of the conducting area A normal to the normal to the flow path, temperature gradient $\partial T/\partial x$ along the path and thermal conductivity k of the material.

Formal defenition of thermal diffusivity arises when deriving an expression for a transient temperature field in a conducting solid from Fourier equation. The equation describing the temperature field in a homogeneous, linear conducting solid with no internal heat source is $\nabla^2 T = 1 / \propto \partial T/\partial x$.

Here $\propto$ is the thermal diffusivity which is related to the thermal conductivity (k),density (ρ) and specific heat capacity C of the material as

$$\propto = k / \rho c$$

The thermal diffusivity α is expressed in m^2/s . Because of its controlling effect and common occurance in heat flow problems, its determination is often necessary and knowledge of the thermal diffusivity can in turn be used to calculate the thermal conductivity. Changes in the thermal parameters such as thermal conductivity can be used to monitor changes with in a material. The significance of α is evident from the above relationship. The reciprocal $1/\alpha$ expressed in sm^{-2} is a measure of the time required to heat the material to some temperature level. Therefore the ratio of heating times for two materials of the same thickness will be inversely proportional to the thermal diffusivity values. Thus α is a significant thermopdynamic parameter that determines the heat diffusion in bulk as well as in film samples.

5.5 Lithium ion battery concepts

These batteries were developed to meet the demand for systems with higher specific capacity, energy and power. Non- aqueous electrolytes have to be employed since lithium decomposes water. The discovery of a new electrolyte based on lithium salt dissolved in an ion conducting organic polymer has led to a solid-state electrochemical device. This has led to the so-called lithium ion battery concept. The lithium battery technology is now quickly replacing the older techniques.[7].The advantages of the type of batteries include their high energy density, wide temperature range and long shelf life.

Lithium metal is used as a lithium battery anode material because of its light weight, good conductivity, high electrochemical equivalence and high voltage. Most cells are limited to 1.5V while the lithium cells have voltages up to

about 4V. This reduces the number of cells required in a multiple cell battery. The storage life of lithium batteries can be as much as ten years at normal temperatures and store well even at elevated temperatures. These lithium batteries are widely used in battery back-ups, watches cameras, calculators, and military equipments and as standby emergency power.

In lithium ion battery, the negative electrode consists of a metallic lithium foil, which exploits the low weight and high reactivity of lithium. The cathode is a transition metal oxide and the electrolyte is a lithium salt dissolved in liquid or polymer gel. Transition metal oxides used in these batteries are mainly complex lithium containing oxides of cobalt, nickel or manganese such as $LiCoO_2$, $LiNiO_2$ & $LiMn_2O_4$. of these $LiCoO_2$ is found in commercially successful rechargeable lithium ion batteries.

The spinel $LiMn_2O_4$ does not have an acceptable cycle life. $LiCoO_2$ is currently used as a cathode material in commercial rechargeable lithium batteries due to its ease of preparation on an industrial scale and its stable electrochemical properties. It suffers form a disadvantage that only half of its theoretical capacity can be used. It is also both toxic and expensive. $LiNiO_2$ is an attractive cathode material because of the relatively abundant natural resources of nickel. This compound is experimentally benign and does not have the toxic effects of $LiCoO_2$. $LiNiO_2$ shows semiconducting property. The stochiometric $LiNiO_2$ compound belongs to the rhombohedral system in which Li+ and Ni^+ ions occupy the octahedral3a and 3b sites, respectively,of fcc packing.Such a structure provides a two diamentional

channel for Lithium ion intercalation and de-intercalation.The hexagonal parameters are a=2.8806A^0 andc=14.2050 A^0 The earlier experiments carried out shows that the electronic conductivity is in the semiconducting range of the order of 10^{-3}-10^{-4} m ho-m^{-1}.

5.6 Experimental techniques.

Layered $LiNiO_2$ compounds are synthesized using a variety of conditions. In this work, solid-state reaction method is used. Although structural investigations using electrochemically obtained samples give direct information of structural changes during charge-discharge processes with controllable rates in a cell, a chemically synthesized sample has several advantages over an electrochemically prepared sample for the purpose of structural analysis,

1. It does not have additives such as binder or carbon, which must be treated as an impurity in the analysis.
2. A large amount of uniform sample can be prepared.
3. The experiment can be performed rapidly because there is no need for cell construction and subsequent charge discharge processes.

5.7 Synthesis of LiNiO2 compounds

A direct solid-state reaction was effected between $LiOH.H_2O$ and NiO to prepare stochiometric $LiNiO_2$. The materials were weighed separately taking the precursors in the molar ratio 1:1 (i.e, to prepare 5 grams of $LiNiO_2$ 2.148 grams of $LiOH.H_2O$ and 3.825 grams of NiO were taken.)

The reactants were mixed thoroughly in an agate mortar and pestle. The mixture was pelletised at 7 tons and the pellets were fired at 700°C in air for about 48 hours.

The chemical reaction taking place is.

$$4\ LiOH.H_2O + 4\ NiO + O_2 \rightarrow 4LiNiO_2 + 6H_2O.$$

the final mixture obtained is $LiNiO_2$. The experiment is repeated taking precursors in the molar ratio 1.05:1 (i.e., to prepare 5 grams of $LiNiO_2$ 2.158 grams of $LiOH.H_2O$ and 3.811grams of NiO were taken).

For the third sample the molar ratio is 1.1:1 (i.e., to prepare 5 grams of $LiNiO_2$, 2.168 grams of $LiOH.H_2O$ and 3.798 grams of NiO are taken).

(1) The layered $LiNiO_2$ compounds with Li:Ni taken in the ratio 1:1, 1.05:1 and 1:1:1 are synthesized.

(2) The three samples have been characterized using X-ray diffraction and are found to be phase pure with rhombohedral structure. There is no considerable change in the rhombohedral structure parameters with varying Li to Ni ratio The intensities of peaks (003) and (104) differ for different samples. It has been reported that the Bragg intensity ratio R(003)=**I** (003) / **I** (104) can be used as a reliable quantitative criterion for the stochiometry of $LiNiO_2$ compounds. It is possible however that the texture of the powder can also influence the intensity of diffraction peaks.

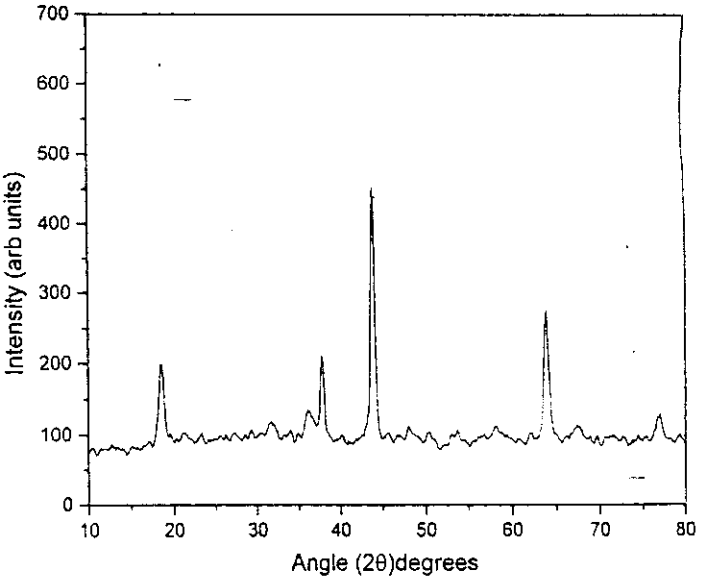

Fig 1. Li:Ni taken in the molar ratio 1: 1

(3)

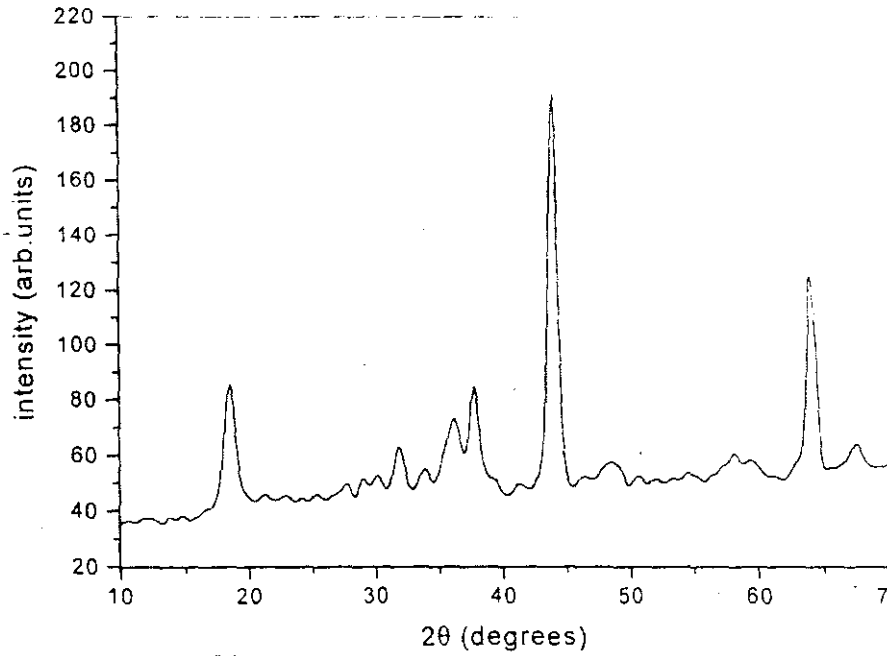

Fig 2. Li : Ni taken in the molar ratio 1.05: 1

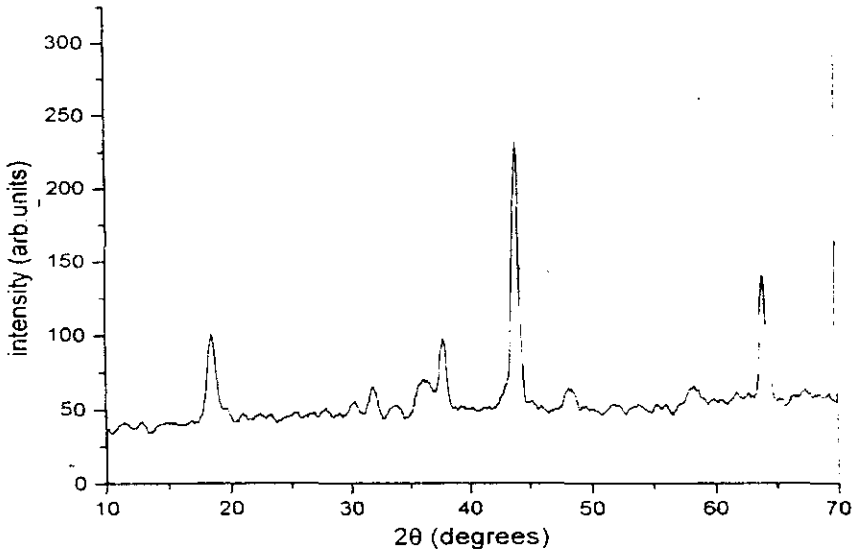

Fig.3. Li : Ni taken in the molar ratio 1.1: 1

5.8 Photoacoutic investigation of Thermal diffusivity of $LiNiO_2$

The versatility and potential of the Photoacoustic (PA) technique has been proved in characterization of materials [8-14] Photoacoustic is essentially a closed cavity detection of energy liberated by atoms or molecules through non radiative dē-excitation mechanism subsequent to the light absorption by a sample. In the PA technique, the sample to be studied is placed in a closed cell or chamber. For gases and liquids the sample generally fills the chamber [15]. However in the case of solids, the sample fills only a portion of the chamber and

the rest of the chamber is filled with non absorbing gas such as air. In the present thesis, we are dealing with only the PA studies on solid samples.

When the sample is irradiated with an electromagnetic radiation, absorption of intermittent radiation and subsequent non radiative de-excitation taking place in the sample material produces acoustic signal in the gas medium with which the sample surface is in contact within the cell or chamber. Acoustic signals thus generated are detected by a sensitive transducer (microphone) kept inside the cell. The theoretical explanation to this effect in condensed media formulated by Rosencwaig and Gersho[15,16] is given in chapter I of the thesis. The Photoacoustic cells are designed depending upon the sample (solid, liquid or gas) and also on the purpose of measurement (trace gas detection, optical absorption, thermal characterization, temperature varying measurements etc.). However, the cells are broadly classified into two: Resonant cells and Non resonant cells. The phase transition measurements in which temperature has to be varied requires a resonant cell, where the microphone is separated from the sample chamber by a long narrow tube. In non resonant cells, the microphone is placed in close proximity of the sample so that the gas volume can be minimized which in turn provides better signal. In the present work, an Open Photoacoustic Cell (OPC) is used for measuring the thermal and transport properties of the copper delafossites.

5.9 OPEN PHOTOACOUSTIC CELL CONFIGURATION:

Open Photoacoustic cell configuration is a modified and convenient form of the conventional Photoacoustic cell. This technique has been successfully applied for the study of optical spectra of liquids [16], discrimination of bulk and surface optical absorption coefficients [17] thermal and transport property determination [18,19] etc. The open photoacoustic theory was developed by Helander etal [20-21] and was later modified by McQueen etal [22].The OPC technique does not require additional transducer medium like air chamber in the case of conventional PA cells and may be called minimal volume PA detection. The solid sample is mounted directly on to the top of microphone leaving a small volume of air in between the sample and the microphone. OPC detection has been widely employed in thermal characterization of samples. A schematic representation of the open Photoacoustic cell is as shown in figure (1). The periodic pressure variation in the air chamber can be derived using the R-G theory. The sample is assumed to be optically opaque so that whole energy is absorbed at the sample surface itself and the heat flux into the surrounding air is negligible.

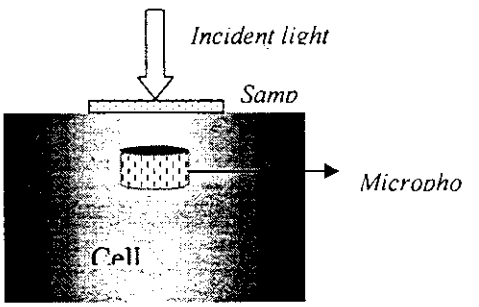

Figure 1: Schematic representation of an open photoacoustic cell.

The expression for the PA signal from the 1-D heat flow model of Rosenwaig and Gersho([15] is obtained as

$$\delta P = \frac{\gamma P_0 I_0 \left(\alpha_g \alpha_s\right)^{1/2}}{2\pi l_g T_0 k_s f \sinh\left(l_s \sigma_s\right)} \exp\left[j\left(\omega t - \pi/2\right)\right]$$

(1)

where γ is the air specific heat ratio, $P_0(T_0)$ is the ambient pressure (temperature), I_0 is the absorbed light intensity, f is the modulation frequency, and l_i, k_i and α_i are the length, thermal conductivity and thermal diffusivity of material I respectively. Here i subscript denotes the sample (s) and gas (g) media respectively and $\sigma_g = (1+j)\, a_g$, $a_g = \{ \Pi f / \alpha_g \}^{1/2}$ is the complex thermal diffusion co-efficient of the material i.

For a sample being thermally thin, ($l_s a_s << 1$) the above equation reduces to
If the sample is optically opaque and thermally thick then equation (1) reduces to

$$P \cong \frac{\gamma P_0 I_0 \left(\alpha_g \alpha_s\right)^{1/2} \exp -l_s \left(\pi f \alpha_s\right)^{1/2}}{\pi l_g T_0 k_s f} \exp\left[j\left(t - \pi/2 - l_s a_s\right)\right]$$

(2)

where l_s and a_s are the thickness and thermal diffusion coefficient of the sample. Thus according to equation (3) the amplitude of the PA signal varies with modulation frequency as $\left(1/f\right)\exp\left[-l_s\left(\pi f/\alpha_s\right)^{1/2}\right]$ and phase varies as $-l_s\left(\pi f/\alpha_s\right)^{1/2}$. Hence, thermal diffusivity can be obtained either from the phase data or amplitude data. However in the case of plate shaped solid samples surrounded by air, the contribution of the photoacoustic signal from the thermoelastic bending of the sample cannot be neglected, especially in the case of thermally thick samples [23]. This effect is mainly due to the temperature gradient inside the sample along the z axis as shown in figure (2).

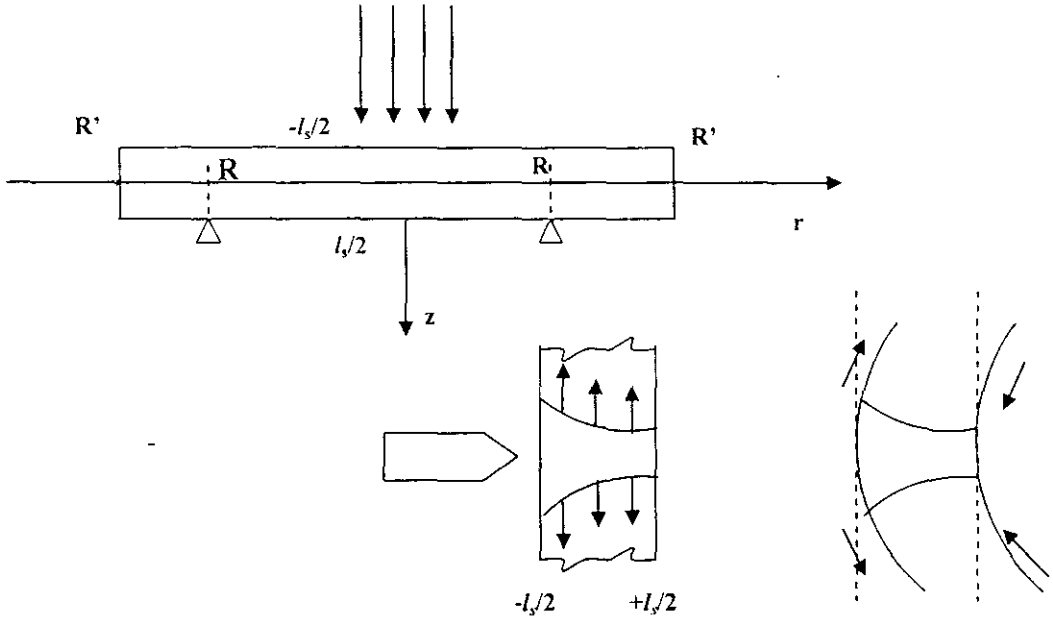

Figure (5): geometry and sources of surface strain for the thermoelastic bending. R' and R are the microphone inlet hole radii

Since the temperature gradient exists in a direction parallel to the z axis, thermal expansion depends on the z. This z dependence of the displacement along the radial direction induces a bending of the plate in the z direction (drum effect)[24].

The contribution from the sample bending is described by a coupled set of equations. The heating caused by the surface displacement (elastic waves) is

neglected. For the configuration shown in figure 2, assuming that all the light is absorbed at the surface ,

$$T_s(z) = \frac{I_0}{k_s \sigma_s} \frac{\cosh\{[z-(l_s/2)]\sigma_s\}}{\sinh(l_s \sigma_s)} e^{j\omega t} \quad (3)$$

neglecting the inertial term also since the experiment is performed at low frequencies. Assuming that the sample is cylindrically symmetric and thin enough such that $l_s << R$'. In this condition the stress condition is applicable i.e one has $\sigma_{zz} = \sigma_{rz} = 0$ along z direction where σ_{ij} is the stress tensor. Then on solving the set of thermoelastic equations for the sample displacement u_r and u_z along the radial and z directions subjected to the boundary conditions that the sample is simply supported at r=R and $z=l_s/2$ and that at the edges r=R' it is free of forces and moments, one gets

$$u_z(r,z) = \alpha_T \left\{ \frac{6(R^2 - r^2)}{l_s^3} M_T + \frac{1+\nu}{1-\nu} \int_{l_s/2}^{z} dz T_s - \frac{\nu}{1-\nu} \times \left[\frac{12 M_T}{l_s^3} \left(z^2 - \frac{l_s^2}{4} \right) + \frac{2 N_T}{l_s} \left(z - \frac{l_s}{2} \right) \right] \right\} \quad (4)$$

with

$$M_T = \int_{-l_s/2}^{l_s/2} dz z T_s \quad N_T = \int_{-l_s/2}^{l_s/2} dz T_s$$

(5)

The first term in equation () represents the bending of the sample and the other ones are due to the thickness dilation. The thermoelastic contribution p_{el} to the pressure fluctuation in the PA chamber can be calculated if the sample displacement along the z direction is known using the piston model as

$P_{el} = \gamma P_0 \Delta V / V_0$ where ΔV is the volume change due to the sample surface displacement.

Hence $P_{el} = \frac{\gamma P_0 2\pi}{V_0} \int_0^R dr r u_z\left(r, \frac{l_s}{2}\right)$

(6)

Combining equations 4, 5 & 6,

$$P_{el} = \frac{3\alpha_T R^4}{R_c^2 l_s^2} \times \frac{\gamma P_0 I_0}{l_g K_s \sigma_s^2} \left(\frac{\cosh(l_s\sigma_s) - \left(\left(l_s\sigma_s/2\right)\sinh(l_s\sigma_s)\right) - 1}{l_s\sigma_s \sinh(l_s\sigma_s)} \right) e^{j\omega t}$$

(7)

where R_c is the eadius of the PA chamber in front of the diaphram. It follows from equation (8) that fro a thermally thin sample $(l_s\sigma_s)<<1$, the thermoelastic contribution to the PA signal reduces to

$$P_{el} \approx \frac{\alpha_T R^4 \gamma P_0 I_0}{8 R_c^2 l_g k_s} e^{j(\omega t+\pi)} \qquad (8)$$

This means that the PA signal becomes independent of the modulation frequency while its phase ϕ_{el} approaches 180^0. AT the same time for a thermally thick sample,

$$P_{el} = \frac{3\alpha_T R^4 \gamma P_0 I_0 \alpha_s}{4\pi R_c^2 l_s^2 l_g k_s f}\left[\left(1-\frac{1}{x}\right)^2+\frac{1}{x^2}\right]^{1/2} e^{j\left[\omega t+\left(\pi/2\right)+\phi\right]}$$

(9)

where $x = l_s a_s = l_s\left(\pi f/\alpha_s\right)^{1/2}$ and

$$\tan\phi = 1/(x-1)$$

(10)

At high modulation frequencies such that x>>1, the thermoelastic contribution varies as

f^1 and its phase ϕ_{el} approaches 90^0 as

$$\phi_{el} = \pi/2 + \arctan\left(1/[x-1]\right)$$

(11)

Thus for a thermally thick sample, if the thermoelastic contribution is dominant then the thermal diffusivity can be evaluated from the modulation frequency dependence of either the signal amplitude or its phase.

Experimental

$LiNiO_2$ powders with molar ratio varying from 1 to 1.1 are pelletised and heated at 750^0C in argon atmosphere. The samples are then ground for X-ray diffraction pattern, which did not show any peaks of impurity phase [26].

In the OPC technique, the sample is attached to the front sound inlet of an electret mirophone. When irradiated by an intensity-modulated light, it absorbs energy, which is converted into heat by non-radiative processes. Three heat sources can be identified in this process: electron-phonon collisions within the conduction band, the non-radiative electron hole recombination in the bulk (bulk recombination) and at the surface (surface recombination).

A He-Ne laser (632.8 nm, 20 mW) is used as the excitation source and is intensity modulated using a mechanical chopper (SR 450). The laser beam is used

without focussing in order to minimize the lateral heat flow. The pressure fluctuations as a result of thermal waves produced are detected using an electret microphone (Knowles FG 3392). The amplitude and phase of the PA signal is obtained from the lock-in-amplifier (SR830). A cross sectional view of the experimental setup used is given by figure 1.The experiment is performed on similar samples of different thickness.

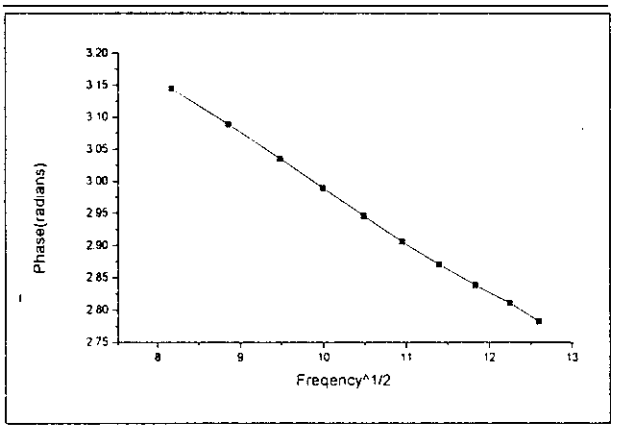

Fig.5.3 shows the plot of phase vs.square root of frequency for Li NiO_2 taken in the molar ratio 1 :1 and Thickness 500 microns

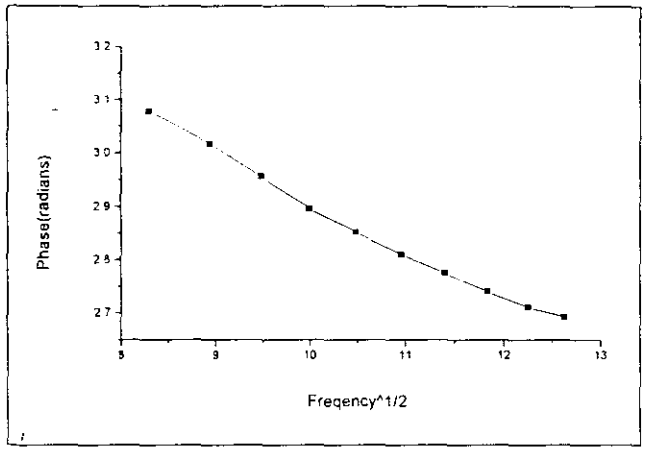

Fig.5.4 shows the plot of phase vs.square root of frequency for Li NiO_2 taken in the molar ratio 1 :1 and Thickness 700 microns

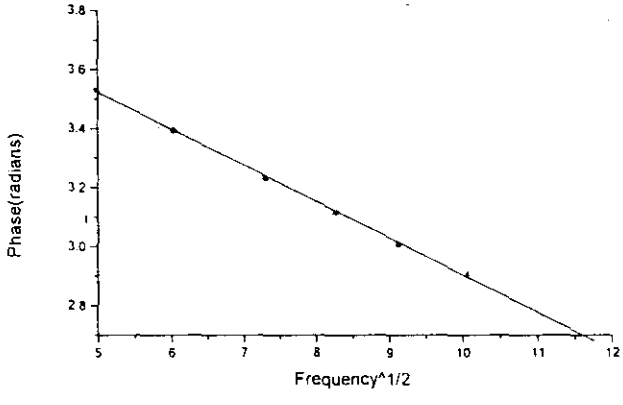

Fig.5.5 shows the plot of phase vs.square root of frequenc

$Li\ NiO_2$ taken in the molar ratio 1 :1 and Thickness 900 microns

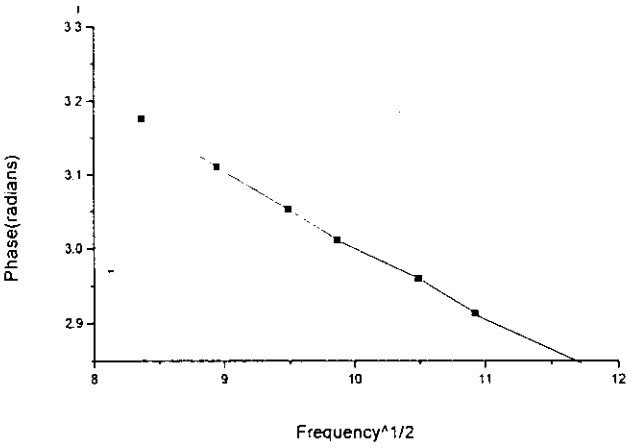

Fig.5.6 shows the plot of phase vs.square root of frequency for

$Li\ NiO_2$ taken in the molar ratio 1 :1.05 and Thickness 500 microns

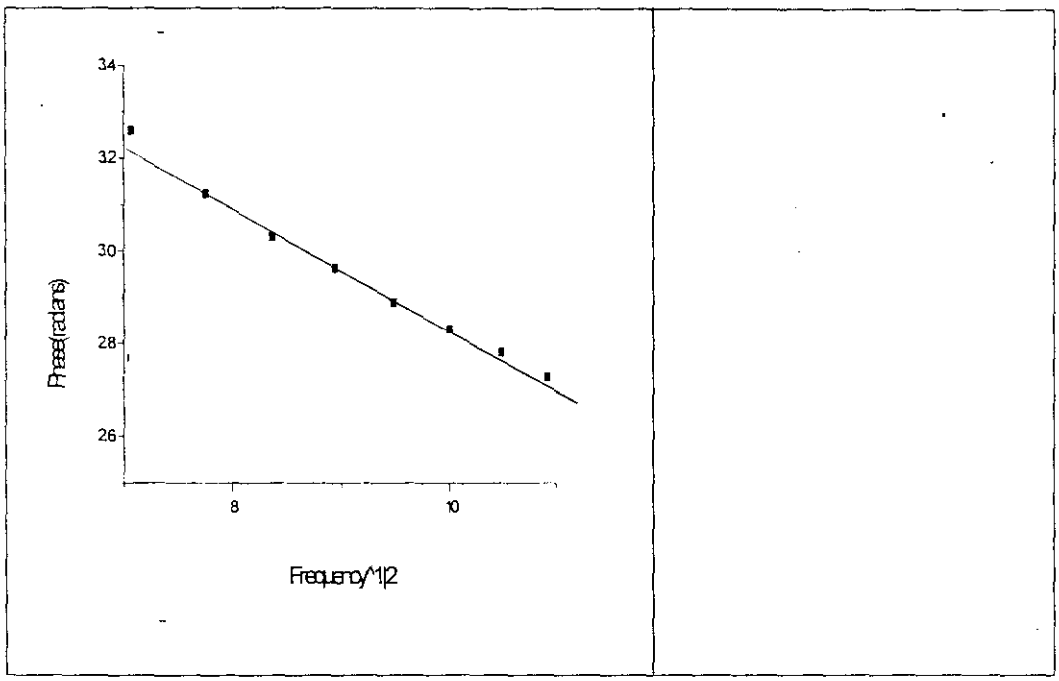

Fig.5.7 shows the plot of phase vs.square root of frequency for

Li NiO_2 taken in the molar ratio 1 :1.05 and Thickness 700 microns

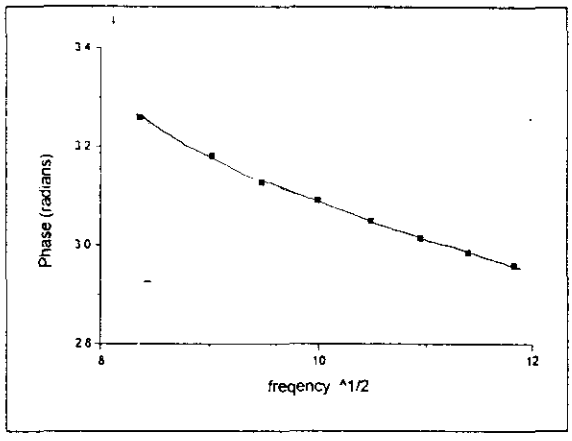

Fig.5.8 shows the plot of phase vs.square root of frequency for

Li NiO_2 taken in the molar ratio 1 :1.05 and Thickness 900 microns

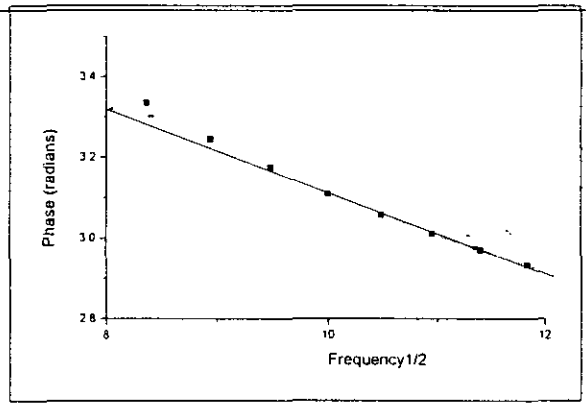

FIG.5 .9 shows the plot of phase vs.square root of frequency

Li NiO_2 taken in the molar ratio 1.1 :1 and Thickness 500 microns

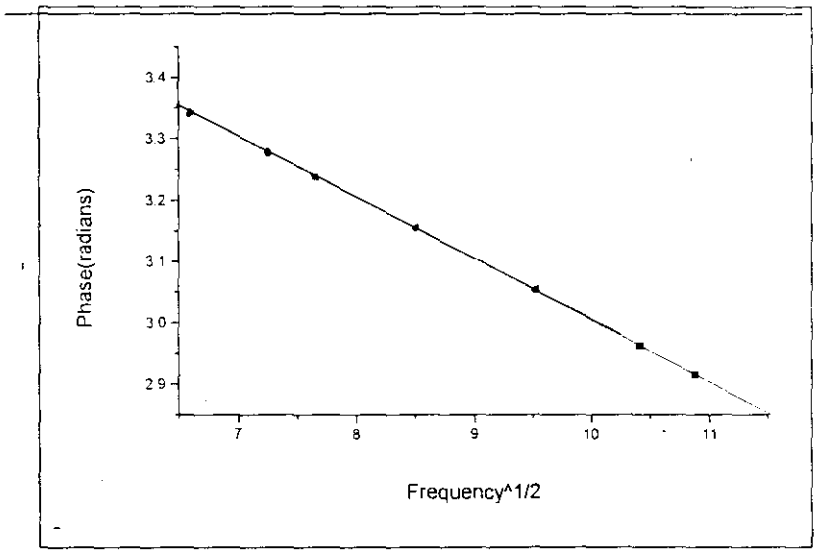

FIG.5 .10 shows the plot of phase vs.square root of frequency for $LiNiO_2$ taken in the molar ratio 1.1 :1 and Thickness 700 microns

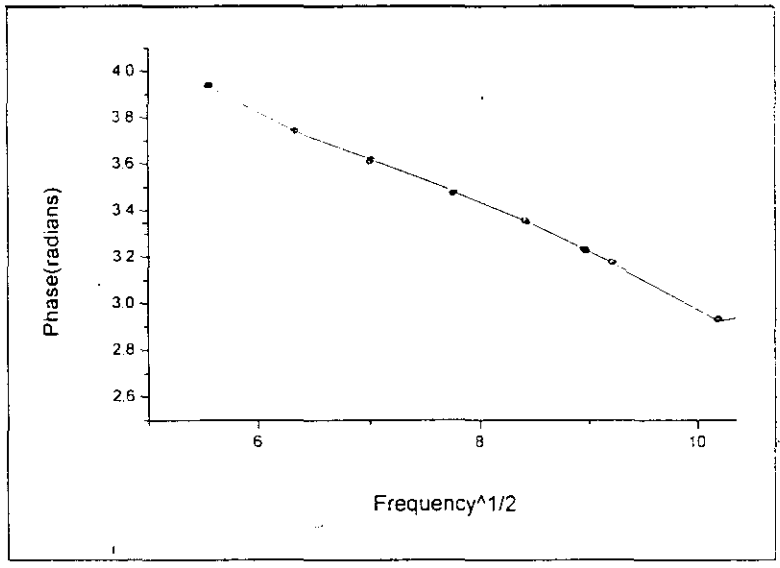

Fig.5.11 shows the plot of phase vs.square root of frequency for Li NiO_2 taken in the molar ratio 1.1 :1 and Thickness 900 microns

Ratio Li : Ni	Thickness (Microns)	Thermal diffusivity (cm^2 / sec)
1 : 1	500	1.07948
	700	0 .99778
	900	1.0728
1.05 :1	500	0 .70912
	700	0 .8922
	900	0 .813
1.1 : 1	500	0.716
	700	0 .7988
	900	0 .6491

Table .5 .1 Thermal diffusivity of $LiNio_2$ for different molar ratios.

5.10 Results and conclusion

In conclusion the thermal diffusivity of $LiNiO_2$ for different molar ratios are determined .The variation of phase with modulation frequency for the same set of samples are shown from figures (3 -11).From the figures it is seen that the phase is varying linearly with squareroot of modulation frequency.Hence the thermal diffusivity can be obtained directly from the slope,which is given by-l_s ($\Pi/\alpha_s)^{1/2}$.[25] From the figures and table it is observed that this sample with Li Ni = 1:1,shows D-value more than that of samples of other molar ratio.This is due to that on changing the molar ratio of Li :Ni lattice gets distorted.This is also evident from the broadening of peaks of XRD pattern.Due to this distortion and also due to the change in the atomic masses,phonons are scattered.The scattering of phonons reduces the thermal conductivity (Thermal diffusivity).

References:

1 .A. Mandelis (Edit) Progress in Photothermal Science and technology in Semiconductors
(Elsevir Science,Newyork)1992

2.YuG.Gurevich,G.Gonzalezdela Cruz,G.Logvinovand M.N Kasyanchuk. Semiconductors, 32 (11), 1179 (1998

3.A.Mandelis (Edit) Photohotoacoustic and Thermalwave Phenomena in Semiconductors (North Holland Newyork)1987.

4 Charles Kittel, Introduction to Solid state Physics, Seventh Edition, Wiley Eastern Limited. 5. M.Ali.Omar .Elementary Solid state Physics : Pearson Educatiion Asia 2002

6_Carlsjaw H.S and Jaeger J. C. Conduction of heat in Solids (Oxford Press) 1959.

7 G.X.Wang. S.Zhong. D,H.Bradhurst,S.X.Dou.HK.Liu (Elsevir Science,Newyork)1998

8. Rosencwaig, J.B.Willis, J.Appl.Phys.51(8) (1980) 4361.

9. J.C.Murphy, L.C.Aamodt, J.Appl.Phys. 48(8) (1977) 3502.

10.F.Scudieri, M.Marinelli, U.Zammit, S.Martellucci, J..Phys.D Appl. Phys. 20 (1987) 1045

11. Nibu A.George, C.P.G Vallabhan, V.P.N. Nampoori, A.K. George P.Radhakrishnan J.Phys.D. Appl.Phys 33 (2000) 3228.

12 J.Bernal-Alvarado, M.Vargas, J.J.Alvarado-Gil,I.Delgadillo,A.Cruz-Orea,H.Vargas, A.Tufino-Velazquez, M.L.Albor-Aguilera, M.A.Gonzalez-Trujillo, J.Appl.Phys. 83(

13 O.Delgado-Vasallo, E.Marin, J.Phys.D:Appl.Phys. 32 (1999) 593

14. A.Rosencwaig, Photoacoustics and Photoacoustic Spectroscopy, John Wiley &Sons,) New York (1980)

15 A.Rosencwaig,A.Gersho, J.Appl.Phys.47,64 (1975).

16. P.Helander, J.Photoacoust.1 (1982) 103

17 .P.Helander, I.Lundstrom, J.Appl.Phys. 54 (1983) 5069

18. M.D.Dramicanin,Z.D.Ristovski,P.M.Nikoli,D.G.Vasilgevic,D.M.Todorovic, Phy.Rev B.51(20)(1995) 14226

19. E.Marin.,H.Vargas,P.Diaz,I.Riech.Phy.stat.sol (a) 179 (2000) 387.

20. P.Helander, J.Photoacoust.1 (1982) 251.
21. . J.Helander.J.Appl.Phys. 59 (1986) 3339.
22. D.H.McQueen, J.Phys.E. 16 (1983) 738
23. A.Rosencwaig,A.Gersho, J.Appl.Phys.47,64 (1975).
24.. G.Rousset, F.Lepoutre, L.Bertrand, J.appl.Phys. 54, (1983), 2383.
25.JyotsnaRavi,M.K.Jayaraj,K.A.Vanaja,K.P.R.Nair and T.M.A Rasheed,Semiconductor Science And Technology 18(2003)693-696.
26. Lleonid V. Azaroff, Martin J. Buerger, the Power Method in X-ray Crystallography. Mc. Graw-Hill Book Company 1958

CHAPTER VI

Summary and Conclusions

Investigations have been carried out using the two most important nondestructive laser induced photothermal methods namely photothermal deflection and photoacoustic technique.

Measurements presented on this thesis reveal the versatility and applicability of these Photothermal techniques for the characterization of a of materials, in addition to providing a better understanding of the physics of heat transport through these materials, which is an essential for the progress of photonic industry. A brief review given on the introductory part of this thesis about the various photothermaltechniques and on the applicability of the techniques, which are employed here on the class of materials so as to reveal the potential of these methods.

Thermal wave physics has been an active area of research as it has created basis for several new and revolutionary measurement technologies. All the photothermal techniques are based on the detection of the thermal waves generated in the specimen following illumination with pulsed or chopped optical radiation. Photothermal deflection and photoacoustic technique, which are based on the generation and propagation of thermal waves and subsequent effects in the

specimen as well as in the coupling medium, allow the evaluation of many of the material parameters which are hard to measure using conventional techniques.

When a solid sample is irradiated with a focused laser beam, thermal waves generated from this point source will propagate in all directions, the characteristics of which are determined by the thermal properties of the sample. The profile of refractive index gradient generated in a coupling fluid in contact with the heated surface of the solid sample is ultimately decided by these thermal waves. A weak probe-beam propagating through this gradient generated in a coupling fluid in contact with the heated surface of the solid sample is ultimately decided by these thermal waves. The weak probe-beam propagating through this gradient gets deflected. The phase of the deflection signal as a function of the distance between the point source and the probe-beam holds a linear relationship and the slope of the plot determines the thermal diffusivity of the solid sample.Thermal transport properties of liquids and gaseseous media can be determined by several photothermal methods.The author has applied the crossed beam probe beam deflection technique to determine the thermal properties of liquids.The drawback of this method is that the gas/liquid must be absorbing to thepump laser radiation to induce heating and transparent to the probe beam.

.Polymerised films are of great importance for the past few decades due to its increased industrial applicationThey are extensively used in electronic packagings

as well as in multicolour printing.biomedical membranes,anti-reflective coatings LCD's etc. The author has prepared the plasma polymerised films of the organic compounds and from the FTIR spectra of the monomer and polymer direct band gap,urbach energyv and refractiveindex are evaluated.The thermal properties of three of them is evaluated by probe beam deflection method. .

In spite of the existence of several photothermal techniques, photoacoustic technique has gained wide popularity due to simplicity in experimental setup as well as the capability of simultaneous measurement of thermal and transport properties with good accuracy. Photoacoustic phase measurements are an excellent approach to investigate the heat transport mechanism in materials. It also enables one to measure the thermal and transport properties viz, thermal diffusivity, diffusion coefficient, surface recombination velocity and nonradiative recombination time of both direct and indirect bandgap semiconductors.

Photoacoutic technique is employed for the thermal characterisation of some Lithium compounds. Li compounds shows the semiconducting property.Samples are prepared taking lithium and Nickel in different molar ratios. Thermal diffusivity measurements decreases when their molar molar ratios are changed.This is due to the scattering of phonons due to lattice distortion.

. Photothermal deflection technique along with its unique features such as noncontact and nondestructive nature allows the measurement of anisotropy in effective thermal parameters of layered structures.

In general, the versatility and applicability of two important photothermal techniques, namely photothermal deflection technique and photoacoustic technique for the evaluation of fundamental properties of organic molecules and its plasma polymerized films are highlighted in this thesis.